PNNL-28379

Puget Sound Energy Glacier Energy Storage System

An Assessment of Battery Technical Performance

July 2019

A Crawford
V Viswanathan
C Vartanian
K Mongird
J Alam
D Wu
P Balducci

PACIFIC NORTHWEST NATIONAL LABORATORY
operated by
BATTELLE
for the
UNITED STATES DEPARTMENT OF ENERGY
under Contract DE-AC05-76RL01830

Printed in the United States of America

Available to DOE and DOE contractors from the
Office of Scientific and Technical Information,
P.O. Box 62, Oak Ridge, TN 37831-0062;
ph: (865) 576-8401
fax: (865) 576-5728
email: reports@adonis.osti.gov

Available to the public from the National Technical Information Service
5301 Shawnee Rd., Alexandria, VA 22312
ph: (800) 553-NTIS (6847)
email: orders@ntis.gov <http://www.ntis.gov/about/form.aspx>
Online ordering: http://www.ntis.gov

This document was printed on recycled paper.
(8/2010)

PNNL-28379

Puget Sound Energy Glacier Energy Storage System

An Assessment of Battery Technical Performance

A Crawford
V Viswanathan
C Vartanian
K Mongird
J Alam
D Wu
P Balducci

July 2019

Prepared for
the U.S. Department of Energy
under Contract DE-AC05-76RL01830

Pacific Northwest National Laboratory
Richland, Washington 99352

Acknowledgments

We are grateful to Mr. Bob Kirchmeier, Senior Energy Policy Specialist at the Washington Department of Commerce, for administering Clean Energy Fund Program financial support to Pacific Northwest National Laboratory (PNNL) and our utility partners, in addition to providing his guidance during this project. We are also grateful to Dr. Imre Gyuk, who is the Energy Storage Program Manager in the Office of Electricity Delivery and Energy Reliability at the U.S. Department of Energy, for providing financial support and leadership on this and other related work at PNNL. We wish to acknowledge Philip Craig from BlackByte Cyber Security; the team members from Puget Sound Energy, including Kelly Kozdras and Shane Richards; and Jason Yedniak from Doosan GridTech.

Executive Summary

Energy storage integration into the U.S. grid has been gathering momentum, especially as renewable generation penetration increases. Several states have storage procurement targets to deal with a variety of issues such as afternoon ramping requirements, frequency regulation/control, and time shifting of renewable energy. The technical attributes of energy storage required to provide benefits to stakeholders, comprised of multiple utilities and their customers, were defined and evaluated. This project was funded jointly by Puget Sound Energy (PSE), the Washington Clean Energy Fund (CEF), and the U.S. Department of Energy Office of Electricity Delivery and Energy Reliability (DOE-OE).

Motivation for this Work

The 2-MW, 4.4-MWh Li-ion battery energy storage system (BESS) near the Glacier substation is installed to provide the following functions:

- Short-term backup power source to a portion of the local Glacier circuit during outages
- Reduce system load during periods of high demand
- Balance energy supply and demand to support integration of intermittent renewable energy generation on PSE's grid.

As part of Washington CEF 1, a $3.8 million grid modernization grant was awarded to PSE. The grant supported exploration of energy storage applications and associated benefits for several use cases including flexibility services (energy arbitrage, regulation up/down), primary frequency response, capacity, and outage mitigation. In addition to temporary backup for outage mitigation, BESS performance was more generally evaluated by applying duty cycles that correspond to the following additional energy storage use cases: arbitrage, capacity, regulation services, load following services, real-world flexibility operation, load shaping services, and distribution upgrade deferral. These use cases or services were identified as applicable for PSE and were defined based on utility- and site-specific characteristics. Not all use cases were ultimately deemed to provide economic value to PSE but the battery's ability to provide each was tested.

Because BESSs have quite diverse characteristics, it was important to first characterize performance over time using a DOE-OE standardized baseline test procedure for energy storage, which includes representative generic duty cycle profiles, test procedure guidance, and calculation guidance for determining key BESS characteristics, including energy capacity, response time, internal resistance, and efficiency. After conducting baseline tests to evaluate the general characteristics of the BESS, the various use cases listed were performed and measurements were taken to evaluate key BESS performance metrics relative to the several aforementioned energy storage use cases. Outcomes of these analyses will help PSE understand the performance of the Glacier BESS at its current state, and in designing appropriate long-term operational strategies for Glacier and future PSE BESS projects.

Summary of Work Performed

This report investigates the technical performance of the Glacier BESS facility, which consists of one 2-MW, 4.4-MWh BESS, based on a number of baseline and use case tests. Baseline tests were intended to assess the general technical capability of the BESS (e.g., stored energy capacity, ramp rate performance, ability to track varying charge/discharge commands, direct current [DC] battery internal resistance). Use case tests were used to examine the performance of the BESS while engaged in specific economic services (e.g., arbitrage, frequency regulation). The project measured and/or calculated parameters that are important for understanding BESS performance when subjected to actual field operation for achieving economic benefits (e.g., round trip efficiency [RTE])[1] with and without rest, with and without auxiliary loads, auxiliary power consumption, signal command tracking performance, temperature variations, parasitic power loss during power electronics switching during rest, and state-of-charge (SOC) excursions. These baseline and use case parameters were analyzed using recorded test results. In addition, the results and lessons presented in this report also will be beneficial for any task or effort that needs technical assessment on similar and different types of BESSs based on field deployment results, because the assessment methodology remains the same.

Key Questions Addressed

A thorough analysis of BESS performance was carried out using metrics developed in the DOE-OE Energy Storage Performance Protocol and additional metrics identified in this project. In combination, these general and project-specific metrics allowed a set of structured evaluations of questions that are key for ultimately determining the cost effectiveness of BESSs used for grid energy storage applications.

The following questions were addressed:

1. How does the BESS perform during baseline and use case testing for energy intensive duty cycles? For example, what is the RTE of the BESS? This analysis determined the RTE for the BESS under various scenarios—ambient temperature, charge-discharge power levels, with and without rest periods, with and without auxiliary consumption.
2. How does the BESS perform during baseline and use case testing for high ramp rate duty cycles?
3. What was the percent of time the BESS was not available?

   An analysis was done on the percent of time the BESS was not available, and the reasons for specific periods of non-availability were attributed to one of the following:

   – BESS Balance of Plant (BOP) Outage
   – Direct Current (DC) Battery Outage
   – Site or System Outage
   – Learning
   – Maintenance
   – Human error
4. What are some of the issues identified in this project that are not very obvious?

Key Outcomes

The PSE BESS was subjected to reference performance or baseline testing, including various rates of charge and discharge, internal resistance measurements, and response time/ramp rate measurements. In addition, duty cycles were developed for various use cases to be performed for this project, and the BESS use case performance was tested and analyzed accordingly.

The following highlighted Outcomes 1 to 4 summarize the most substantial findings from both base line and use case performance testing.

[1] The RTE is simply the ratio of discharge energy to charge energy.

Outcome 1

Outcome 1 revealed findings related to discharge capacity and RTE.

A thorough analysis of BESS performance was carried out using metrics developed in the DOE-OE Energy Storage Performance Protocol and additional metrics identified in this project. We determined that average power levels determine the RTE. The BESS performance during Reference Performance Tests (RPT) and use case testing was analyzed. RPTs consisted of Baseline tests prior to use case testing. Two cycles of use case testing were performed. After each cycle, the RPTs were performed. The RPT results after Cycle 1 are referred to as Post Cycle 1, while results after Cycle 2 are referred to as Post Cycle 2. Analysis was done in the 10 to 82% SOC range for all tests for two reasons:

1. Because of the flat voltage profile of the lithium iron phosphate ($LiFePO_4$) cathode, the discharge energy varied linearly with SOC down to 10%. At <10% SOC, the delivered energy increased more rapidly per unit change in SOC, indicating the reported SOC was lower than the actual SOC. Because not all discharges were carried out to very low SOCs, these extreme SOCs were not considered when comparing the Baseline vs. Post Cycle 1 and Post Cycle 2. Hence, we used a lower SOC limit of 10% for analysis.
2. Because of string imbalance issues, the SOC at the end of charge could not reach the target 90% value during the RPTs. We used an upper limit of 82% SOC for the analysis.

Discharge Energy Capacity

The range of discharge energy capacity for all RPTs and C rates ranged from 3,175 to 4,060 kWh.

The discharge energy capacity and Ah capacity at C/6 rate[2] decreased by 6% from Baseline to Post Cycle 1 and Post Cycle 2. Post Cycle 1 had the same 6% decrease at C/4 and C/2, while the decrease was 19 to 20% for Post Cycle 2. This was due to a large gap in testing during which BYD and the PSE Whitehorn crew did SOC software updates and rebalancing, respectively, thus affecting battery status. The estimated discharge energy at 100% depth of discharge was in the 3,685 kWh to 3,940 kWh range at the C/6 rate, while excluding auxiliary losses, the corresponding range was 3,710 to 3,985 kWh. There were four cycles at various rates for which discharge was done from 88% to 1%. The highest energy content was obtained for the Baseline at the C/6 rate, with discharge energies of 4,570 kWh and 4,630 kWh with and without auxiliary consumption, respectively. The corresponding numbers for Post Cycle 1 at the C/2 rate was 3,840 and 3,844 kWh, respectively, while those for Post Cycle 2 were 3,815 and 3,845 kWh, respectively. This clearly indicates there was loss of energy capacity, possibly related to loss of Ah capacity, and not an increase in internal resistance, as described below.

RTE

Inclusive off all loss sources, the range of RTE's for all tests performed was 37.0 to 87.6%.

The RTE remained relatively unchanged during testing. This is consistent with the internal resistance of the BESS remaining relatively unchanged during the course of testing, thus indicating loss of energy capacity could be related to capacity loss or inaccuracy in SOC reporting. RTE increased with C rate, especially when auxiliary losses were taken into account.

---

[2] C rate corresponds to discharging or charging the BESS at C kW, where C is the rated energy of the BESS. For example, the PSE BESS rated energy is 4,400 kWh. Hence, 1 C rate discharge or charge corresponds to 4,400 kW for 1 hour. Because the BESS rated power is 2,000 kW, the BESS can be discharged or charged at a maximum rate of C/2.2

The charge, discharge energy, and RTE are shown in Figure ES.1 for the RPT. The RTE for the RPTs ranged from 82.9 to 87.6%.

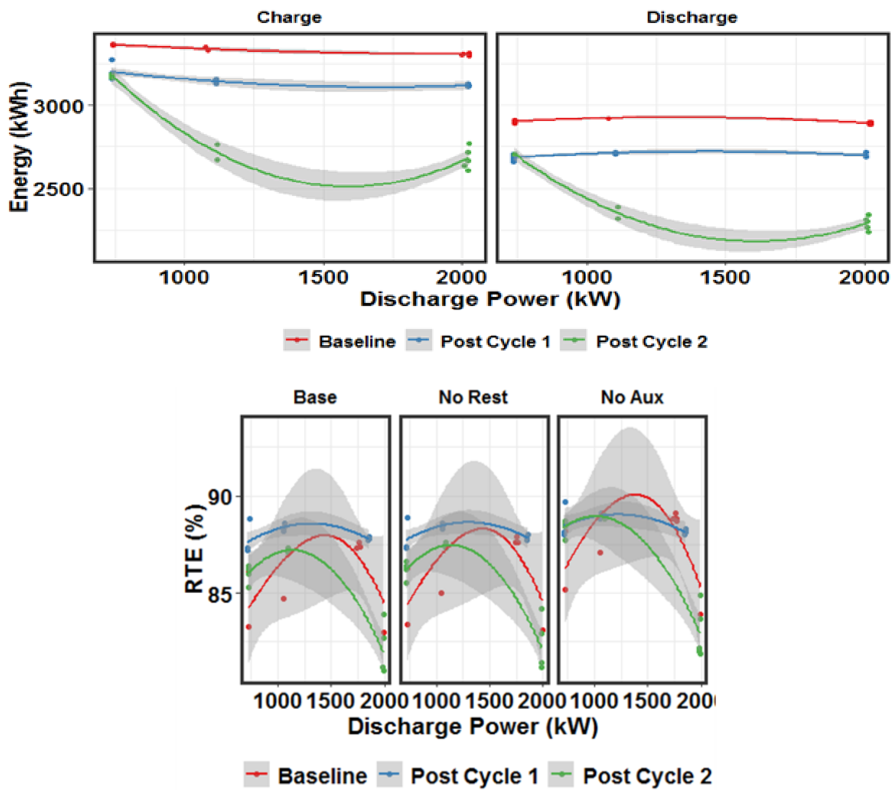

Figure ES.1. RPT for Energy Capacity – Charge, Discharge Energy and RTE at Various Power Levels

The RTE for volatile signals such as frequency regulation increased with average power. The RPT results gave an RTE in the 80 to 82% range at an average power of ~ 600 kW, while the frequency regulation RTE was in the 54 to 75% range at an average power of 130 to 220 kW.

The PCS was sometimes placed in disabled mode and sometimes in connected mode during rest, based on a BYD algorithm. The DC power consumption from the battery was higher during PCS switching, while auxiliary consumption was unchanged. From the current draw during PCS switching, the rate of change of SOC during rest was 0.5 percent per hour, while without switching, it was 0.25 percent per hour. While for the most part, the PCS switched during rest, about 20 percent of the time after charge and 15 percent of time after discharge, the PCS did not switch. This non-switching state followed BYD visits to limit SOC drift during rest. The faster rate of decrease of SOC when the PCS is in switching state needs to be accounted for when optimally deploying the BESS for various use cases.

The arbitrage use case resulted in an RTE of 61 to 78 percent, depending on power, and whether rest and auxiliary loads were included. This supports the conclusion that there is no single RTE that represents BESS performance. Assuming an artificially high RTE makes the BESS more attractive than it actually is, especially for use cases such as arbitrage whose benefits are directly tied to the BESS RTE, in addition to the high/low price differential. The rest times for arbitrage were 65 to 90 percent of total test duration, with an average of 81 percent for all 4 runs. Removing the rest resulted increased the RTE to 85 percent. Hence, if arbitrage is the only use case being considered, it may be useful to have the BESS in a disconnected state to avoid loss of energy during rest.

The RTE range for the system capacity test was in the 66 to 72 percent range. The average power ranged from C/8 to C/2.5, and the rest duration was only 10 to 64 percent of total test duration. Tests that had double the C rate and double the rest time had nearly the same RTE, with electrochemical losses balanced by rest time related losses. For distribution deferral, the average charge rate was only 0.01C and the average discharge rate was only 0.02C, mainly due to large periods where the requested power was extremely low (< 30 kW). This resulted in a low RTE of 37 percent even though the rest time was only 6 percent of total test duration with an increase of RTE to 48 percent when auxiliary consumption is excluded.

Outcome 2

Outcome 2 reports findings related to response time and internal resistance.

Response Time

The response time of the BESS ranged from nearly instantaneous to 4 seconds for the range of test cycles performed.

The response time of the BESS hardware was instantaneous to 4 seconds, corresponding to ramp rates of 25% of rated power per second at the low end to instantaneous response. There was a communication lag of 4 to 6 seconds, indicating the responsiveness of the BESS is limited by this communication lag. Because of the unique nature of this installation, with communication occurring via telephone lines, this lag should be taken into account for rapidly changing signal tracking.

BESS Internal Resistance

The BESS charge and discharge internal resistance was in the 2 to 4 milliohm range, with resistance decreasing slightly with increasing SOC. The resistance decreased by 33% from Baseline tests to Post Cycle 1 tests, possibly due to a conditioning effect, and remained unchanged for Post Cycle 1. The measured resistance, on an Ah-normalized basis, was 2 to 4 times that of a high power A123 26650 cell with the same cathode chemistry.

The RTE was in the 54 to 75% region due to average power being much lower in the 75 to 275 kW range. Signal tracking volatile signals such as frequency regulation was excellent within 2% of power, while tracking was poor within 2% of signal value. This is because at these low power levels, the meter may not be sufficiently accurate.

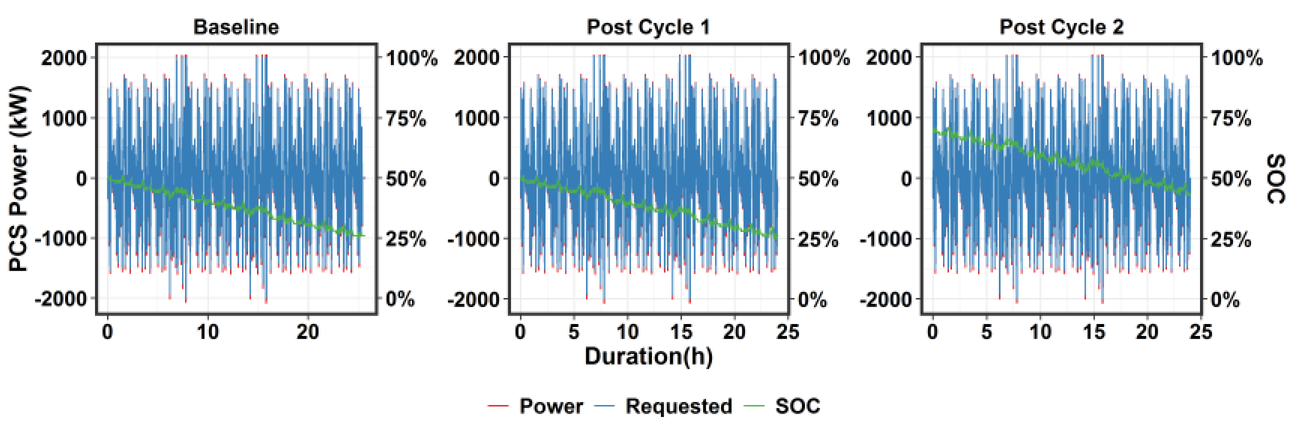

Figure ES.2. RPT for Frequency Regulation

Outcome 3

Outcome 3 reports findings on system availability.

The aggregate availability of the BESS over the test period was 64%.

The total test duration was 551 days, out of which 199 days (36% of the time) were lost for various reasons. Forty-eight days, or 9% of the test duration, were lost because of BOP-related issues, which include BESS external communication hardware and internal communication within the BESS and uninterruptable energy supply. Thirty lost days or 5% of the test duration were related to Battery Management System (BMS) control, SOC drift during rest, and string balancing. Twenty-one lost days or 4% of the test duration were site related including outage, communication error at the recloser network switch for communication. Details are shown in Figure ES.3.

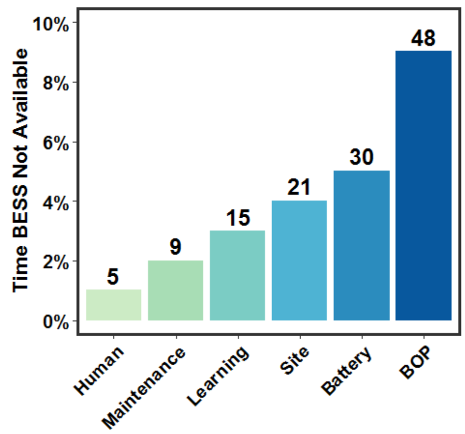

Figure ES.3. Contribution to Lost Time from Various Categories

Outcome 4

Outcome 4 captures findings for issues that surfaced during testing and were outside of specific structured objectives (e.g., testing to measure and report RTEs).

Multiple issues identified during testing that were not obvious or necessarily anticipated leading up to testing are listed in detail in the Appendix.

- It took several months to establish a virtual private network connection for data transfer. Synchronization of data from various meters was a challenge.
- The inability of the BMS to control SOC to target end of charge or discharge values resulted in string imbalances that required periodic onsite maintenance by BYD or the Whitehorn crew. Strings are considered balanced when their SOCs are within 10 to 15% of each other. This is a wide range, and is sustainable only if the Battery Master Controller allocates power to each container based on the SOC of each container.
- The discharge energy is linear with respect to depth of discharge until ~3% SOC. Deviation of a reported SOC from an actual SOC due to a potential flaw in how the BMS estimates SOC results in significant energy to be released after the SOC drops below 3%, with this effect pronounced at <1% SOC.

- The BESS SOC drifted unpredictably during rest. BYD retrofit all modules with new Battery Management Units to improve balancing and reduce SOC drift. Our work indicates the DC battery powers auxiliary load and PCS during rest, with average power for each being 10 kW. This results in an SOC drop of 0.25% per hour for auxiliary load, and another 0.25% per hour for PCS switching. At times, the DC power draw during rest was as high as 100 kW, resulting in an SOC drop rate of 2.3% per hour.
- Thermal management was done based on deviation from a set point of thermostats in each container. This resulted in a 20ºC temperature range between the maximum and minimum module temperatures, which can be deleterious to the battery state of health.
- The Doosan Gridtech Intelligent Controller, which is the system operator interface, required special formatting for test durations >24 hours. Tests having multiple commands every few seconds needed a manual start, hence cannot be scheduled sequentially in automatic mode.
- The power following mode of the Doosan Gridtech Intelligent Controller was not applicable to the load following use case. The frequency/watt mode was more applicable. This mode has not been used by PSE, hence duty cycles were sent by Pacific Northwest National Laboratory for load following.

Additional findings explored in the report include:

- The internal resistance of the DC battery decreased with use, possibly due to a conditioning effect.
- The DC battery powers auxiliary loads during rest, reducing battery SOC and compromising its ability to provide required energy after rest.
- The seasonal effect on auxiliary power consumption was determined.
- The effect of inverter switching state during rest on battery self-discharge was determined.
- While the BYD BMS was supposed to allow charge and discharge to the target SOC, this was not achieved in practice. The reported SOC was lower than actual SOC during discharge and vice-versa. The root mean square error decreased with average signal power, while signal tracking increased with average signal power.

Acronyms and Abbreviations

A	amperes
AC	alternating current
ACE	area control error
Ah	ampere-hours
BESS	battery energy storage system(s)
BMU	Battery Management Unit
BMS	battery management system
BOP	balance of plant
BSET	Battery Storage Evaluation Tool
CEF	Clean Energy Fund
DC	direct current
DERO	GridTech's Distributed Energy Resources Optimizer
DG	Doosan GridTech
DG-IC	Doosan GridTech Intelligent Controller
DNP3	Distributed Network Protocol
DOD	depth of discharge
DOE	U.S. Department of Energy
DOE-OE	Office of Electricity Delivery and Energy Reliability
EMS	energy management system
ES	Energy Storage
ESS	Energy Storage Systems
GLA	Great Lakes Automation Supply
kV	kilovolts
kVA	kilovolt-ampere
kvar	kilovolt-ampere reactive
kW	kilowatts
kWh	kilowatt-hours
MESA	Modular Energy Storage Architecture
MW	megawatt(s)
MWh	megawatt hour(s)
OE	Office of Electricity Delivery and Energy Reliability
PCS	power conversion system
PNNL	Pacific Northwest National Laboratory
PSE	Puget Sound Energy
RMSE	root mean square error
RPT	Reference Performance Test

RTE	round-trip efficiency
SOC	state of charge
SOH	state of health
T	temperature
UPS	uninterruptable energy supply
V	volts
W	watt
Wh	watt hour(s)

Contents

Figures

Tables

1.0 Introduction

1.1 Project Synopsis

Pacific Northwest National Laboratory (PNNL) was chosen to provide analytical support under the Washington Clean Energy Fund (CEF) Use Case Analysis Project. This project is designed to aid battery energy storage system (BESS) grid integration efforts by providing a framework for evaluating the technical and financial benefits of the BESSs deployed under this program, and exploring the role of energy storage in delivering value to utilities and their customers. This framework, and the tools used to implement it, evaluated a number of use cases as applied to energy storage projects deployed by the participating utilities under the Clean Energy Fund (CEF) program. The methodologies that emerged from this project for evaluating multiple storage benefits, and the detailed operational results from utility utilization of energy storage, has broad national relevance and applicability. The three main components related to use case testing and evaluation are depicted in Figure 1.1.

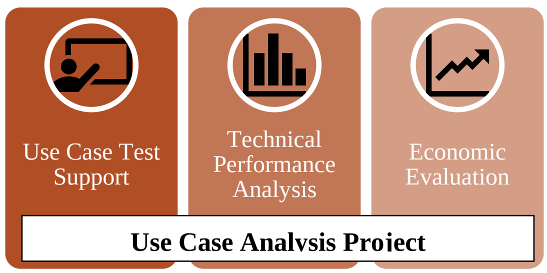

Figure 1.1. Main Components of the Use Case Analysis Project

This report documents baseline and use case technical performance of the PSE BESS based on the framework and approaches defined by PNNL in the test plan report, and the lessons learned on the technical aspects of the PSE BESS. The Reference Performance Test (RPT) vs. use case comparative analytic approach was used to evaluate the effectiveness of BESSs when operated to deliver sets of energy storage applications combined into use cases. This technical support included:

1. Development of protocols and duty cycles to test the ability of the BESS to safely and effectively be used for the project's tested use cases
2. Determination of performance metrics (e.g., ramp rate, round trip efficiency [RTE], internal resistance) to be evaluated
3. Analysis of test results against a predefined set of performance metrics to determine the effectiveness of storage for each use case.

Baseline testing used cycles intended to quantify basic BESS characteristics, including power and energy capacities, ramp rate/response time, and signal tracking. Reference performance for the BESS considered in this project used several duty cycles defined and described in the U.S. Department of Energy (DOE) Energy Storage Protocol and were performed at the beginning of the project (Baseline tests), after Cycle 1 of use case testing (Post Cycle 1) and after Cycle 2 of use case testing (Post Cycle 2).

This project designed and tested five use cases, some of which included sub use cases. These use cases combined several energy storage applications as follow:

- Use Case 1 – Energy Arbitrage and System Capacity
- Use Case 2 – Regulation, Load Following, and Real-World Flexibility

- Use Case 3 – Deferment of Distribution Upgrades and Load Shaping
- Use Case 4 – Outage Mitigation
- Use Case 7 – Optimal Utilization of the BESS across Use Cases 1 through 4.

These use cases were selected from the full set of use cases being evaluated across several CEF BESS projects. Table 1.1 lists the full range of use cases under investigation and which of those are relevant to this specific project.

Table 1.1. Use Cases Considered in Testing of the CEF Projects

Use Case and Application as Described in PNNL Catalog	Avista	PSE	Sno-MESA1	Sno-MESA2	Sno-Controls Integration
UC1: Energy Shifting					
Energy shifting from peak to off-peak on a daily basis	X	X	X	X	
System capacity to meet adequacy requirements	X	X	X	X	
UC2: Provide Grid Flexibility					
Regulation services	X	X		X*	
Load following services	X	X		X*	
Real-world flexibility operation	X	X		X*	
UC3: Improving Distribution Systems Efficiency					
Volt/Var control with local and/or remote information	X		X	X	
Load-shaping service	X	X	X	X	
Deferment of distribution system upgrade	X	X			
UC4: Outage Management of Critical Loads		X			
UC5: Enhanced Voltage Control					
Volt/Var control with local and/or remote information and during enhanced CVR events	X				
UC6: Grid-connected and islanded micro-grid operations					
Black Start Operation	X				
Micro-grid operation while grid-connected	X				
Micro-grid operation while in islanded mode	X				
UC7: Optimal Utilization of Energy Storage	X	X			X

*Use case relies on simulated signals because these services are not provided by SnoPUD.

This project developed the composite cycle profiles and used them for testing the project BESS for these use-case scenarios. The duty cycles and associated test results are described and discussed in the body of the report.

Finally, PNNL evaluated the economics of energy storage using commonly used characteristics such as rate of return and payback periods, starting with a preliminary economic analysis using the BESS manufacturer specifications. The use cases were optimized (Use Case 7) to determine the potential financial benefit of BESS deployment over the economic life of the unit. This work was used to characterize the performance of the BESS, and the economic models were updated to develop the use case based duty cycles.

Understanding a battery's technical features and limitations is essential and provides necessary input data used to perform the economic evaluation of the services a BESS can provide. Technical information on the PSE BESS is provided in the following section.

1.2 PSE Battery

1.2.1 Battery Architecture

The project's 2-MW, 4.4-MWh rated BESS consists of lithium iron phosphate ($LiFePO_4$)-graphite cells. This chemistry is the safest among all Li-ion cells. This chemistry's relative safety among the broader general family of Li-ion batteries is mainly due to delayed onset of thermal runaway for the $LiFePO_4$ electrode and the low energy content for the runaway reaction for this electrode, relative to other Li-ion chemistries (e.g., nickel-manganese-cobalt or nickel-cobalt-aluminum Li-ion).

The BESS consists of four containers, each with a 1.1-MWh DC battery unit, and a BYD 500-kVA inverter. The inverters are tied in parallel to provide or absorb the full system rated power. Each container has six battery strings connected in parallel. There are four cabinets per string, with each cabinet housing 10 slots. Thirty-five of these slots have battery modules consisting of eight series-connected cells, while the BMS control box occupies one slot, leaving four open slots. All modules within a string are connected in series, resulting in a 280-cell connection. Per the BYD Glacier Battery Technical Specifications, the operating voltage range for the BESS is estimated at 780 to 1,000 VDC, which corresponds to a single-cell voltage range of 2.8 to 3.6V per cell, which is consistent with $LiFePO_4$-graphite chemistry.

The battery cabinet layout within one string is shown in Figure 1.2.

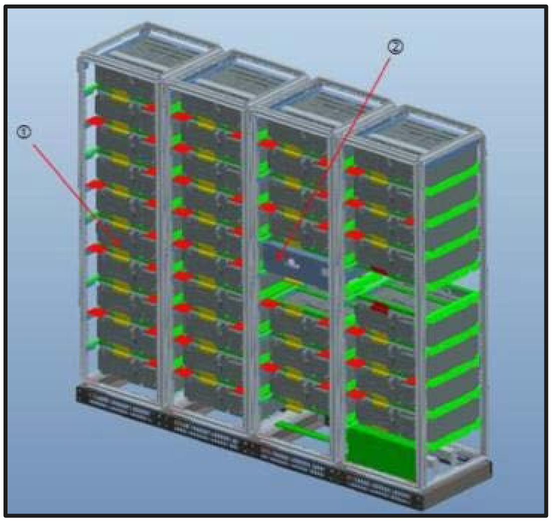

Figure 1.2. Battery Cabinet Layout within One String. (1) Battery Module, (2) BMS Control Box.

Table 1.2 summarizes the architecture of the BESS.

Table 1.2. BESS Architecture

Level	Quantity	Total per container	Total in BESS
# Containers	4	NA	4
# parallel connected strings per container	6	6	24
# modules per string	35	210	840
# series-connected cells per module	8	1680	6720

1.2.2 Battery Technical Specifications

The DC voltage range of operation is 780V to 1,000V, corresponding to 2.78V to 3.57V per cell. This operating range corresponds to the usable SOC range: a lower allowed SOC corresponds to 780V and an upper allowed SOC corresponds to 1000V.

The BESS PCS is a 500-kW BYD model BEG500KTL-U inverter. Its DC voltage range is 780 V to 1,000 VDC, matching the DC battery technical specifications. The nominal alternating current (AC) power rating per inverter is 500 kW. The efficiency of the inverter impacts the power at the DC bus during the charge and discharge cycles as follows. During discharge, the maximum DC power was 2,140 kW, while during 2,000 kW charge, the maximum DC power was 1,970 kW. On the AC side of the inverter, the nominal grid voltage is 480 V, with a permissible grid voltage range of 423 to 528 VAC, with a maximum efficiency of 97.5%.

The containers are rated at National Electrical Manufacturers Association 3R, "… intended for outdoor use primarily to provide a degree of protection against rain, sleet, and damage from external ice formation" [BYD undated]. The response time of the BESS was specified to be <100 milliseconds at the BYD interface. The definition of response time was not specified; it is assumed the hardware responds at >100 milliseconds of receiving a signal. With data collected every 2 seconds, it was not possible to verify this. The communication protocol for the BESS is Transmission Control Protocol/Internet Protocol.

1.2.3 Battery Management System

Each module has a Battery Management Unit (BMU) that communicates to the container BMS. The container BMS communicates to the BYD master controller. The Doosan GridTech Intelligent Controller (DG-IC), also referred to as the PSE Operator Interface, is installed on top of the BYD master controller. The BYD master controller distributes the power among the four containers when it receives signals or commands from the DG-IC. In July 2018, BYD retrofitted all modules with advanced BMUs. It is not clear specifically what benefits these BMUs offered.

During operation, the BMS allows the battery SOC to go to 0% during discharge and 100% during charge when the strings are balanced. When the strings become unbalanced, low cell voltages in two or more strings during discharge will kick the container out of discharge. The other containers continue to discharge until the same situation arises. The reverse happens during charge, when high cell voltages in two or more strings cause that container to drop off charge. Clearly, if the strings are well balanced, it is possible to approach the extremes of 0% and 100% SOC during discharge and charge, respectively.

The battery discharge energy increased linearly with depth of discharge (DOD) until the SOC decreases to ~3% SOC. The battery reported SOC swings in the direction of charge or discharge power during a sudden power change, resulting in underestimated SOC during discharge and overestimated SOC during charge as seen in Figure 1.3. This resulted in additional energy obtained at very low SOC during discharge.

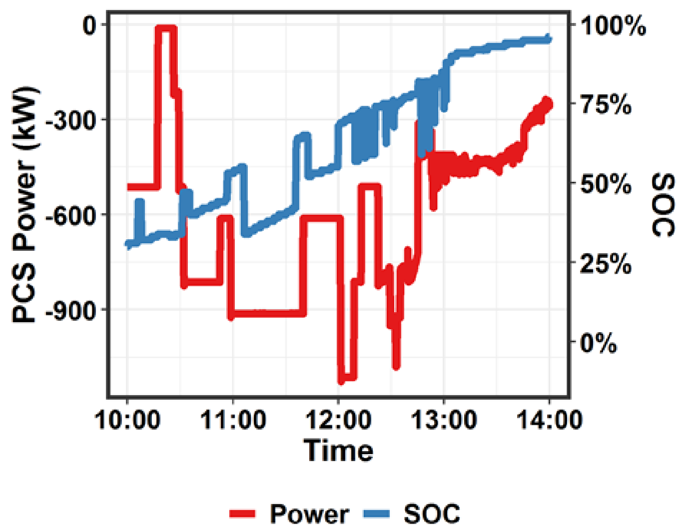

Figure 1.3. SOC Change with Rapid Power Swings

1.2.4 Balancing Procedure

Periodically, the strings within a container become unbalanced when their SOCs differ by >10%. The DG-IC has the ability to set the minimum and maximum SOC, which can be overridden to re-balance the strings. The balancing procedure is described below:

- The battery is discharged to “empty” state
- The PCS and DC battery are placed in stop state
- For each container, the open circuit voltages and SOCs for all strings are recorded
- The highest SOC string is discharged at 50 kW until its voltage is 15 V lower than the other strings’ voltage (the 15 V value probably is chosen to account for the internal resistance decrease that occurs during discharge). After 1 minute, the string voltage is compared with other strings’ voltages to ensure all six string voltages are close (within 6 V of each other)
- If more than one string was at high SOC, the process is repeated with a second string.
- The six strings are charged to the desired SOC
- The process is repeated for the other containers.

Figure 1.4 shows the status of six strings in container 1. Note that the String 2 SOC is out of balance with respect to other strings.

Figure 1.4. BYD String Status for Container 1

1.2.5 DC Round-Trip Efficiency

The maximum DC current was specified as 700 A. As seen in Figure 1.5, the DC current during discharge decreases from 2,390 A (or 600 A per inverter) at ~2% SOC to 2,310 A (or 580 A per inverter) at 88% SOC. The charge and discharge current are plotted as a function of SOC to account for deviation of the reported SOC from the actual SOC. During charge, the DC current was 2,120 A at 6% SOC, which decreased to 1,970 A at 90% SOC. Hence the maximum current of 700 A was not observed during testing. Note that the mismatch of SOC during charge and discharge is due to underestimation of SOC during discharge and overestimation during charge as explained earlier.

The product of current and voltage is power. Therefore, at a fixed/set power setting, the ratio of charge to discharge current is an estimate of the RTE of the DC battery. The ratio of DC charge to discharge current, at fixed DC power flow, is shown in Figure 1.5. The DC-DC RTE is in the 95 to 98% range. The RTE increases with increasing SOC. For baseline tests, the RTE range was 95.6 to 96.6%, while for Post Cycle 1 and Post Cycle 2, the RTE was in the 96.0 to 96.8% range, which is a slight improvement. Similar plots for C/4 rate and C/6 rate also are shown. All of them show the same trend of increasing RTE with SOC and with test duration. This is consistent with a slight decrease in DC internal resistance from Baseline to Post Cycle 1.

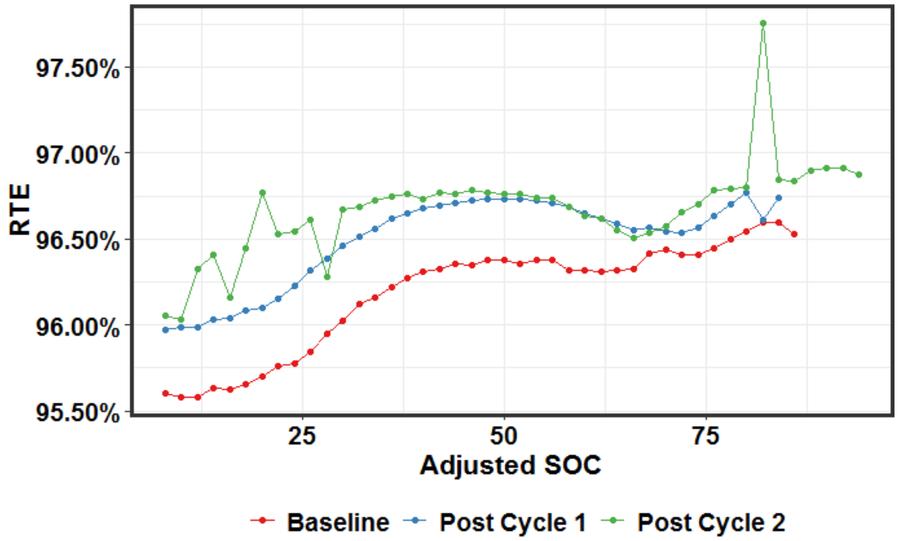

Figure 1.5. Battery DC RTE Calculated from Ratio of DC Charge Current to DC Discharge Current at a Fixed 2,000 kW DC Power.

1.2.6 PCS One-Way and Round-Trip Efficiency

The ratio of requested power to charge power is plotted as a function of SOC for C/6, C/4, and C/2 rates to determine one-way inverter efficiency as a function of SOC and rate. This was repeated for the ratio of discharge AC power at the PCS to DC power for C/6, C/4, and C/2 rates to get one-way inverter efficiency for the PCS during discharge. The results are shown in Figure 1.6 for charge and discharge respectively.

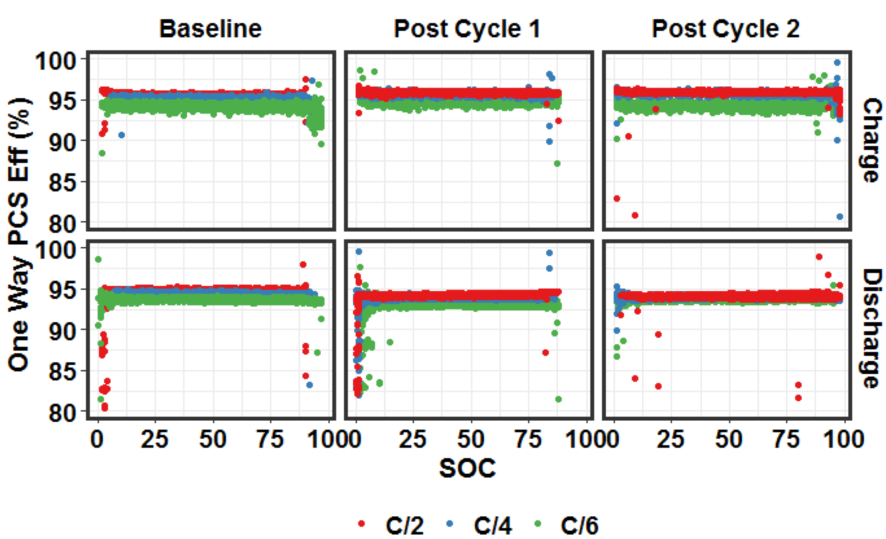

Figure 1.6. One-Way PCS Efficiency for RPT at Various Rates for Charge and Discharge

The results indicate that in this rate range, the one-way inverter efficiency was 93 to 96% for both charge and discharge, with lower efficiency at lower rates. Per the technical specifications provided by the manufacturer, the maximum PCS one way efficiency is 97.5 percent. The PCS conversion loss was determined by subtracting the AC power at the PCS from the DC power at the PCS. This loss was found to be parabolic with an R^2 of 0.95, with low efficiency at low power. These results are presented in Table 1.3, and visualized in Figure 1.7.

Table 1.3. PCS Conversion Loss Regression

Parameter	Coefficient	Standard. Error
Intercept (kW)	3.77E+01	3.00E-02
PCS Power (kW/kW)	8.54E-03	1.70E-05
PCS Power^2 (kW/kW^2)	1.60E-05	1.48E-08

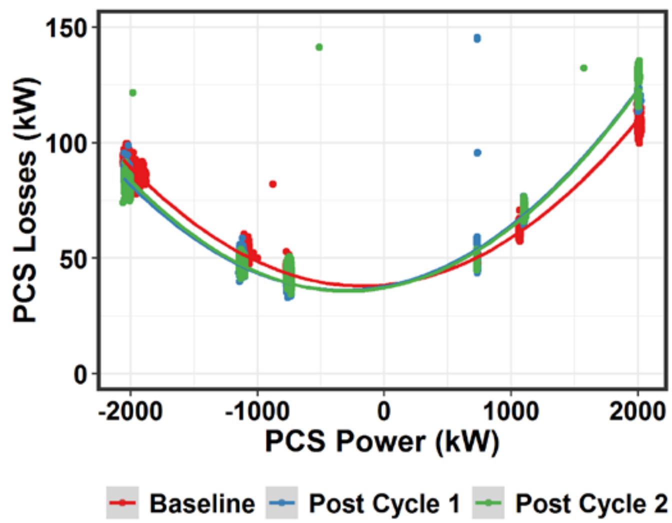

Figure 1.7. PCS Conversion Power Losses

The results are consistent with the Factory Acceptance Test (FAT) results at >200 kW per container (or >800 kW for the BESS) as shown below. At low power levels (40 kW for BESS), the PCS one-way efficiency for discharge was 73%. FAT tests are summarized in the Appendix.

- PCS Power/DC Power during discharge – 73% at 10 kW, 88% at 50 kW, 90% at 100 kW, >94% at ≥200 kW.
- DC Power/PCS Power during charge – 92% at 100 kW, 98% at 250 kW, 99% at 500 kW.

The ratios of charge to discharge power at PCS level, which is the inverter RTE, for C/6, C/4, and C/2 rates, also are plotted as a function of adjusted SOC.

1.2.7 One-Way Efficiency of 12 kVAC to 480 VAC Transformer

The efficiency of the 12 kilovolts (kV) AC to 480 VAC transformer was determined as follows: During charge, transformer efficiency = (PCS power + auxiliary)/ESS Ion meter power, where all power levels are expressed in absolute terms. During discharge, transformer efficiency equals PCS power/ESS ion meter power. The efficiency is >1 in the -1,500 kW < PCS Power < 1,800 kW range. Hence, reliable results for transformer efficiency could not be obtained for this project. Figure 1.8 shows the transformer efficiency in for regions where the efficiency is <1.

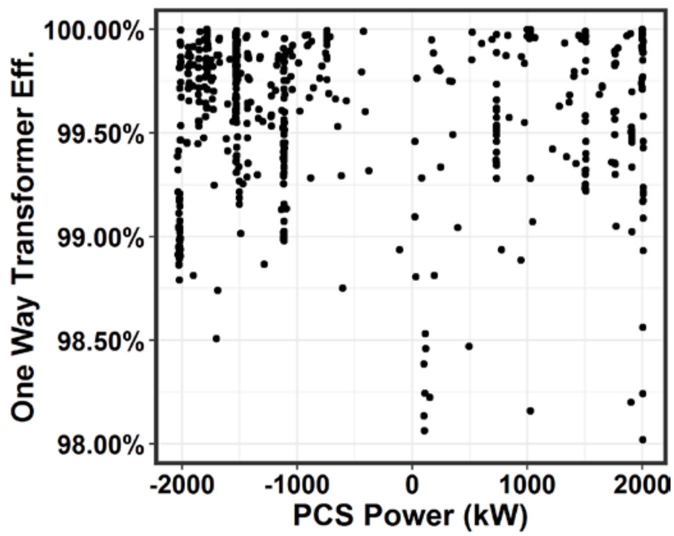

Figure 1.8. One-Way 480 VAC to 12 kVAC Transformer Efficiency

1.2.8 Thermal Management

Per the technical specifications, cooling is done by forced air. Subsequent correspondence with PSE engineers indicates there is a heat pump/air conditioning system that is used for heating or cooling as needed.

Thermal management is done using a set point of 22°C for four thermostats located inside each container as seen as per communication from PSE staff. Figure 1.9 shows the thermostats in one container, along with the heat pump/air conditioning unit located outside the container.

Figure 1.9. Thermostats inside the Container (left) Control Ductless Heat Pump/Air Conditioning Units (right)

Figure 1.10 plots the auxiliary load as a function of temperature for battery temperature, external temperature, container temperature, and weather temperature. The external temperature corresponds to PCS temperature. The weakest correlation was obtained for battery module temperature. The adjusted R^2 for PCS temperature was 5 to 10 times better as shown in Table 1.4. The adjusted R^2 with respect to container temperature and ambient temperature was about twice that of the PCS temperature. The slope for heating was 2.5 to 4 times that for cooling the BESS. Thermal management is done by a heat pump/air conditioning unit located outside each battery container based on deviation from 22°C of four thermostats located inside each container. Communication from PSE indicated the auxiliary power stays constant until the thermostat measurements fall within a deadband around 22°C. Our analysis indicates the auxiliary power is proportional to deviation from 24 to 26°C inside the container.

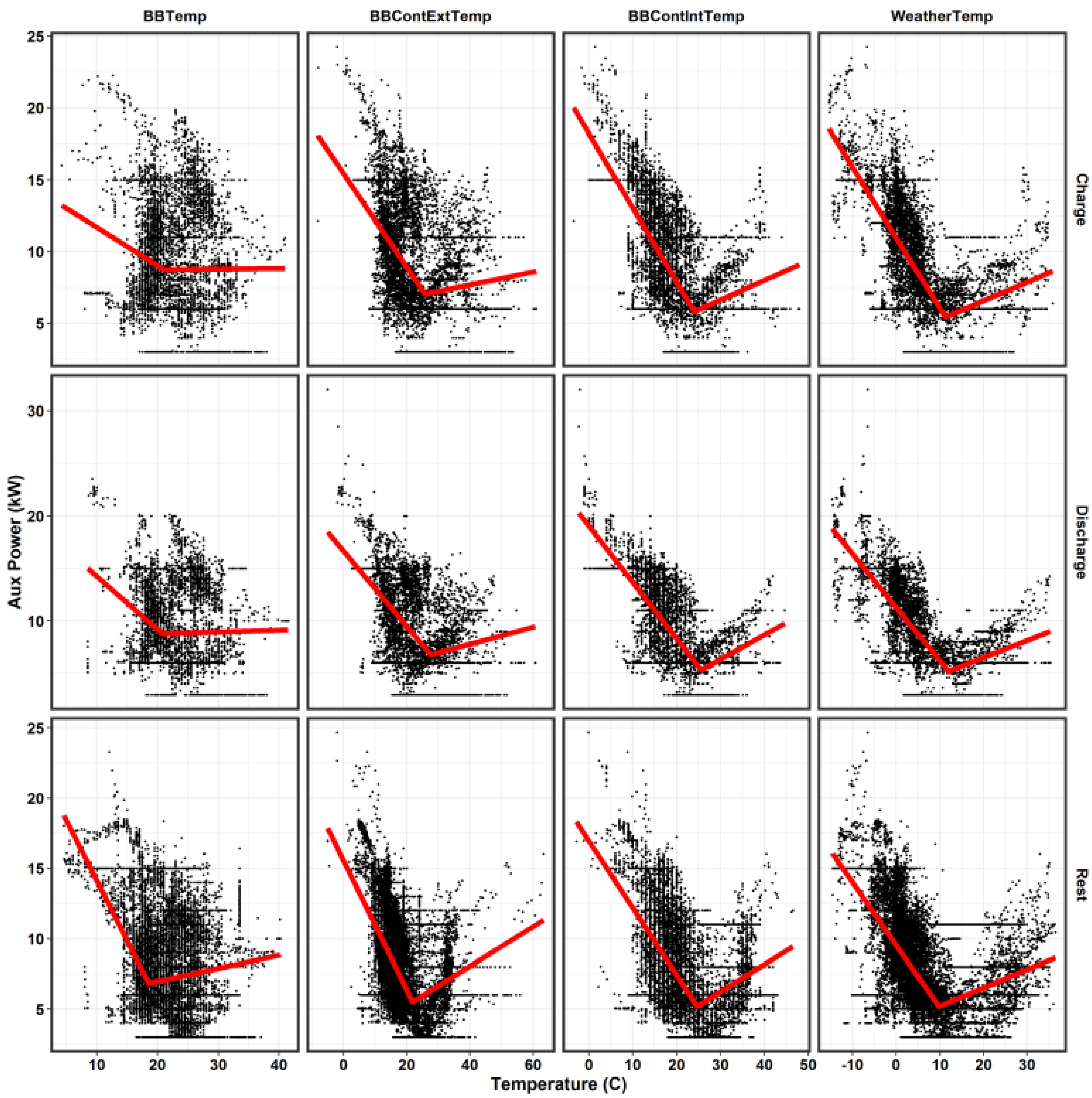

Figure 1.10. Auxiliary Power Consumption during Charge, Discharge and Rest as a Function of Deviation from Various Temperatures.

Table 1.4. Auxiliary Power Regression

Variable	State	Ad R Sq	SetPoint.Estimate	Heating Slope	Cooling Slope
BBContExtTemp	Charge	0.187	2.6E+01	-3.3E-01	4.5E-02
BBContExtTemp	Rest	0.266	2.2E+01	-4.6E-01	1.4E-01
BBContExtTemp	Discharge	0.259	2.8E+01	-3.6E-01	8.1E-02
BBContIntTemp	Charge	0.450	2.4E+01	-5.2E-01	1.4E-01
BBContIntTemp	Rest	0.287	2.5E+01	-4.8E-01	1.9E-01
BBContIntTemp	Discharge	0.522	2.6E+01	-5.4E-01	2.3E-01
BBTemp	Charge	0.015	2.1E+01	-2.7E-01	4.8E-03
BBTemp	Rest	0.124	1.9E+01	-8.5E-01	9.3E-02
BBTemp	Discharge	0.043	2.1E+01	-5.1E-01	1.7E-02
WeatherTemp	Charge	0.498	1.1E+01	-4.9E-01	1.3E-01
WeatherTemp	Rest	0.370	9.7E+00	-4.5E-01	1.3E-01
WeatherTemp	Discharge	0.559	1.2E+01	-5.1E-01	1.6E-01

1.2.9 SOC Drop during Rest

The technical specifications and the single-line drawings for the energy storage project are included in the Appendix. The single-line diagram does not provide details on how auxiliary load is powered during rest. The team found the BESS powers auxiliary loads during rest. During rest, the DC power is sometimes lower than auxiliary power, sometimes equal, and sometimes far greater than auxiliary power. Figure 1.11 shows results during rest after charge (left) and discharge (right) for PCS disabled (top) or PCS switching (bottom).

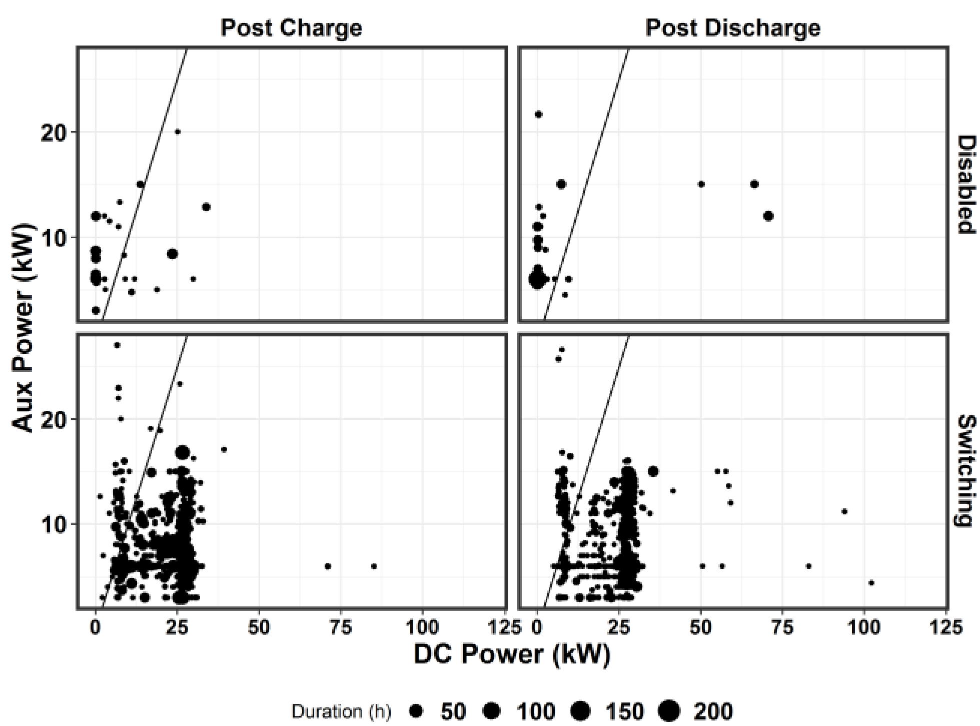

Figure 1.11. Auxiliary Power and DC Power during rest after Charge and Discharge for (top) PCS Disabled, (bottom) PCS Switching. Line for each graph denotes y = x line.

There are several runs where the discharge power is less than auxiliary consumption (as seen from the points to the left of the y = x line). These could correspond to auxiliary power (and/or PCS switching power) being partially provided by the grid. About 25% of the time during rest, the PCS is in a disabled state. With the PCS not switching, these are instances when the DC power is 0, indicating the auxiliary power is entirely powered by the grid. There are occasions when the DC power is >0, but less than auxiliary consumption, while on some occasions the DC power is much greater than auxiliary consumption. Hence it is not straightforward to predict the SOC drop during rest, even with PCS disabled.

When the PCS is disabled, during rest after discharge, the DC power is 0 or <5 kW for 55% of the time, just less than or greater than auxiliary load 14% of the time, and ≥50 kW for 21% of the time. For rest after charge, the DC power is 0 about 25%, nearly equal to the auxiliary load 55% of the time, and between 20 and 30 kW 18% of the time.

When the PCS is switching, the minimum DC power is 5 kW (not 0). A majority of data points correspond to DC power greater than the auxiliary load, with DC power around 25 kW for several runs. For some runs, the DC power was 70 to 80 kW after charge, and as high as 100 kW after discharge.

Interestingly, the maximum DC power was higher during rest after discharge for both PCS states, while for PCS in the disabled state, DC power was >0 on more occasions after charge.

About 75% of the time during rest, the PCS is in a switching state. During this time, the DC power for the most part is much greater than auxiliary consumption, with a majority of the points significantly to the right of the y = x line. This leads to a steeper drop in SOC.

To estimate the effect of PCS switching, the difference between average discharge power consumption during rest and auxiliary consumption during rest was determined as a function of PCS switching (left hand image in Figure 1.12). The average power during rest was calculated by dividing the discharge energy corresponding to the measured SOC drop during rest by the rest duration. Because the SOC meter resolution is only 1%, the regression was done by weighting the runs by their durations.

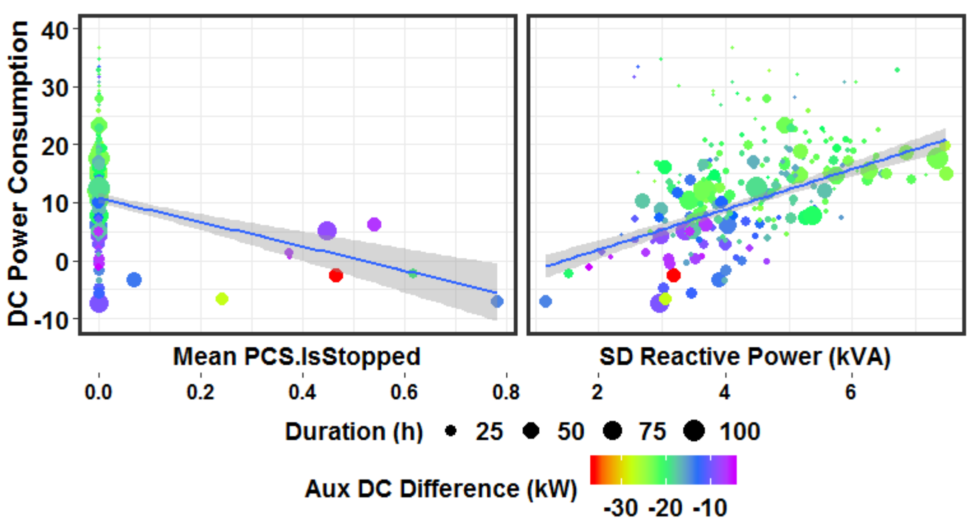

Figure 1.12. Effect of PCS State and Reactive Power on DC Power Consumption during Rest

The average power during switching was estimated to be 15 kW, based on the difference between the values for PCS switching and PCS disabled state. Because PCS switching consumes reactive power, the results are plotted vs. the standard deviation of the PCS reactive power during rest. As expected, the incremental DC power increased linearly with the standard deviation of reactive power. Table 1.5 provides regression results. Note that the mean of the absolute magnitude of reactive power was unchanged, thus indicating that it was the volatility in reactive power that determined DC power consumption, and not magnitude of reactive power.

Table 1.5. Regression for Average Discharge Power during Rest

Parameter	Coefficient	Standard Error	Pr(>|t|)
Intercept (kW)	-8.79	1.56	1E-07
Reactive SD (kW/kVA)	2.71	0.336	0E+00
Auxiliary DC Diff (kW/kW)	-0.383	0.076	1E-06

1.2.10 Site Control System

Control system integration of the PSE ESS is performed using the Modular Energy Storage Architecture (MESA) standard. At the planning stage, PSE explored different standards for software and control system integration of ESSs and experienced a lack of adequate open standards. Therefore, in collaboration with a number of partners, the MESA standard was used (MESA 2016). The MESA standard is open, non-proprietary, and helps accelerate interoperability, scalability, safety, quality, and affordability in energy storage components and systems. Both BESS units at SnoPUD MESA-1 are built on this standard. There are two major components of the MESA standard as shown in Figure 1.13. One is the MESA-Device that addresses how energy storage components within an ESS communicate with each other and other operational components, and is built on the Modbus protocol. The other component is the MESA-ESS that addresses ESS configuration management, ESS operational states and the applicable ESS functions from the Institute of Electrical and Electronics Engineers 1815 Distributed Network Protocol (DNP3) profile for advanced distributed energy resource functions.

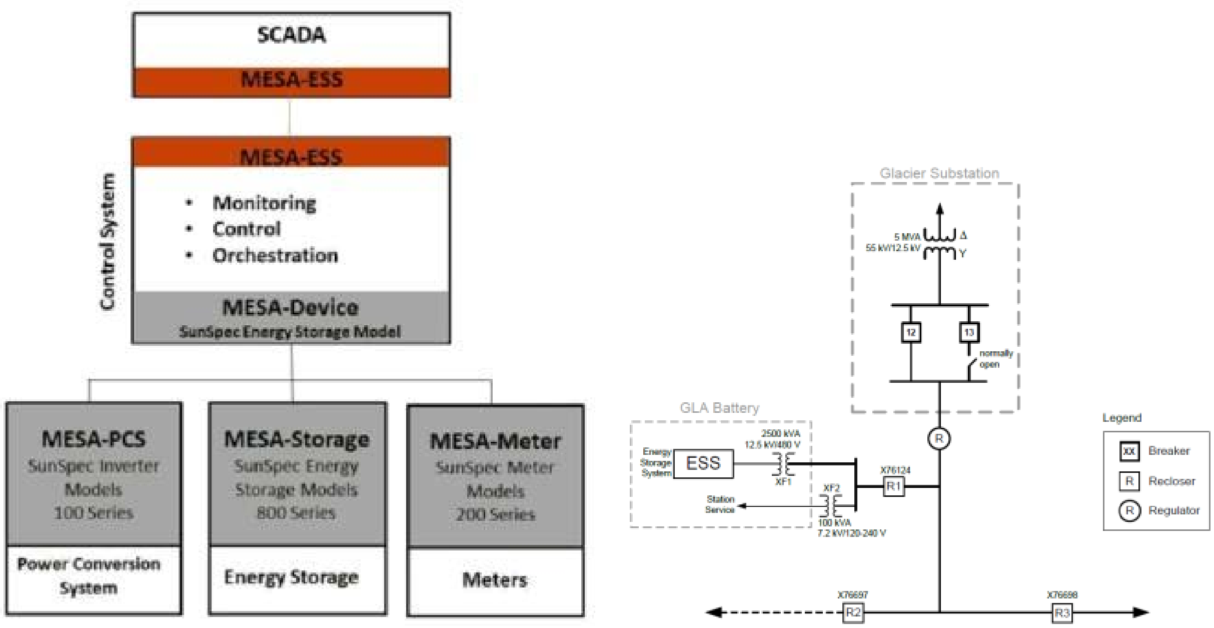

Figure 1.13. MESA Standard Architecture (left) and Electrical Schematic (right)

Control is accomplished by the 1Energy-Intelligent Controller, which has now been acquired by Doosan GridTech and renamed the DG-IC (Doosan 2016a). This control and communication platform for the ESS includes built-in operating modes that can be configured and fine-tuned to reach maximum economic benefits for changing grid and market conditions. Capabilities of DG-IC can also be extended by creating new operating modes through an Application Programming Interface. Built-in operating modes of DG-IC include Market-Based Charge/Discharge, Frequency Correction, Forecast Assurance, Power Following, Peak Power Limiting, Power Factor Correction, Volt/VAr, Volt/Watt, Power Smoothing, Islanding, SOC Maintenance. Supervisory control, including optimal control for different use cases for PSE ESS is performed by manual entry of duty cycles provided by PNNL. Data tags for the energy storage were set based on the SunSpec Alliance Interoperability Specification (SunSpec 2017).

2.0 Battery Performance Test Results

During the first phase of tests, the BESS was subjected to baseline testing as described in the Office of Electricity Delivery and Energy Reliability (DOE-OE) Performance Protocol (Viswanathan 2014), with discharge at various C rates for a constant C rate charge. Response time and ramp rate were measured at various SOCs, along with charge and discharge resistance. The results of these tests are presented in this section of the report. The battery still seemed to discharge to power the auxiliary while at rest, despite the PCS meter not registering any power flow. Hence, the battery was hypothesized to be set up as shown in Figure 2.1.

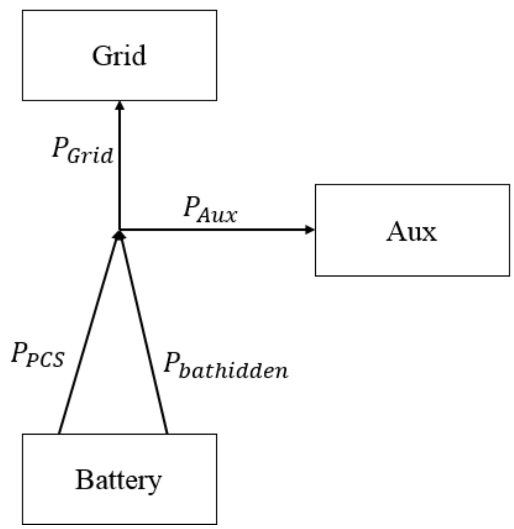

Figure 2.1. Hypothesized Power Diagram

In this setup, the hidden power is hypothesized to be:

$$P_{batthidden} = P_{aux}(P_{Req} > 0)$$

This leads to the following definitions:

$$P_{batt} = P_{PCS} + P_{aux}(P_{Req} > 0)$$

$$P_{grid} = P_{batt} - P_{aux}$$

$$E_{Chg} = \int (P_{grid} < 0)P_{grid}dt$$

$$E_{Dis} = \int (P_{grid} > 0)P_{grid}dt$$

$$E_{Chgnorest} = \int (P_{req} < 0)P_{grid}dt + E_{SOCdroprest}$$

$$E_{Disnorest} = \int (P_{req} > 0)P_{grid}dt$$

$$E_{Chgnoaux} = \int (P_{req} < 0)P_{batt}dt + E_{SOCdroprest}$$

$$E_{Disnoaux} = \int (P_{req} > 0)P_{batt}dt$$

$$E_{SOCdroprest} = E_{Disnoaux100} \int (P_{req} = 0) \frac{dSOC}{dt} dt$$

$$RTE = -\frac{E_{Dis}}{E_{Chg}}$$

$$RTE_{norest} = -\frac{E_{Disnorest}}{E_{Chgnorest}}$$

$$RTE_{noaux} = -\frac{E_{Disnoaux}}{E_{Chgnoaux}}$$

2.1 Baseline Test Results

Note that for baseline analysis, SOC limits were different for each capacity. For comparison, SOCs were held in the 10 to 82% range. Because only data in that range were analyzed, we made the following changes in definitions for baseline capacity test only:

$$E_{Chg} = \int (P_{grid} < 0) P_{grid} dt - E_{SOCdroprest}$$

$$E_{Chgnorest} = \int (P_{req} < 0) P_{grid} dt$$

$$E_{Chgnoaux} = \int (P_{req} < 0) P_{batt} dt$$

$$E_{SOCdroprest} = \frac{1}{RTE_{noaux}} \int (P_{req} = 0) P_{aux} dt$$

The change in how the energy associated with SOC drop is calculated is due to the SOC meter only having a resolution of 1%, which doesn't capture how the SOC changes in the small 0.5h rest periods.

The energy capacity stability of the ESS shall be reported as a percent of initial performance as determined in accordance with Section 8.4.5 of the *Washington Clean Energy Fund: Energy Storage System Performance Test Plans and Data Requirements* (Viswanathan et al. 2017), along with the date of the test upon which the reported value is based and the ambient temperature and barometric pressure encountered during the test.

Baseline capacity tests were done for multiple power levels—C/2, C/4, and C/6—where the C rate corresponds to 2,000 kWh/1h = 2,000 kW. The limitations for testing were that the battery SOC could not be controlled. Figure 2.2 shows the Ah as a function of SOC for the RPTs. The cumulative Ah discharged is linear down to 10% SOC. When the SOC nears 0%, the Ah discharged increases without a significant change in SOC, as denoted by the vertical line at low SOC. This appears to be due to the fact that the reported SOC fluctuates when there is a change in power, thus indicating that the SOC is simply a proxy for operating voltage. At the high end, while the target was 90%, there were some runs where string imbalance led to a maximum SOC of only 82%. Hence the analysis was completed for an SOC range of 10 to 82% SOC. Results for the actual SOC range for each test are presented in Appendix A.

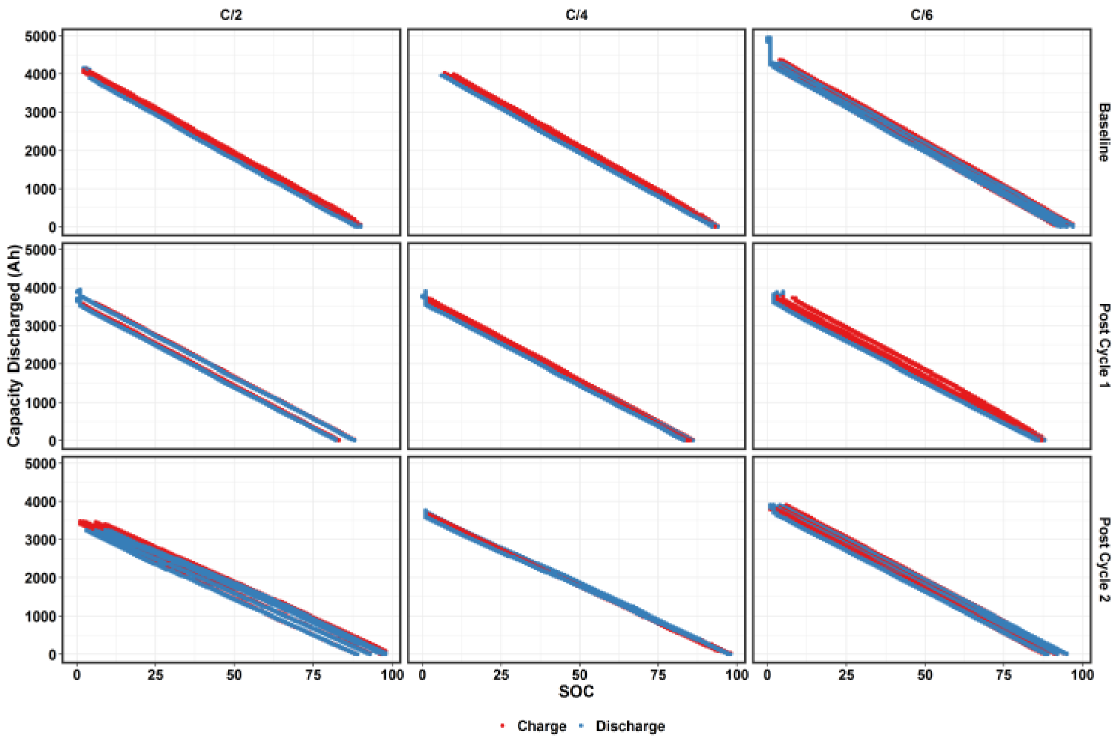

Figure 2.2. Capacity Discharged for Baseline Capacity Tests

Figure 2.3 shows the power and SOC profile during the reference performance energy capacity tests. The results for the capacity tests are shown in Table 2.1 and in Figure 2.4.

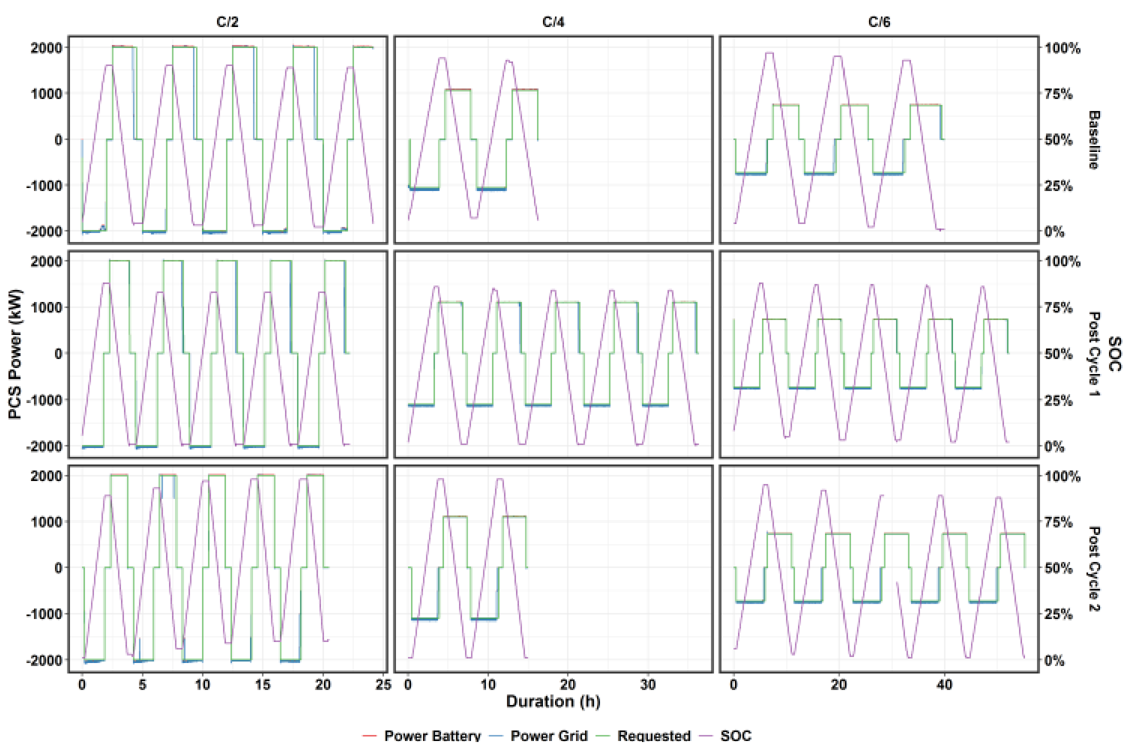

Figure 2.3. Power and SOC Profiles for BESS at C/2, C/4, and C/6 rates for Reference Performance Capacity Baseline, Post Cycle 1 and Post Cycle 2 Tests

Table 2.1. Baseline Capacity Test Results

Scenario	Baseline	Baseline	Baseline	Post Cycle 1	Post Cycle 1	Post Cycle 1	Post Cycle 2	Post Cycle 2	Post Cycle 2
Date	Jan 7, 2017	Feb 14, 2017	Mar 17, 2017	Oct 2, 2017	Sep 28, 2017	Sep 25, 2017	Jun 11, 2018	Jun 7, 2018	Mar 23, 2018
C Rate	C/2	C/4	C/6	C/2	C/4	C/6	C/2	C/4	C/6
Duration (h)	24	16	40	22	36	52	21	15	55
Average Charge Power (kW)	2027	1093	750	2023	1116	743	2027	1127	748
Average Discharge Power (kW)	1994	1052	725	1998	1098	730	1991	1092	721
SOC Range	10-82	10-82	10-82	10-82	10-82	10-82	10-82	10-82	10-82
Cycles	5	2	3	5	5	5	5	2	4
Charge Energy (kWh)	3335	3390	3407	3123	3153	3215	2702	2749	3225
Discharge Energy (kWh)	2872	2886	2869	2694	2706	2675	2285	2336	2674
RTE	86.1	85.1	84.2	86.3	85.8	83.2	84.6	85.0	82.9
Charge Energy No Rest (kWh)	3324	3377	3396	3120	3149	3212	2693	2739	3216
Discharge Energy No Rest (kWh)	2872	2886	2869	2694	2706	2675	2285	2336	2674
Discharge Energy No Rest per SOC (kWh)	3990	4008	3985	3742	3758	3715	3173	3244	3714
RTE No Rest	86.4	85.5	84.5	86.3	85.9	83.3	84.8	85.3	83.1
Charge Energy No Auxiliary (kWh)	3304	3336	3360	3116	3141	3199	2681	2717	3177
Discharge Energy No Auxiliary (kWh)	2890	2922	2902	2698	2713	2686	2295	2355	2707
Discharge Energy No Auxiliary per SOC (kWh)	4013	4058	4030	3748	3768	3730	3187	3271	3759
RTE No Auxiliary	87.5	87.6	86.4	86.6	86.4	84.0	85.6	86.7	85.2
Discharge (Ah)	3351	3360	3356	3151	3157	3148	2673	2718	3119
Charge (Ah)	3363	3389	3383	3184	3220	3251	2740	2777	3203
Couloumbic Efficiency	99.6	99.1	99.2	99.0	98.1	96.8	97.6	97.9	97.4
Mean Charge Temperature (ºC)	30	27	22	33	33	27	33	31	26
Mean Discharge Temperature (ºC)	33	28	22	33	33	28	35	31	26
Mean Temperature (ºC)	31	27	23	32	33	28	34	31	26
Mean Ambient Temperature (ºC)	-12	1	3	9	13	14	11	13	3

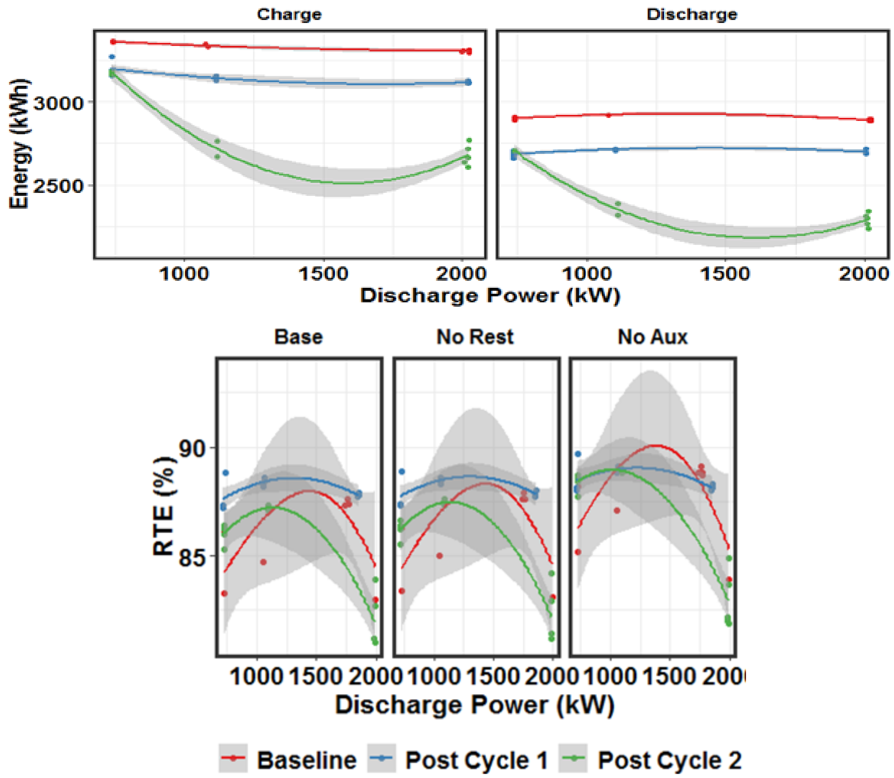

Figure 2.4. Reference Performance Test for Energy Capacity – Charge, Discharge Energy and RTE at Various Power Levels.

The RTE was calculated for energy flow in and out of the grid including and excluding rest periods, and energy flow at the PCS level, excluding auxiliary losses. As expected, the RTE increases in the following order: RTE, RTE without rest, RTE without auxiliary. RTE at the grid including rest is lower than the RTE at the grid excluding rest, which is lower than the RTE at the PCS excluding auxiliary losses. Energy capacity tests were done at C/6, C/4, and C/2 rates. The RTE increased with the C rate and was highest at 86% for baseline and Post Cycle 1. The corresponding RTE without auxiliary consumption was 87 to 87.5% at the C/2 rate. The seasonal effect was evident at the C/6 rate where the RTE without auxiliary for baseline capacity test performed in January was 2% points higher compared to RTE with auxiliary, while for Post Cycle 1, performed at the end of September, the increase in RTE without auxiliary was only 0.5% higher. The small rest duration of 0.5 hours resulted in the difference in RTE with and without rest being <0.2%. For perspective, the RTE when just considering PCS losses is 90 percent for the C/6 and C/4 rates and 93 percent for the C/2 rate.

The RTE peaked at the C/4 rate for the baseline and Post Cycle 2 tests, and increased with the C rate for the Post Cycle 1 test, which indicates the C/4-C/2 rate is the sweet spot that balances electrochemical losses vs. losses due to auxiliary load. When the auxiliary load is excluded, RTE again peaks in the C/4-C/2 range, but the difference in RTE for each scenario and across all scenarios is small for various C rates. The fact that the RTE for the baseline was lower than the RTE for the Post Cycle 1 and Post Cycle 2 tests for all rates, while discharge energy was highest, appears to indicate that there may be a symmetric expansion of the SOC range when going from the baseline to the Post Cycle 1 and Post Cycle 2 tests. Hence, what was 12 to 80% SOC may be represented at the 10 to 82% SOC range for the Post Cycle 1 and Post Cycle 2 tests. This has the effect of reducing the charge and discharge energy across this SOC range while increasing the RTE due to the SOC range extremes being further away from 0 and 100% SOC.

The BESS was discharged between 82% and 10% SOC, which corresponds to 72% DOD. The estimated discharge energy at 100% DOD was calculated by dividing the measured energy by the DOD at 72%. Including auxiliary losses, a maximum of 3,965 kWh was delivered at the C/2 rate for the Baseline Capacity Test. Excluding auxiliary consumption, the energy delivered was maximum at 4010 kWh at the C/4 rate. The estimated maximum energy content was 3,750 kWh for the Post Cycle 1 capacity test at the C/4 rate, while the maximum energy content without auxiliary load consumption was highest for the C/4 rate at 3,760 kWh. For the Post Cycle 2 test, as stated earlier, the battery performance decreased after the C/6 rate test due to a time gap of nearly 3 months after the C/6 capacity test. The C/6 rate discharge energy content at 100% DOD was 3,685 kWh, while the energy content was 3,715 kWh excluding auxiliary consumption.

Figure 2.4 shows the charge and discharge energy as a function of power for the RPTs in the 10 to 82% SOC range. The lower charge energy with increasing rate may be due to better performance at high rates related to higher temperature and/or to the error in SOC reporting, with overestimation during charge and underestimation during discharge as will be discussed later. The charge energy also decreased by 6% from the Baseline to Post Cycle 1. The discharge energy remained nearly constant with changing C rates, with a 6% drop in energy from the Baseline to Post Cycle 1. For Post Cycle 2, due to a large gap between the C/6 and C/4-C/2 tests, the steep drop in charge and discharge energy at the C/4-C/2 rates can be assigned to BESS balancing and maintenance that have not been documented adequately. The RTE increases slightly with increasing rate, possibly due to higher performance at higher rates.

Appendix A provides the results corresponding to Table 2.1, but for the actual SOC range for each test.

The DC Ah discharged and charged per unit change in SOC was calculated for the Baseline, Post Cycle 1, and Post Cycle 2 scenarios for testing done in the 10 to 82% SOC range. The Ah capacity decreased from 4,500 to 4,200 Ah at the C/6 rate for the Baseline to Post Cycle 2 tests, respectively, with the capacity for the Post Cycle 2 test being 4,300 Ah. The rate of decrease was similar for the C/4 and C/2 rates through Post Cycle 1. However, the Ah capacity and energy capacity of the BESS decreased at the C/4 and C/2 rates for the BESS during Post Cycle 2 testing, possibly because there was a 2 month gap after C/6 rate testing, during which undocumented maintenance was carried out on the BESS.

To determine the effect of SOC on the calculated Ah/SOC, the calculations were done for 20 to 80% SOC in 10% SOC increments. As seen in Figure 2.5, the Ah capacity per 100% change in SOC decreased linearly from 4,600 Ah to 4,000 Ah for the Baseline through Post Cycle 2 tests, respectively. At 20% SOC, the rate of decrease was lower, decreasing from 4,600 Ah to 4,200 Ah. The results appear to indicate that there may be a slight capacity loss for this BESS as testing progresses. This is further reinforced by the decreasing coulombic capacity for the BESS registered from the Baseline to Post Cycle 2 tests. It would be instructive to do a differential capacity analysis to verify this from the movement of peaks. This can be done by using a same starting point of 82% SOC, and plot dV/dQ as a function of Ah discharged. The movement of peaks would help us understand the capacity loss.

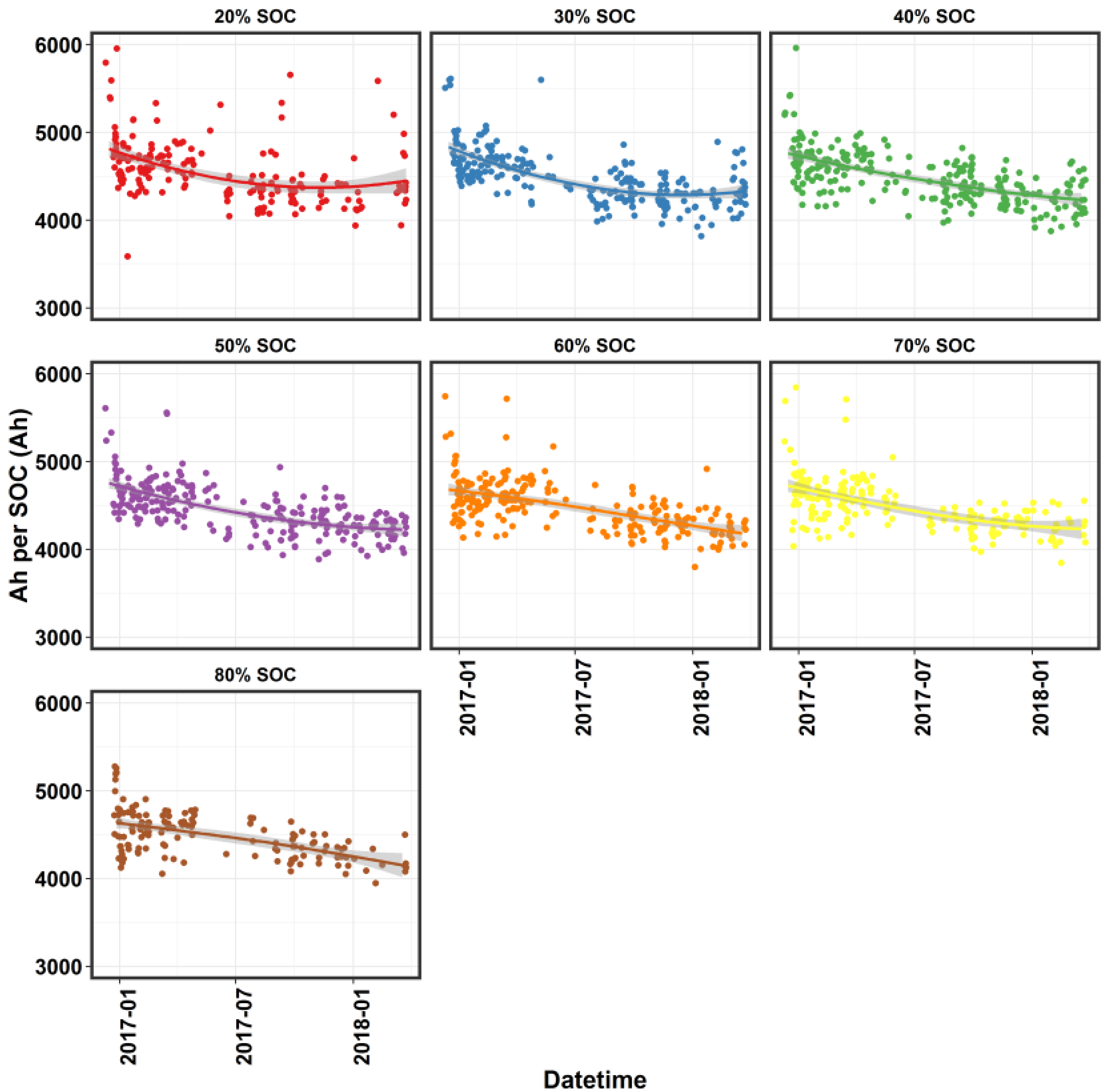

Figure 2.5. In Situ Capacity per 100% SOC at Each SOC

Figure 2.6 shows temperature profiles for the battery modules (maximum, minimum), internal container temperature, and the ambient temperature obtained from the weather report. The following points stand out:

- The container temperature was higher than the outside ambient temperature from the weather forecast. For the most part, the container temperature fell between the minimum and maximum module temperatures.
- Thermal management worked well for the C/6 to C/4 rates, with the maximum module temperature remaining below 35 to 40°C. At the C/2 rate, the temperature reached 45ºC during Baseline testing in January 2017, and 48ºC for Post Cycle 2 testing in June 2018.

- At the C/2 rate, the Baseline test done in January had the highest rate of change of module temperature, with the lowest initial container temperature. This is probably related to a greater I^2R related heating effect at the lower starting module temperature. The container temperature is in the 18 to 27°C, while for Post Cycle 1 tests, container temperature reaches 38°C, and for Post Cycle 2, container temperature reaches a high of 44°C. This shows that the thermal management system is not able to control the container temperature within a narrow band around of the thermostat set point. Regardless of the container temperature, the maximum module temperature does not exceed 48°C at C/2, thus indicating the BMS appears to be effective in maintaining the module temperature within design-specific levels.

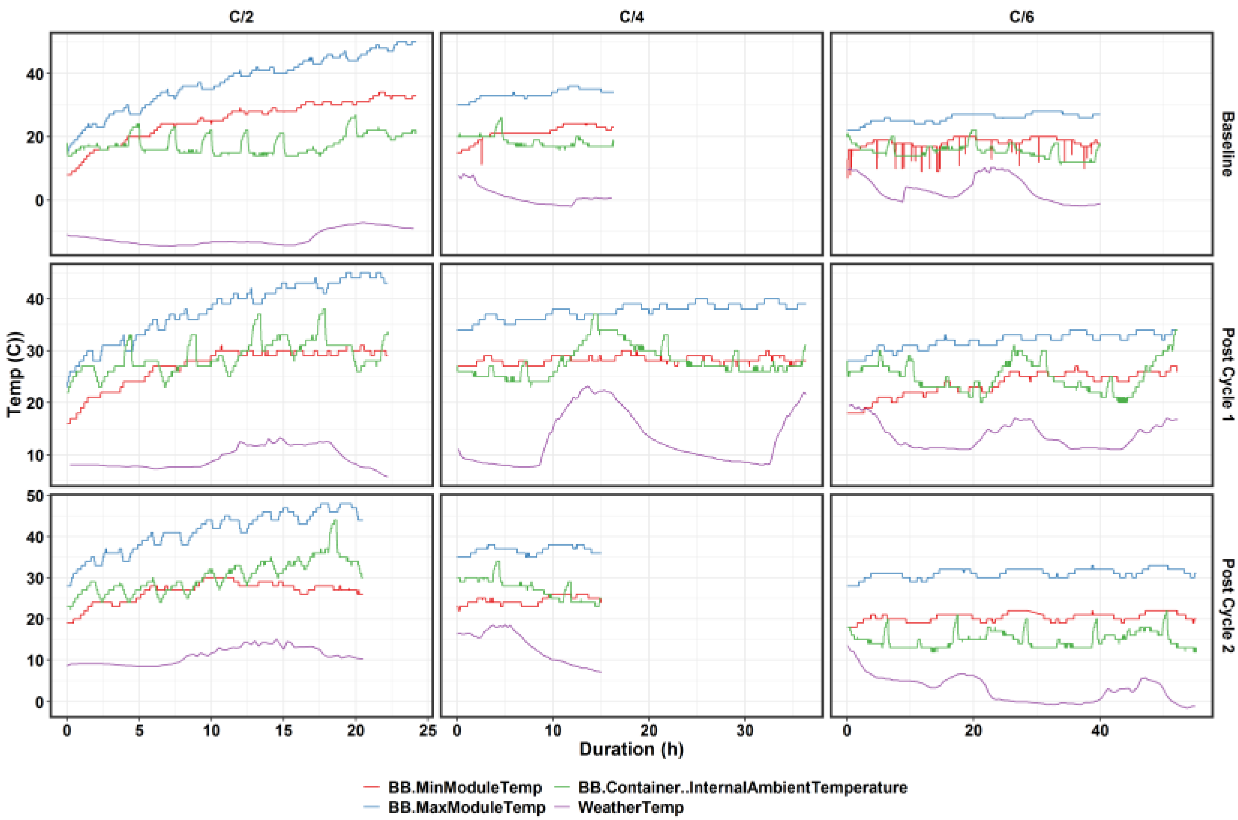

Figure 2.6. Battery Module Minimum and Maximum, Container and Weather Temperature for Reference

2.2 Response Time/Ramp Rate Test

The response time of the BESS hardware was instantaneous to 4 seconds, corresponding to ramp rates of 25% of rated power per second at the low end to instantaneous response. Because the resolution of the meter is 2 seconds, any response between 0 to 2 seconds registers as 2 seconds. There was a communication lag of 4 to 6 seconds, indicating the responsiveness of the BESS is limited by this communication lag. Because of the unique nature of this installation, with communication occurring via telephone lines, this lag is not expected to be present with high-speed communication. However, for installations that do not have infrastructure for high-speed communication, this limitation should be kept in mind.

The internal resistance of a battery can be measured by various methods. One way is to pulse the battery at high rate and measure the change in voltage ΔV after a fixed duration. Depending on the duration, the ΔV would be different, resulting in different reported internal resistances. At high durations, the ΔSOC would be high, resulting in a high reported internal resistance, part of which is due to the change in SOC. As shown in Figure 2.7 (Schweiger et al. 2010), as the ΔSOC increases, the measured internal resistance increases linearly.

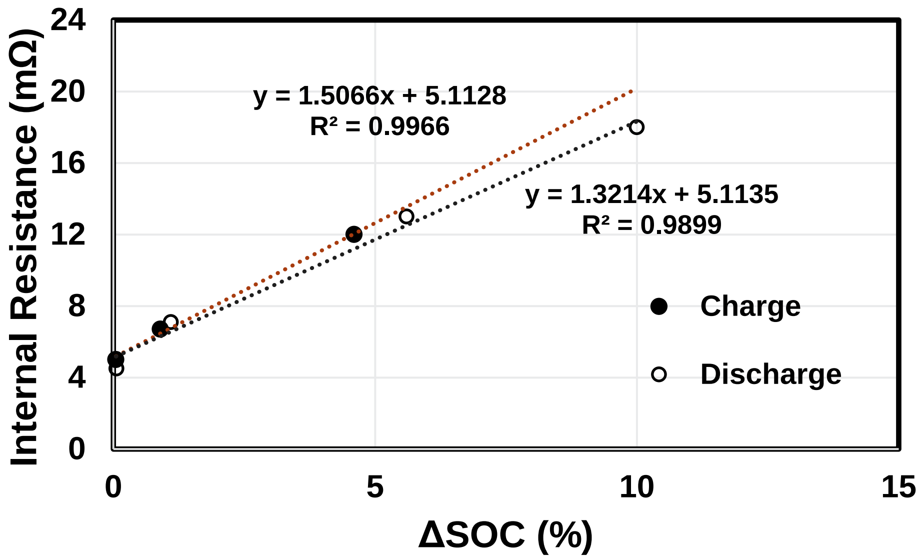

Figure 2.7. Internal Resistance of a 1.8 Ah Li-Ion Cell as a Function of Change in SOC during Charge or Discharge Pulse (Schweiger et al. 2010)

The internal resistance was reported in accordance with the provisions in Section 7.2 of the test plan report (Balducci 2017). This test is done as part of Baseline testing, and as RPTs after use case testing. Results are shown in Figure 2.8 and Table 2.2 and Table 2.3 for 10-second 1C rate pulses, which correspond to a 0.13% ΔSOC respectively, which is sufficiently low not to affect the results. The system charge and discharge internal resistance was in the 2 to 4 milliohm range, with resistance decreasing slightly with increasing SOC. The resistance decreased by 33% from Baseline tests to Post Cycle 1 tests possibly due to a conditioning effect, and remained unchanged for Post Cycle. This may be a sign of the beginning of degradation of state of health (SOH). The measured resistance on an Ah-normalized basis was 34 to 69 mΩ-Ah. As a reference point, the Ah-normalized resistance of a high-power A123 26650 cell with the same cathode chemistry is 16 mΩ-Ah.

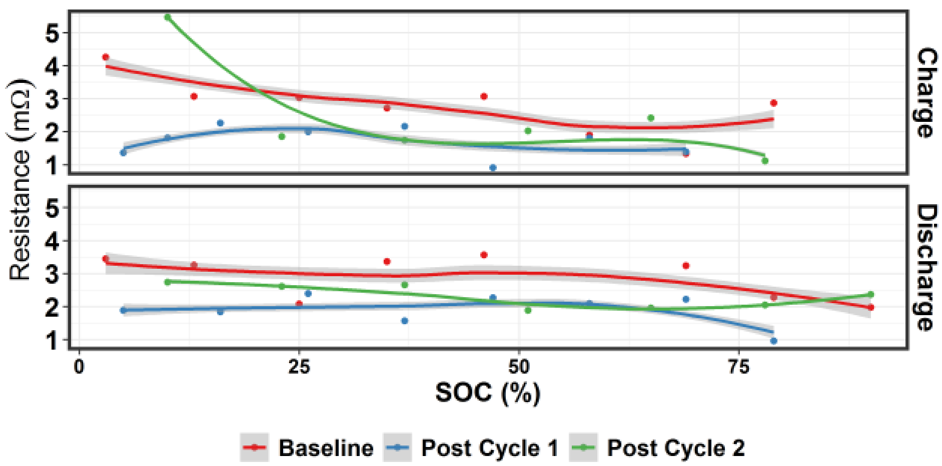

Figure 2.8. Pulse Test Resistance

Table 2.2. Response Time for Pulse Test

SOC	Baseline Charge	Baseline Discharge	Post Cycle 1 Charge	Post Cycle 1 Discharge	Post Cycle 2 Charge	Post Cycle 2 Discharge
0	4	2	4	2	NA	NA
10	4	0	2	NA	NA	4
20	2	2	4	4	2	4
30	NA	NA	2	4	NA	NA
40	2	4	2	2	2	4
50	4	2	2	2	2	2
60	2	0	4	4	2	2
70	0	4	2	2	NA	NA
80	4[(a)]	2	NA	2	2	2
90	NA	4	NA	NA	NA	NA

(a) Only reached 1,500 kW after 4 seconds.

Table 2.3. Ramp Rate (kW/s) for Pulse Test

SOC	Baseline Charge	Baseline Discharge	Post Cycle 1 Charge	Post Cycle 1 Discharge	Post Cycle 2 Charge	Post Cycle 2 Discharge
0	500	1000	500	1000	NA	NA
10	500	>1000	1000	NA	NA	500
20	1000	1000	500	500	1000	500
30	NA	NA	1000	500	NA	NA
40	1000	500	1000	1000	1000	500
50	500	1000	1000	1000	1000	1000
60	1000	>1000	500	500	1000	1000
70	>1000	500	1000	1000	NA	NA
80	375[(a)]	1000	NA	1000	1000	1000
90	NA	500	NA	NA	NA	NA

(a) Only reached 1,500 kW after 4 seconds.

Figure 2.9 shows the in situ resistance for the BESS, calculated for a change in current corresponding to when power levels changed by more than C/8. The results are in line with the pulse test results shown in Figure 2.8.

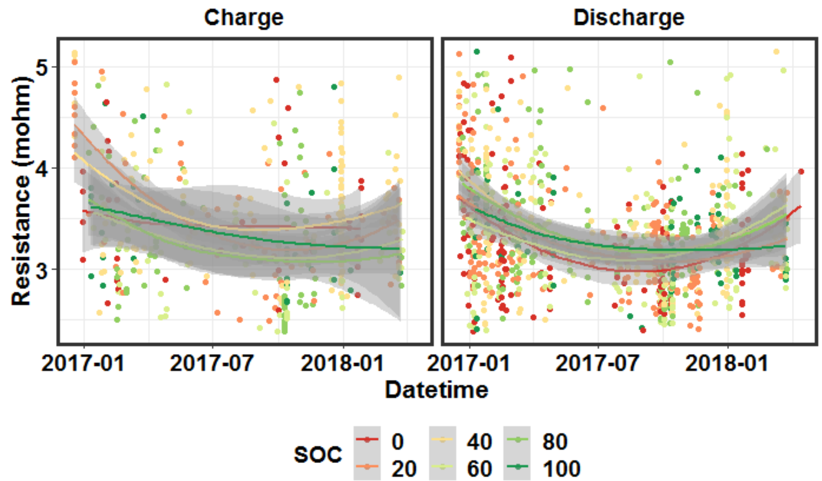

Figure 2.9. In Situ Resistance

2.3 Frequency Regulation Test

The BESS was subjected to the DOE-OE Frequency Regulation Signal as part of the RPT. The average discharge power was ~600 kW, while the average charge power was ~635 kW. While the starting SOC was 50% for Baseline and Post Cycle 1 tests, the starting SOC was increased to 70% for Post Cycle 2 tests to account for SOC drift.

The RPT results gave RTEs in the 80 to 82% range, with the RTE increasing to 83 to 85% when auxiliary consumption was excluded. Signal tracking was excellent within 2% of the power, while tracking was poor within 2% of the signal value. This is because at these low power levels, the meter may not be sufficiently accurate. The results of these tests are shown in Figure 2.10 and Table 2.4.

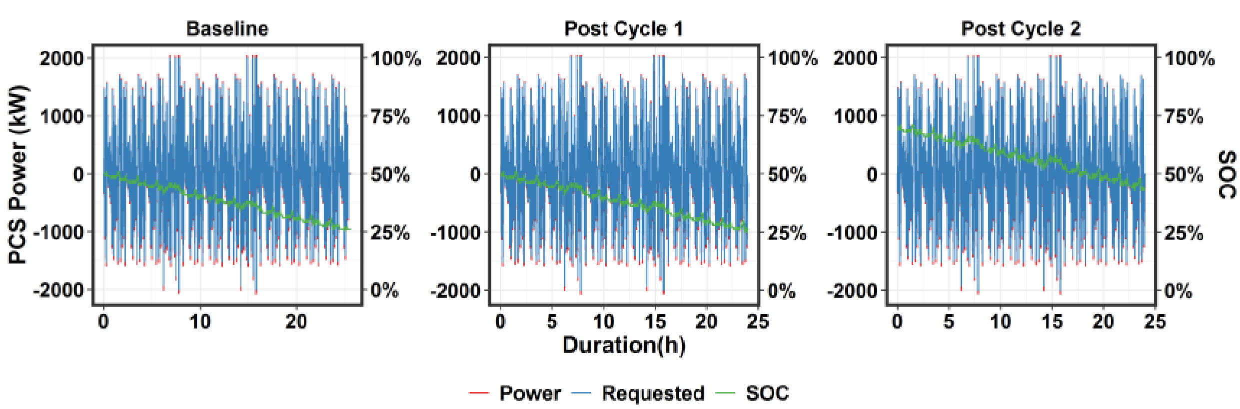

Figure 2.10. Frequency Regulation DOE Protocol Tests

Table 2.4. Frequency Regulation Test Results

Scenario	Baseline	Post Cycle 1	Post Cycle 2
Date	Jan 27, 2017	Oct 6, 2017	Jun 15, 2018
Duration (h)	26	24	24
Start SOC (%)	50	50	70
End SOC (%)	26.0	26.4	44.0
Average Charge Power (kW)	641	631	635
Average Discharge Power (kW)	593	599	597
RTE (%)	81	82	80
RTE No Auxiliary (%)	85.2	83.2	82.8
Normalized Root Mean Square Error (RMSE)	0.022	0.019	0.020
Normalized RMSE No Auxiliary	0.019	0.018	0.018
Tracking 2%	0.96	0.97	0.97
Tracking 2% No Auxiliary	0.91	0.96	0.95
Signal Tracking 2%	0.41	0.44	0.44
Signal Tracking 2% No Auxiliary	0.28	0.43	0.40
Signal Tracking 2% Deadband Removed	0.39	0.43	0.43
Signal Tracking 2% No Auxiliary Deadband Removed	0.27	0.42	0.39

The remainder of this section is dedicated to presenting the results of the use case-based tests.

2.4 Use Case 1: Energy Arbitrage

2.4.1 Duty Cycle Summary

The energy arbitrage duty cycle was modeled using PNNL’s Battery Storage Evaluation Tool (BSET) by maximizing ESS revenue for a 1-week period using historic Mid-Columbia (Mid-C) wholesale energy price data.

2.4.2 Test Results

The arbitrage use case resulted in an RTE of 61 to 78%, depending on power and whether rest and auxiliary loads were included. Average discharge power ranged from 930 kW to 1,470 kW, while average charge power ranged from 850 to 1,555 kW.

The rest times for arbitrage were 65 to 90% of total test duration, with an average of 81% for all four runs. At 89% rest time, the RTE for the Post Cycle 1 test at ~1,400 kW was lowest at 62%, with a steep increase to 85% when rest was excluded. While higher power is conducive to increasing RTE, at ~900 kW power, the RTE still was quite high at 76% for the Post Cycle 1 test, thanks to lower rest duration of 62%.

This supports the conclusion that there is no single RTE that represents BESS performance. Assuming an artificially high RTE makes the BESS more attractive than it actually is, especially for use cases such as arbitrage whose benefits are directly tied to the BESS RTE, in addition to the high/low price differential.

Our model shows that at 81% rest time, increasing average charge and discharge rate from C/6 to C/2.2 leads to decrease in rest related RTE losses from 21% to 7%. At C/6, reducing rest time from 90% to 10% reduces RTE-related losses from 23.4% to 2.6%. Hence, if arbitrage is the only use case being considered, it may be useful to have the BESS in a disconnected state to avoid loss of energy during rest. More importantly, this shows the importance of keeping the BESS under operation because keeping it under rest simply drains energy from it. Energy arbitrage test results are presented in Figure 2.11 and Table 2.5. The RTE without auxiliary losses increases with average power in the 800 to 1,500 kW range for this use case. This result is in line with the increase in PCS one way efficiency from 95.0 to 96.3 percent in this power range.

The discharge Ah was 5 to 10 percent higher than charge Ah for all runs, adjusted for end SOC being brought to start SOC. This is not feasible and could have been caused by at least three issues:

- Measurement error
- Holes in data collected
- The Ah exchanged during maintenance of strings that are out of balance was not recorded.

Since about 50 percent of runs did have charge Ah equal to or 1-4 percent greater than discharge Ah, measurement error does not seem plausible. The runs analyzed for which the anomaly existed did not have data holes. Hence, it appears that the Ah exchanged during balancing may not have been captured.

This anomaly does not affect the results of this work. The various metrics reports, such as RTE, response time, and ramp rate are not affected. The scope of this Ah analysis was to determine the degradation mechanism of the Li-ion BESS. While the Ah numbers cannot be used for this analysis, signature curves during discharge can be used to further analyze the degradation mechanism of this BESS.

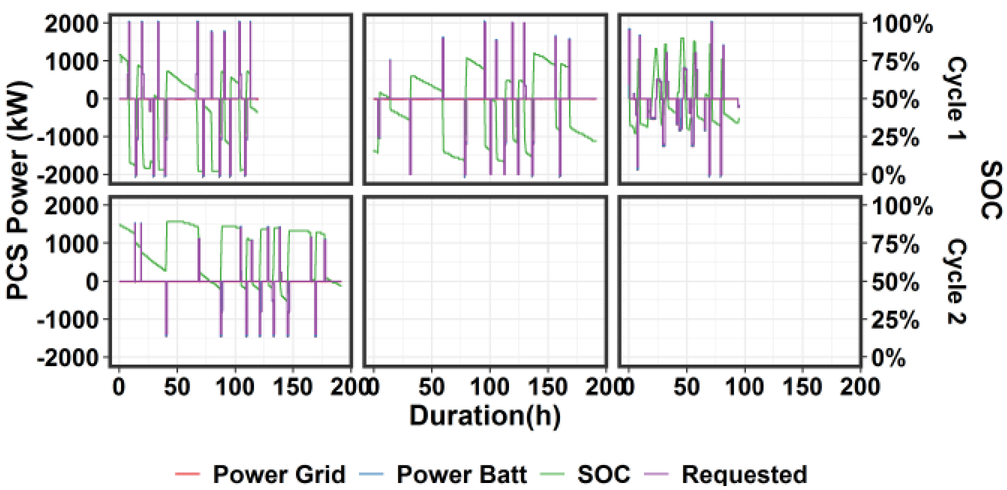

Figure 2.11. Energy Arbitrage Test

Table 2.5. Energy Arbitrage Test Results

Scenario	Cycle 1	Cycle 1	Cycle 1	Cycle 2
Date	Feb 16, 2017	Feb 24, 2017	Mar 11, 2017	Oct 26, 2017
Duration (h)	120	192	95	192
Percent Charging	10%	7%	21%	6%
Average Charge Power (kW)	1556	1373	850	1029

Scenario	Cycle 1	Cycle 1	Cycle 1	Cycle 2
Percent Discharging	10%	4%	17%	4%
Average Discharge Power (kW)	1469	1443	928	1111
Percent Resting	80%	89%	62%	90%
SOC Range (%)	2-79	8-80	27-90	37-89
Charge Energy (kWh)	21472	19674	19458	14370
Discharge Energy (kWh)	16814	12229	14873	9158
RTE (%)	78.3	62.2	76.4	63.7
Charge Energy No Rest (kWh)	18537	14418	17574	10576
Discharge Energy No Rest (kWh)	16811	12228	14871	9158
RTE No Rest (%)	90.7	84.8	84.6	86.6
Charge Energy No Auxiliary	18373	14250	17321	10470
Discharge Energy No Auxiliary	16955	12345	15053	9233
RTE No Auxiliary (%)	92.3	86.6	86.9	88.2
Discharge (Ah)	22,440	18630	19109	14091
Charge (Ah)	20097	17587	18113	12604
Mean Discharge Temperature (ºC)	25	18	21	20
Mean Rest Temperature (ºC)	25	18	21	19
Mean Charge Temperature (ºC)	27	21	20	20
Mean Ambient Temperature (ºC)	2	0	3	6

2.5 Use Case 1: System Capacity

2.5.1 Duty Cycle Summary

The capacity duty cycle was developed as a 7-day schedule of charging/discharging power with discharge periods varying from 1 to 4 during peak hours and charging adequately to maintain SOC.

2.5.2 Test Results

Because of multiple issues with the BESS, data for only one run were available for Cycle 1. Testing had to stop due to a windstorm that interrupted communication between the BYD master controller and each container. This interruption was followed by an outage on the line to Glacier. Testing was attempted a month later and ran for 120 hours. This was followed by another outage, after which point testing proceeded to the next use case. Run 1 had an average charge rate of 615 kW, and average discharge rate of 570 kW, with a rest duration of 46%. The RTE was 77.5%, increasing to 82.6% when rest was excluded, and to 85.3% when auxiliary consumption was excluded. Because auxiliary consumption is ~1.5% of charge and discharge rated power, the long rest times do not adversely impact RTE significantly. System Capacity Test results are shown in Figure 2.12 and Table 2.6.

For Cycle 2, charge power ranged from 570 to 840 kW, while discharge power ranged from 440 to 835 kW. The rest duration was long, and ranged from 50 to 65% of the test duration, with RTEs ranging from 65 to 77%. The average auxiliary load ranged from 1 to 2.5% of charge and discharge power for these tests, slightly higher than the 1.5% for the Cycle 1 test. Hence, as expected, the RTE was slightly lower for Cycle 2 tests. The general trend of RTE decreasing with rest duration and lower average charge/discharge power was observed for all tests. For tests with the greatest rest percentage, the RTE increase without rest was the highest, as seen from the increase of 73.5% to 84.2% for Cycle 2 run 3. Excluding auxiliary losses, the RTE was 85 to 87 percent for the last three runs, while it was only 74 percent for the first Cycle 2 run. The average power level for this run is similar to other runs. There does not appear to be any clear reason for this discrepancy. Since the power fluctuates for this use case, it is possible that for this run, the power stays at low levels where PCS efficiency is low longer than for other runs. The BESS performs well under the low ambient temperature conditions.

The SOC-adjusted charge Ah is lower than discharge Ah reported in Table 2.6, which in not feasible. Our analysis suggests that the most likely reason for this anomaly is that maintenance-related charging was not captured. This anomaly does not affect any other metrics reported in this table.

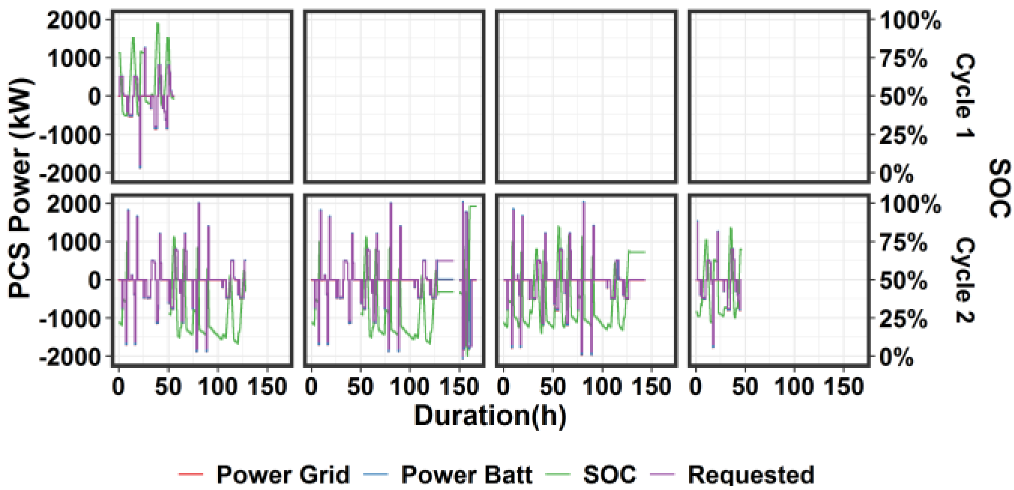

Figure 2.12. System Capacity Test

Table 2.6. System Capacity Test Results

Scenario	Cycle 1	Cycle 2	Cycle 2	Cycle 2	Cycle 2
Date	Mar 24, 2017	Nov 8, 2017	Nov 8, 2017	Nov 17, 2017	Dec 8, 2017
Duration (h)	56	128	168	143	46
Percent Charging	27%	24%	22%	22%	33%
Average Charge Power (kW)	615	757	828	770	588
Percent Discharging	27%	16%	24%	14%	17%
Average Discharge Power (kW)	558	811	449	815	667
Percent Resting	46%	61%	52%	64%	50%
SOC Range (%)	37-97.8	8-78	0-98	15-85	22-84
Charge Energy (kWh)	10805	16267	22295	24705	9038
Discharge Energy (kWh)	8370	10560	16840	18152	6967
RTE (%)	77.5	64.9	75.5	73.5	77.1
Charge Energy No Rest (kWh)	10133	14603	20453	21545	8424
Discharge Energy No Rest (kWh)	8370	10560	16839	18152	6965
RTE No Rest (%)	82.6	72.3	82.3	84.2	82.7
Charge Energy No Auxiliary	9968	14423	20222	21192	8289
Discharge Energy No Auxiliary	8503	10667	17135	18398	7060
RTE No Auxiliary (%)	85.3	74.0	84.7	86.8	85.2

Discharge (Ah)	10678	22518	29257	22762	8220
Charge (Ah)	9941	22981	28969	23650	8660
Mean Discharge Temperature (ºC)	20	22	21	23	20
Mean Rest Temperature (ºC)	20	22	22	22	20
Mean Charge Temperature (ºC)	20	21	22	22	20
Mean Ambient Temperature (ºC)	7	4	4	4	-1

2.6 Use Case 2: Regulation

2.6.1 Duty Cycle Summary

The duty cycle for this test was developed by scaling down the area control error (ACE) signal (MW) provided by PSE using a response factor (kW/MW) to match the rated power capacity of the ESS. The value of the response factor is negative to direct the ESS to act against ACE. A recent 1-week sample of ACE signal was collected from PSE. The test was conducted with the duty cycle based on only one day's ACE signal, depending on the day of the week it starts. Three 1-day runs were performed using the same ACE, but with three response factors. Initial assumptions of these factors were made based on statistical analysis of the signal to determine the range where 99% of the ACE signal values fall (mean ±3σ rule). However, response factor values were finalized by observing the resulting SOC spread. The starting SOC of the test was determined based on the signal's energy neutrality. If the signal is charge (or discharge) intensive, the starting SOC needed to be near the minimum (or maximum) limit so that the duty cycle does not cause SOC limits to be crossed at the end of each run. The ESS was discharged (or charged) as necessary to reduce the SOC down to a specific level before the next run was started. This level depended on the SOC spread resulting from the signal.

2.6.2 Test Results

Three runs with 24-hour durations each were conducted for Cycle 1 and Cycle 2. The duty cycles were biased towards charge, with SOC increasing with time. The power levels decreased from Run 1 to Run 3, with average charge power decreasing from 277 kW to 149 kW, and average discharge power from 160 kW to 73 kW. As expected, the RTE decreased from 75% to 60% for Cycle 1, and from 75 to 54% for Cycle 2. The RTE without auxiliary increased by 4 to 5%, which is in line with the ratio of auxiliary consumption to average charge-discharge power. The RMSE for the response is quite low in the 1 to 3% range, with a 0.3% improvement when auxiliary consumption is excluded. The signal tracking as a percent of rated power is in the 97 to 100% range. The signal tracking within 2% of signal is low in the 20 to 25% range. One reason could be due to low ability for DERO to follow the signal within a deadband of ±50 kW. Frequency regulation test results are shown in Figure 2.13 and Table 2.7.

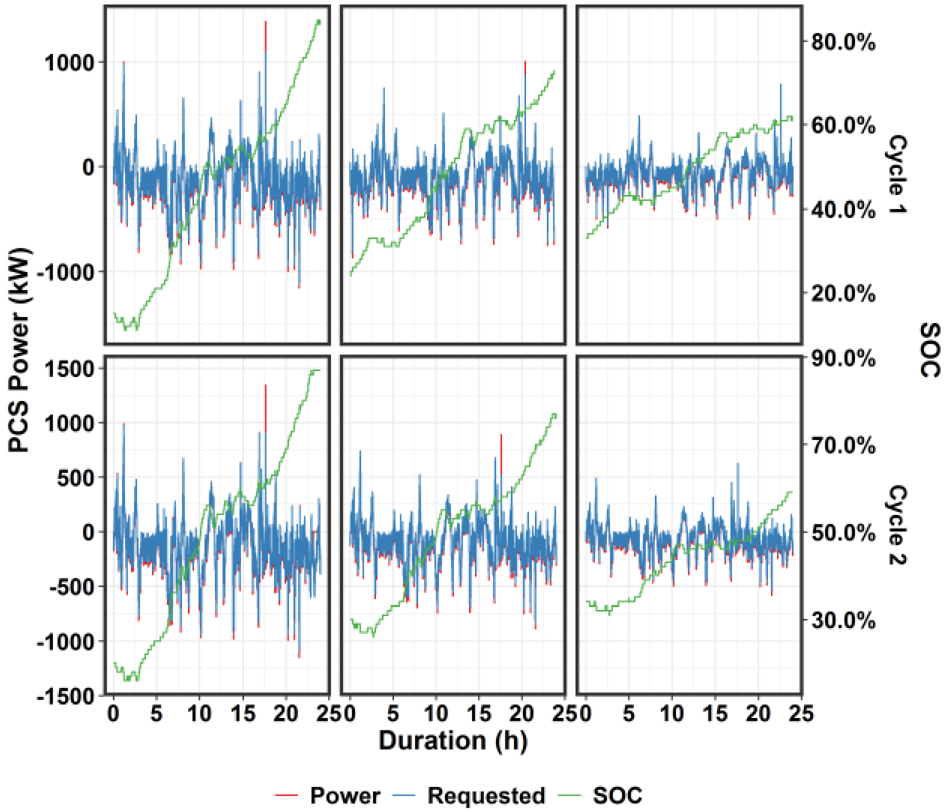

Figure 2.13. Frequency Regulation Test

Table 2.7. Frequency Regulation Test Results

Scenario	Cycle 1	Cycle 1	Cycle 1	Cycle 2	Cycle 2	Cycle 2
Date	Mar 28, 2017	Mar 30, 2017	Apr 3, 2017	Dec 12, 2017	Dec 14, 2017	Dec 18, 2017
Duration (h)	24	24	24	24	24	24
Start SOC (%)	15	24	33	20	30	34
End SOC (%)	85	73	62	87	77	59
Average Charge Power (kW)	277	213	149	270	217	148
Average Discharge Power (kW)	160	117	73	159	116	73
RTE (%)	75	70	60	75	66	54
RTE No Auxiliary (%)	79.4	74.2	64.7	80.7	71.4	58.2
Normalized RMSE	0.016	0.014	0.013	0.031	0.016	0.012
Normalized RMSE No Auxiliary	0.012	0.011	0.009	0.030	0.011	0.010
Tracking 2%	1.00	1.00	1.00	0.97	1.00	1.00
Tracking 2% No Auxiliary	1.00	1.00	1.00	0.97	1.00	1.00
Signal Tracking 2%	0.24	0.25	0.25	0.27	0.25	0.25
Signal Tracking 2% No Auxiliary	0.22	0.22	0.24	0.21	0.20	0.24
Signal Tracking 2% Deadband Removed	0.21	0.21	0.20	0.24	0.21	0.20
Signal Tracking 2% No Auxiliary Deadband Removed	0.19	0.19	0.19	0.19	0.16	0.19

2.7 Use Case 2: Load Following

2.7.1 Duty Cycle Summary

The duty cycle for this test was developed by smoothing the regulation duty cycle. Smoothing is performed by taking the 5-minute moving average of the regulation duty cycle.

2.7.2 Test Results

Three runs of 24-hour duration each were conducted for Cycle 1 and two runs for Cycle 2. The duty cycles were biased towards charge, with the SOC increasing with time. The charge power for Runs 1 and 2 of Cycle 1 was 140 kW, while the discharge power was 69 kW, the same as for Run 2 of Cycle 2. The charge and discharge power levels for Run 3 were 260 kW and 150 kW, the same as for Run 1 of Cycle 2. The RTE for all the runs increased with average charge-discharge power level. A 3 to 5% increase in RTE was observed when auxiliary consumption was excluded. The RMSE for the response is quite low in the 1 to 2% range, with a 0.2% improvement when auxiliary consumption is excluded. The signal tracking as a percentage of rated power is in the 99 to 100% range. The signal tracking within 2% of signal is low in the 23 to 28% range. One reason could be due to the low ability for DG-IC to follow the signal within a deadband of ±50 kW. Frequency regulation test results are shown in Figure 2.14 and Table 2.8.

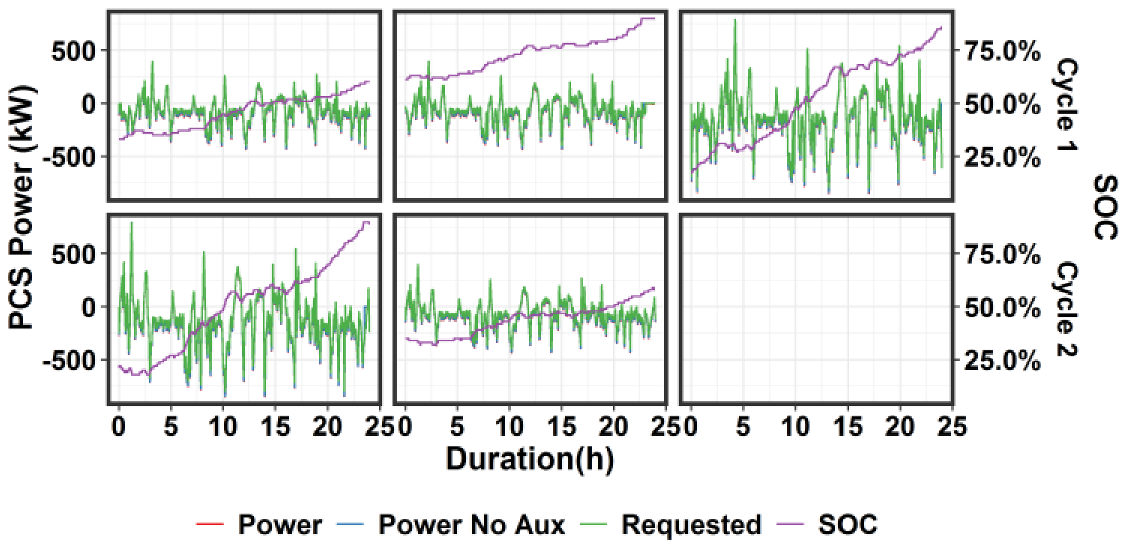

Figure 2.14. Load Following Test

Table 2.8. Load Following Test Results

Scenario	Cycle 1	Cycle 1	Cycle 1	Cycle 2	Cycle 2
Date	April 4, 2017	April 5, 2017	April 7, 2017	Dec 21, 2017	Dec 26, 2017
Duration (h)	24	24	24	24	24
Start SOC (%)	33	61	17	21	35
End SOC (%)	60	90	86	89	58
Average Charge Power (kW)	141	140	260	259	141
Average Discharge Power (kW)	69	69	150	150	69

Scenario	Cycle 1	Cycle 1	Cycle 1	Cycle 2	Cycle 2
RTE (%)	57	64	75	75	51
RTE No Auxiliary (%)	61.5	69.7	79.0	78.0	55.0
Normalized RMSE	0.011	0.011	0.018	0.017	0.011
Normalized RMSE No Auxiliary	0.008	0.009	0.016	0.015	0.009
Tracking 2%	1.00	0.99	1.00	0.99	1.00
Tracking 2% No Auxiliary	1.00	0.99	1.00	0.99	1.00
Signal Tracking 2%	0.24	0.28	0.24	0.25	0.24
Signal Tracking 2% No Auxiliary	0.23	0.25	0.24	0.25	0.23
Signal Tracking 2% Deadband Removed	0.18	0.20	0.21	0.22	0.18
Signal Tracking 2% No Auxiliary Deadband Removed	0.18	0.19	0.21	0.22	0.18

2.8 Use Case 2: Real-World Flexibility

2.8.1 Duty Cycle Summary

This service is related to capacity firming of variable generation resources, such as wind or solar farms. The idea is to control ESS power such that the wind or solar farm output could be used as a “firm” generation capacity for a given period of time. The level where the output will be firmed up and for how long would depend on many aspects, including system conditions and market or hosting utility’s requirements. ESS will import power (charge) from the wind/solar farm if there is over generation with respect to a given firm level and will export power (discharge) if there is under generation with the same reference firm level. For PSE, the duty cycle for this test is developed using total wind generation and system load data provided by PSE at 10-second intervals. The difference between hourly average of system load and base generation is considered as the hourly firm capacity for this duty cycle. The average of the difference between 10-second samples of system load and wind generation taken at 12-hour intervals is used as base generation for this duty cycle. The ESS output obtained using this approach is then scaled down to PSE’s ESS rated power levels by retaining the signal’s asymmetry (i.e., unequal maximum charge and discharge power) and maintaining the SOC limits between 20 and 80%.

2.8.2 Test Results

Real-world flexibility test results for 48-hour runs are shown in Figure 2.15 and Table 2.9. The rest period was negligible for these runs. RTE was low at 58 to 74%, due to a higher percentage of auxiliary loss and possibly due to low power levels resulting in low PCS efficiency. The RTE without auxiliary losses is still low at 66 to 86%, again possibly due to low PCS efficiency.

The SOC-adjusted charge Ah is lower than discharge Ah reported in Table 2.9, which in not feasible. Our analysis suggests that the most likely reason for this anomaly is that maintenance-related charging was not captured. This anomaly does not affect any other metrics reported in this table.

The BESS follows the signal well, and provides the expected performance.

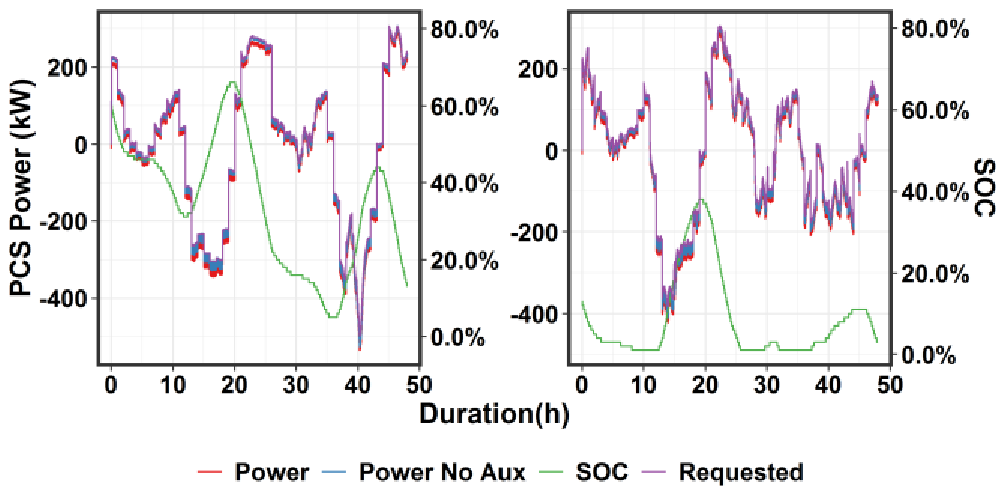

Figure 2.15. Real-World Flexibility Test

Table 2.9. Real-World Flexibility Test Results

Scenario	Cycle 2	Cycle 2
Date	Jan 3, 2018	Jan 7, 2018
Duration (h)	48	48
Percent Charging	31%	36%
Average Charge Power (kW)	210	164
Percent Discharging	39%	44%
Average Discharge Power (kW)	129	113
Percent Rest	1%	0%
SOC Range (%)	5-66	1-38
Discharge Energy (kWh)	3623	2951
Charge Energy (kWh)	6295	3996
RTE (%)	57.5	73.8
Charge Energy No Rest (kWh)	6291	3992
Discharge Energy No Rest (kWh)	3621	2949
RTE No Rest (%)	57.6	73.9
Charge Energy No Auxiliary	6014	3751
Discharge Energy No Auxiliary	3948	3232
RTE No Auxiliary (%)	65.7	86.1
Discharge (Ah)	4978	4164
Charge (Ah)	5005	3207
Mean Discharge Temperature (ºC)	20	19
Mean Rest Temperature (ºC)	20	20
Mean Charge Temperature (ºC)	20	20
Mean Ambient Temperature (ºC)	-2	3

2.9 Use Case 3: Deferment of Distribution Upgrade

2.9.1 Duty Cycle Summary

The Glacier substation serves only one feeder with a typical peak load of 2.5 MVA. The maximum observed load on the feeder during 2016 was 4 MVA, but that peak was mostly due to ESS charging during baseline testing. The transformer is rated at 5 MVA but could be loaded up to 6.6 MVA. The feeder circuit breaker is rated at 5 MVA. There is little load growth predicted for this feeder. The possibility of avoiding reconductoring by having an ESS is not under consideration because the ESS is adjacent to the substation site. Therefore, based on a result of a screening process undertaken with utility personnel, this use case component was not considered for economic evaluation. To verify the technical ability of the ESS to provide this service at any later time or at any other location in the PSE area, we decided to conduct the test. The same load data used for load shaping was used for this duty cycle. A typical load shaving approach was used, with a threshold of 0.95 MW. During the periods when load is lower than the threshold, the ESS is charged so that stored energy is available for peak shaving. Charging is accomplished at such a rate that the total load including the charging load does not exceed 0.95 MW.

Charge/discharge commands for the duty cycle are developed in a way that maintains SOC limits applicable for the ESS at PSE.

2.9.2 Test Results

There was a data error for the Cycle 1 run, hence only the results for Cycle 2 testing are presented here. The RTE for a 1-week duty cycle was only 37%, in spite of the fact that rest time was only 6% of test duration. This was due to low average charge and discharge powers of 44 kW and 88 kW, respectively. There were long periods when the power was within a ±10 kW band. Because DG-IC does not track signals in the ±50 kW deadband, the observed percent charge and discharge durations correspond to absolute magnitude power of >50 kW. As expected, when auxiliary consumption was excluded, the RTE increased to 46%. Because of long durations at low power levels, the SOC decreased from 25% to 5% before the 140 kW peak discharge around hour 150. This shows that the SOC drop due to auxiliary consumption and PCS switching during rest and low power discharge can adversely impact the ability of the BESS to provide peak power at the end of long durations of rest or low power discharge, unless the SOC drop rate is accounted for. Distribution deferral test results are shown in Figure 2.16 and Table 2.10.

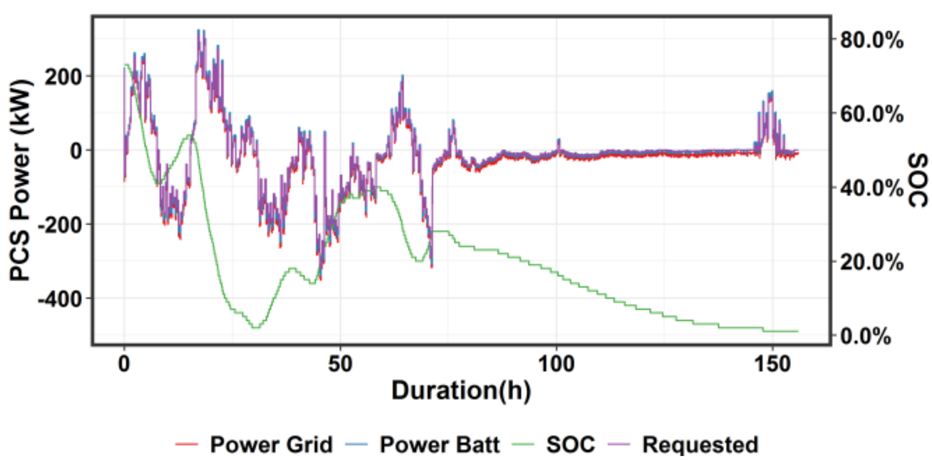

Figure 2.16. Distribution Test

Table 2.10. Distribution Test Results

Scenario	Cycle 2
Date	Jan 13, 2018
Duration (h)	156
Percent Charge	19%
Average Charge Power (kW)	56
Percent Discharge	16%
Average Discharge Power (kW)	99
Percent Rest	6%
SOC Range (%)	1-77
Charge Energy (kWh)	9816
Discharge Energy (kWh)	3620
RTE (%)	36.9
Charge Energy No Rest (kWh)	9699
Discharge Energy No Rest (kWh)	3620
RTE No Rest (%)	37.3
Charge Energy No Auxiliary	8637
Discharge Energy No Auxiliary	3988
RTE No Auxiliary (%)	46.2
Discharge (Ah)	6781
Charge (Ah)	5923
Mean Discharge Temperature (ºC)	19
Mean Rest Temperature (ºC)	18
Mean Charge Temperature (ºC)	20
Mean Ambient Temperature (ºC)	4

2.10 Use Case 3: Load Shaping

2.10.1 Duty Cycle Summary

Understanding the capability of the ESS to perform this use case is important from a distribution deferral and renewable energy integration perspective. This use case could be tested using a number of different approaches. For example, a typical peak shaving approach could be used to control the battery power in such a manner that the loading of the circuit does not exceed a predefined level. This is relevant to the distribution investment deferment application. Another method could be to control ESS power to limit the load ramp rate dP/dt within a limit. This is more relevant to renewable energy penetration into the circuit. Discussions with PSE personnel determined that there was no economic benefit associated with load shaping near Glacier, Washington, because photovoltaic penetration and distribution constraints are not factors in the area. However, a decision was made to conduct the battery tests for this use case to learn if the ESS is technically able to provide this service if necessary at any later time or at any other location in the PSE area. The approach used for developing the load shaping duty cycle is described below. Peak load shaving to defer distribution upgrades and load ramp rate control to manage renewable integration are not issues of immediate concern on the test feeder. One of the next best candidates for load shaping could be to reduce the gap between the peak and valley in the daily load profile. Distribution system operators need to engage resources (e.g., voltage regulator, tap changer, capacitor bank, operation) to mitigate the impact of this gap on a daily basis. Using storage to “flatten” daily load profiles could provide some benefit by reducing voltage regulator, tap changer, and capacitor bank operation. To achieve a flatter load profile, first a reference load is selected approximately in the mid-region between the peak and valley of a daily load profile. If multiple daily load profiles have to be considered, as in the case for this duty cycle, the reference load could be varied by observation. Then, the difference between the reference load and actual load is scaled down by a "flatness factor" and added (if actual load is smaller than the reference load) to or subtracted (if actual load is greater than the reference load) from the actual load. If the flatness factor is "1," the resultant load profile would be a constant flat load profile (i.e., the same as the reference load). Therefore, to achieve a load profile that is flatter but still retains the signature of the variations in the actual load profile, a flatness factor greater than "1" is used. As the power needed to achieve this load profile would be generated/consumed by the ESS, the value of the flatness factor is tuned by observing SOC variations and considering applicable SOC limits. To accomplish a reasonable match in time of the year for use case testing, we used load data measured at 15-minute intervals at the Glacier substation from April 22–30, 2016. A closer match in time could not be achieved due to data quality issues. Observing the nature of load variations, we used reference loads of 0.98 MW for the April 22–25 data and 0.82 MW for the April 26–30 data. We used a flatness factor of 1.8, which considers the SOC limits of 20% and 80% for the ESS at PSE

2.10.2 Test Results

The rest durations were quite low for this test at 3 to 4% of test duration. However, the average power levels were low at 44 kW for Cycle 1 and 66 kW for Cycle 2. This led to a low RTE of 57% for Cycle 1 and 43% for Cycle 2. Because of the low power levels, the RTE is as low as 43%, with an increase to 57% once auxiliary load consumption is excluded. The low average power results in low PCS efficiency. In addition, extended durations at low power levels lead to the auxiliary power plus PCS switching power being a high percent of the average power levels. Hence, sufficient attention should be given to the anticipated SOC drop at these low power levels due to these losses. For Cycle 1, at hour 90, the BESS is no longer able to support the requested discharge power, as its SOC has reached its lower limit. This shows the importance of accounting for SOC drop, especially at low average charge and discharge power levels.

The SOC-adjusted charge Ah is lower than discharge Ah reported in Table 2.11, which in not feasible. Our analysis suggests that the most likely reason for this anomaly is that maintenance-related charging was not captured. This anomaly does not affect any other metrics reported in this table.

Load shaping test results are shown in Figure 2.17 and Table 2.11.

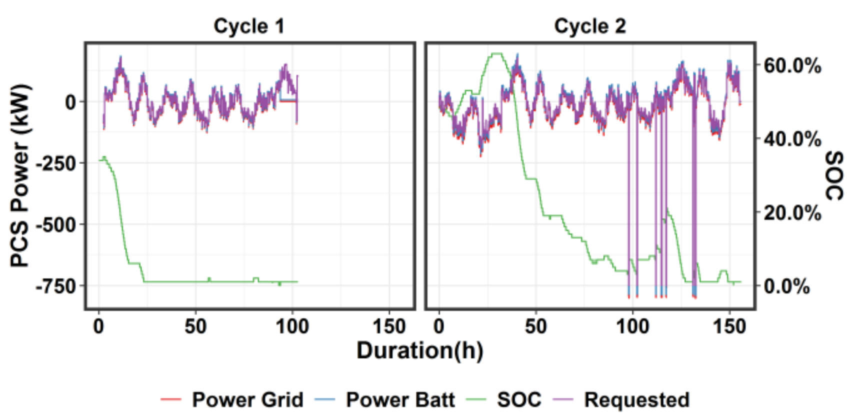

Figure 2.17. Load Shaping Test

Table 2.11. Load Shaping Test Results

Scenario	Cycle 1	Cycle 2
Date	May 6, 2017	Jan 21, 2018
Duration (h)	100	156
Percent Charging	16%	27%
Average Charge Power (kW)	49	85
Percent Discharging	23%	21%
Average Discharge Power (kW)	39	55
Percent Rest	4%	3%
SOC Range (%)	0-35	0.2-63
Charge Energy (kWh)	3671	9122
Discharge Energy (kWh)	2076	3919
RTE (%)	56.6	43.0
Charge Energy No Rest (kWh)	3649	9088
Discharge Energy No Rest (kWh)	2076	3918
RTE No Rest (%)	56.9	43.1
Charge Energy No Auxiliary	3371	8191
Discharge Energy No Auxiliary	2394	4689
RTE No Auxiliary (%)	71.0	57.2
Discharge (Ah)	4100	6766
Charge (Ah)	1898	5758
Mean Discharge Temperature (ºC)	19	19
Mean Rest Temperature (ºC)	20	20
Mean Charge Temperature (ºC)	20	19
Mean Ambient Temperature (ºC)	13	2

2.11 Use Case 4: Outage Mitigation

2.11.1 Duty Cycle Summary

This use case tests the ability of an ESS to manage supply interruption to a critical load due to weather-induced events or unplanned outages. PSE has the capacity to island a connected load of 510 KVA with a 350-400 KVA peak. In developing the duty cycles for this use case, PNNL obtained outage data from 2011-2015 at the Glacier Site. Of the 17 outages that occurred during that time period, seven were randomly selected. Outage data for those seven outages were used to establish the outage dates and durations. Load data were obtained for the calendar days when the outage occurred (load data were from the 2016 time period). The load data for the entire feeder were reduced by 80% to account for the share of the feeder's load that could be islanded. We then assumed that the ESS would meet the load on the island for as long a period during the outage as feasible.

2.11.2 Test Results

This test was done for one week, with the BESS resting 60 to 70% of the time. Run 1 of Cycle 2 had the highest RTE at 60%, due to high charge and discharge power. Run 1 of Cycle 1 and Run 2 of Cycle 2 had a very low discharge power of 114 kW, compared to 287 kW for Run 1 of Cycle 2. This low discharge, coupled with long rest times, led to an RTE of ~50% for these runs. As expected, removing the rest period resulted in a jump in RTE of 18 to 20 percentage points, with an additional 5% increase when auxiliary consumption is excluded. The RTE without auxiliary load increases with average power as expected and is maximum for run 1, Cycle 2. Because of an SOC decrease during rest, the BESS should not be left on rest, especially with PCS switching, when it is being used for outage mitigation service.

The SOC-adjusted charge Ah is lower than discharge Ah reported in Table 2.12, which in not feasible. Our analysis suggests that the most likely reason for this anomaly is that maintenance-related charging was not captured. This anomaly does not affect any other metrics reported in this table.

PSE successfully islanded the Glacier BESS circuit in August 2018. The procedure and other details are provided in Section A.9 of Appendix A. Outage mitigation test results are shown in Figure 2.18 and Table 2.12.

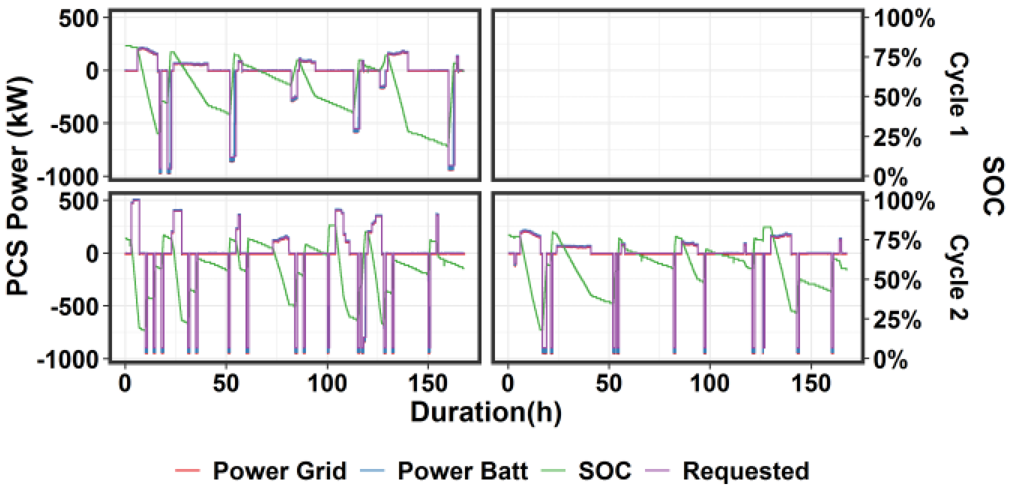

Figure 2.18. Outage Mitigation Test

Table 2.12. Outage Mitigation Test Results

Scenario	Cycle 1	Cycle 2	Cycle 2
Date	May 26, 2017	Jan 31, 2018	Feb 9, 2018
Duration (h)	168	168	168
Percent Charging	11%	10%	7%
Average Charge Power (kW)	510	893	798
Percent Discharge	29%	20%	29%
Average Discharge Power (kW)	114	287	114
Percent Rest	60%	70%	64%
SOC Range (%)	19-82	17-84.2	18-83
Charge Energy (kWh)	10529	16317	11573
Discharge Energy (kWh)	5604	9765	5602
RTE (%)	53.2	59.8	48.4
Charge Energy No Rest (kWh)	7823	12216	8336
Discharge Energy No Rest (kWh)	5604	9765	5602
RTE No Rest (%)	71.6	79.9	67.2

Charge Energy No Auxiliary	7706	12060	8215
Discharge Energy No Auxiliary	5898	10071	6042
RTE No Auxiliary (%)	76.5	83.5	73.5
Discharge (Ah)	10793	15309	10507
Charge (Ah)	9460	14896	10227
Mean Discharge Temperature (ºC)	24	21	20
Mean Rest Temperature (ºC)	23	21	19
Mean Charge Temperature (ºC)	24	21	20
Mean Ambient Temperature (ºC)	17	NA	NA

2.12 Use Case 7: Optimal Utilization

At the end of the use cases 1 through 4, the BESS was deployed to optimize benefits by responding to all use cases addressed.

2.12.1 Duty Cycle Summary

The Battery Storage Evaluation Tool (BSET) considers the battery system SOC, energy available at various power levels, and the benefits of each use case. It simulates battery operation for 1 year and the charging and discharging patterns reflect the demands placed on the battery system by the highest-value applications at any given point in time. BSET sets 24-hour operating schedules that are updated on an hourly basis. These optimized charging and discharging schedules served as the bases of the duty cycles used in Use Case 7.

2.12.2 Test Results

Optimal utilization test results are shown in Figure 2.19 and Table 2.13. The RTE is in the 70 to 75% range at an average charge and discharge power of 15 percent of rated power. An estimated 30 kW loss each way can be assigned to the PCS, resulting in a PCS RTE of 82% assuming no other losses. Per the Energy Storage System Technical Specifications, the maximum efficiency for the PCS was 97.5 percent. Manufacturer’s data needs to be obtained for the PCS efficiency as a function of power to avoid losses at power levels where efficiency is low.

Excluding the 20 to 33 percent rest period, the RTE jumped by about 3 percentage points. A further gain of 3 percentage points in RTE was obtained when auxiliary losses were excluded, with an RTE in the range of 77 to 85 percent.

The SOC-adjusted charge Ah is lower than discharge Ah reported in Table 2.13, which in not feasible. Our analysis suggests that the most likely reason for this anomaly is that maintenance-related charging was not captured. This anomaly does not affect any other metrics reported in this table.

The BESS tracked the signal extremely well within 2 percent of rated power, with a normalized RMSE of 0.005 to 0.041.

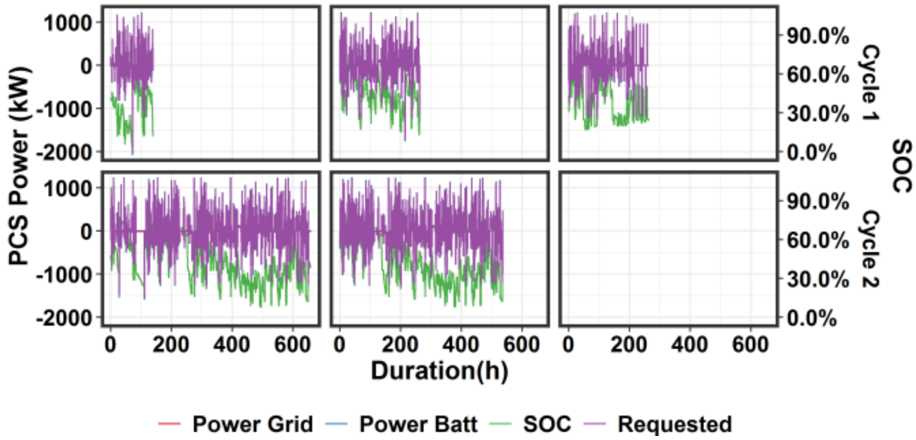

Figure 2.19. Optimal Utilization Test

Table 2.13. Optimal Utilization Test Results

Scenario	Cycle 1	Cycle 1	Cycle 1	Cycle 2	Cycle 2
Date	Jun 16, 2017	Aug 14, 2017	Sep 8, 2017	Feb 21, 2018	Feb 26, 2018
Duration (h)	142	264	264	659	537
Percent Charging	41%	38%	30%	NA%	41%
Average Charge Power (kW)	271	282	326	290	285
Percent Discharging	28%	28%	27%	NA%	30%
Average Discharge Power (kW)	314	296	297	307	308
Percent Rest	20%	24%	33%	26%	20%
SOC Range (%)	4-57	13-75	17-64	8-77	8-76
Charge Energy (kWh)	20,298	35,016	31,720	84,387	73,921
Discharge Energy (kWh)	14,325	24,321	24,545	61,072	55,073
RTE (%)	70.6	69.5	77.4	72.4	74.5
Charge Energy No Rest (kWh)	19,461	33,255	30,033	79,970	71,480
Discharge Energy No Rest (kWh)	14,324	24,317	24,542	61,067	55,068
RTE No Rest (%)	73.6	73.1	81.7	76.4	77.0
Charge Energy No Auxiliary	19,030	32,461	29,546	77,408	69,200
Discharge Energy No Auxiliary	14,597	24,885	24,970	62,857	56,675
RTE No Auxiliary (%)	76.7	76.7	84.5	81.2	81.9
Discharge (Ah)	18,283	31,944	32,192	78,844	69,778
Charge (Ah)	17,971	31,637	29,706	76,003	66,783
Mean Discharge Temperature (ºC)	24	28	24	21	21
Mean Rest Temperature (ºC)	24	29	22	20	21
Mean Charge Temperature (ºC)	24	29	23	21	22
Mean Ambient Temperature (ºC)	14	17	14	1	2
Normalized RMSE	0.005	0.021	0.033	0.037	0.041
Normalized RMSE No Auxiliary	0.004	0.021	0.032	0.037	0.041
Tracking 2%	1.00	1.00	1.00	0.97	0.97
Tracking 2% No Auxiliary	1.00	1.00	1.00	0.97	0.97
Signal Tracking 2%	0.62	0.63	0.75	0.62	0.60
Signal Tracking 2% No Auxiliary	0.68	0.65	0.68	0.58	0.58

3.0 Lessons Learned

This section provides an at-a-glance view of important lessons learned on the technical aspects of the PSE BESS based on experience gained during the testing process and the test results. Conclusive remarks on the overall testing effort and the importance of the test results are provided in Section 4, Conclusions.

3.1 Lessons Learned from Test Results

1. The BESS was discharged between 90% and 5% SOC (85% DOD). Because of a lack of tight control of the end SOCs during charge or discharge, analysis of RPTs were done in the 82 to 10% SOC range. The estimated discharge energy at 100% DOD was calculated by dividing the measured energy by the DOD of 72%. Including the auxiliary losses, 3685 to 3940 kWh was delivered at the C/6 rate. Excluding auxiliary consumption, the energy delivered was 3710 to 3985 kWh.
2. The RPT RTE ranged from 83 to 88%, depending on the power, and whether the rest periods and auxiliary consumption were included. The RTE increased slightly with increasing rates. The RPT RTE was unchanged throughout the test period.
3. PCS one way efficiency ranged from 93 to 96 percent for the C/6 to C/2 range. This leads to RTE of 90 to 93 percent for this range. Tests run at average power levels of less than 15 percent of rated power result in low RTE primarily due to auxiliary losses and PCS losses.
4. When auxiliary consumption during 0.5-hour rest periods were excluded, the RTE rose by only 0.1 to 0.4% due to the low hourly SOC decrease of 0.25% due to auxiliary load. When auxiliary consumption was excluded throughout the test, the RTE increased by 0.6 to 2.5%, with larger increases at lower rates
5. The distribution of power among the four containers was not available; therefore, individual container performance could not be assessed.
6. No taper of power was observed in the SOC range of 5 to 95% investigated.
7. The high RTE at >C/6 rate, along with good signal tracking after accounting for a 5 to 7 second communication lag makes this BESS versatile for multiple applications.
8. Auxiliary power consumption was proportional to deviation of temperature from a set point of 22 to 24°C, and increased at a steeper rate for negative deviations from the set point.
9. The DC internal resistance of the BESS decreased slightly from the Baseline to Post Cycle 1 and then remained unchanged. This decrease appears to be due to a conditioning effect on the BESS. From the perspective of exchanging high power, the BESS SOH can be assumed to be unchanged.
10. The discharge energy decreased by 6% from the Baseline to Post Cycle 1 test, and by another 1% to Post Cycle 2. This was accompanied by an ampere-hour capacity loss, probably due to loss of lithium at the graphite anode. Hence, the BESS can be assigned an energy capacity related SOH of 93%. A direct impact is lower durations at rated power for a fixed DOD.
11. At the Electric Power Research Institute Energy Storage Integration Council meeting held in November 2017, SOC calibration procedure, seasonal testing for auxiliary loads, SOC loss rate due to reactive power injection, and SOH definition and tests were identified as key gaps that merit further studies. This project addressed all of these gaps.
12. During discharge and rest modes, the DC battery supports auxiliary load, resulting in an SOC reduction during rest that is detected for rest durations >5 hours. The SOC reduction rate for some rest periods was much greater than for other rest periods. It was found that during rest, at times the

PCS was in a switching state (reactive power exchanged with the grid) and at other times the PCS was in a disabled state. When the PCS was in a disabled state, the DC discharge power on several occasions was zero, indicating the auxiliary load was being supported by the grid. However, there were some occasions when the DC discharge power supported the auxiliary load. On other occasions, the DC power was as high as 100 kW. When the PCS was switching, the DC power was around 10 kW more than the auxiliary load, with DC power at times reaching >100 kW. This makes it very difficult to estimate the battery SOC during tests when there are long rest periods, especially with PCS enabled (switching mode). The rate of change of SOC (or magnitude of DC discharge power) during rest with PCS switching did not depend on reactive power but increased linearly with the standard deviation of reactive power.

13. BMS-related issues included SOC drift and unbalanced strings, along with inability to control the SOC end points during operation to target SOCs. This inability to control end SOCs can result in:
    - String imbalance
    - Unexpected shutdown when the BMS detects an SOC that crosses the lower or upper limits
    - Incomplete use of the BESS energy, which is further complicated by the varying rate of decrease of SOC during rest associated with PCS state.
14. The SOC-adjusted charge Ah was lower than discharge Ah for several tests, which in not feasible. Our analysis suggests that the most likely reason for this anomaly was that maintenance-related charging was not captured. This anomaly does not affect any other metrics reported here.

3.2 Lessons Learned in Design of Data Transfer

1. A secure file transfer protocol had to be established to get the data out of PSE to PNNL. PNNL's contractor placed software on the BESS computer to automate data transmittal. Sending data to PNNL required initiation from the DG-IC to create and push the files out.
2. Synchronizing data flow from various meters was labor intensive because each meter makes new comma-separated-value files when the file size reached 10 MB.
3. It took several months to establish a virtual private network connection to the Glacier BESS computer. Copying comma-separated-value files in 10 MB chunks took 3 minutes, resulting in a labor-intensive process.
4. The process of selecting files, compressing them on the Glacier computer via a Remote Desktop Protocol session, and retrieving them via a network mapped drive was automated.
5. Files from different meters were combined together into MySQL database on the PNNL computer.
6. Data for the Use Case 3 distribution deferral test run on April 29, for 7 days was not available and could not be recovered.

3.3 Lessons Learned in Design of Test Setup

1. The drawings provided to PNNL by PSE showed a separate line to power auxiliary load. Neither the battery discharge during rest to support auxiliary load nor the additional power draw from the battery during PCS were anticipated. These conditions were quantified during testing and analysis.
2. The detailed procedure for string balancing, shared by BYD, could be done only by human machine interface onsite because individual string information within each container could be only assessed at the site.

3. The inability to control the end SOC during charge or discharge to target values, coupled with varying SOC drop rates during rest, along with changes in BESS state after maintenance by BYD or the Whitehorn crew made it a challenge to accurately predict the SOC change during testing to various duty cycles. The reported SOC during discharge was lower than the actual SOC while the reverse was true during charge. This results in the BESS providing significantly more energy towards the end of discharge at low SOCs for a fixed change in SOC. Because not all discharges were carried out to the SOC range (SOC <0.5%) where this was observed, data analysis was restricted to 10% at the low end.
4. Because of string imbalance issues and an inability of the BMS to lock the end SOC to the target SOC, the high end of SOC for the RPT capacity tests did not reach the target 90% and was as low as 82% for some runs. Hence analysis of data was restricted to the 10 to 82% SOC range. There were some occasions during use case testing when SOC did not exceed 75%, with the target SOC during charge of 90%.
5. SOC drift during rest was addressed in BMS software updates by BYD, the details of which are not known. Analysis of DC battery discharge power flow during rest at the two PCS states provided insights on potential reasons for the SOC drift.
6. BYD retrofit all modules with new BMUs to improve balancing and reduce SOC drift. Details about the retrofit were not shared by BYD.
7. The original 5-minute uninterruptable energy supply (UPS) caused the container BMS to shut down, resulting in the BYD master controller seeing no further information from the BMS. The situation was corrected when PSE learned how to reset the BYD master controller and replaced the 5-minute UPS with a 1-hour UPS.
8. Thermal management is based on temperature deviation from a set point within each container, and not on battery module temperature.
9. Thermal management using heat pump/air conditioning unit outside each container is based on deviations from set points of 22 to 24ºC of four thermostats located inside each container. Thermal management for the BMS is not based on cell or module temperature.
10. Based on our analysis, auxiliary power consumption increases as the temperature deviates from 24ºC. This is in line with PSE input that set points for the thermostats inside the containers are 22ºC. The power to heat the BESS for a fixed deviation was greater than the power to cool the BESS.
11. A similar relationship was found with respect to the ambient temperature. Because the container interior temperature does depend on the ambient temperature, it is not surprising the relationships are similar.
12. A high-temperature condition was found in containers after a 2,000 kW capacity test performed October 1–2, 2017, with the container temperature reaching 37ºC twice. The maximum battery temperature at the end of the test reached 45ºC, which is 5°C lower than observed during capacity tests done in January and February of 2017. For Post Cycle 2 testing, the internal ambient temperature reached 42°C, but this did not generate a high-temperature condition. This indicates that the availability of the BESS is dependent on an unknown algorithm to control container temperature and an inconsistent criterion for a high temperature condition. The high rate test was subsequently done in June 2018, when the battery reached a maximum of 48°C, with the container temperature not displaying the high-temperature condition, even though it reached a maximum of 42°C. The inconsistency in terms of when a high-temperature condition is generated may adversely affect BESS reliability.
13. The difference between minimum and maximum module temperature was as high as 20°C at the C/2 rate and 10°C at the C/6 rate. Separate data were not available for each container; hence, it is not possible to conclude if this disparity exists within a container or across containers. With better

thermal management, this wide range of module temperatures can be narrowed, thus mitigating SOH disparity among modules.

14. Strings are considered balanced when their SOCs are within 10 to 15% of each other. This is a wide range, and is sustainable only if the master controller allocates power to each container based on its SOC.

15. Power flow information across various containers was not available. SOC information also was not available for each container separately. Hence it was not possible to determine if the central BMS controller allocates power depending on each string status—SOC and temperature. For example, at 2,000 kW, each container has to provide 500 kW, which is its maximum rating. However, at power levels <2,000 kW, there is opportunity for the central BMS controller to direct power flow so containers with lower SOCs and/or higher temperatures during discharge are allocated less power.

3.4 Lessons Learned from Site-Related Issues

1. Tests lasting more than 24 hours require special formatting at PSE end to ensure testing continues beyond 24 hours.
2. Tests that have commands every few seconds require a manual start. Hence these tests cannot be scheduled sequentially in automatic mode.
3. With multiple test interruptions, it was a challenge to synchronize runs with the schedule files sent by PNNL.
4. Having a process that names files in an easy-to-track manner at either end would have helped
5. UPS powering the DG-IC faulted due to defective batteries and could not be run on bypass mode. It required a manual DG-IC restart before data could be assessed.
6. There was an occasion when the DG-IC sent a signal, but the BESS did not respond. The cause was unknown.
7. Staff need to be onsite to verify strings are balanced using the human-machine interface.
8. The power-following mode of the DG-IC was not applicable to the load following use case. The frequency/watt mode was more applicable. This mode has not been used by PSE, hence duty cycles were sent by PNNL for load following.

4.0 Novel Findings

4.1 RTE Analysis

Figure 4.1 plots the RTE without rest, referred to as adjusted RTE, vs. average module temperature at various power levels, which are color coded. It is obvious that there is a distinct change in behavior at about 20°C. Therefore, we applied a piecewise linear regression to these adjusted RTEs with respect to temperature and weighted by discharge energy. We found that the breakpoint occurs at 20.3 ±0.5 C. At temperatures colder than 20.3°C, the RTE increases rapidly at a rate of 5.6%/ºC. Above this breakpoint, the RTE increases much less rapidly at a rate of 0.4%/°C, a rate that is 14 times lower. Both of these rates have a standard uncertainty of 2.1%/°C.

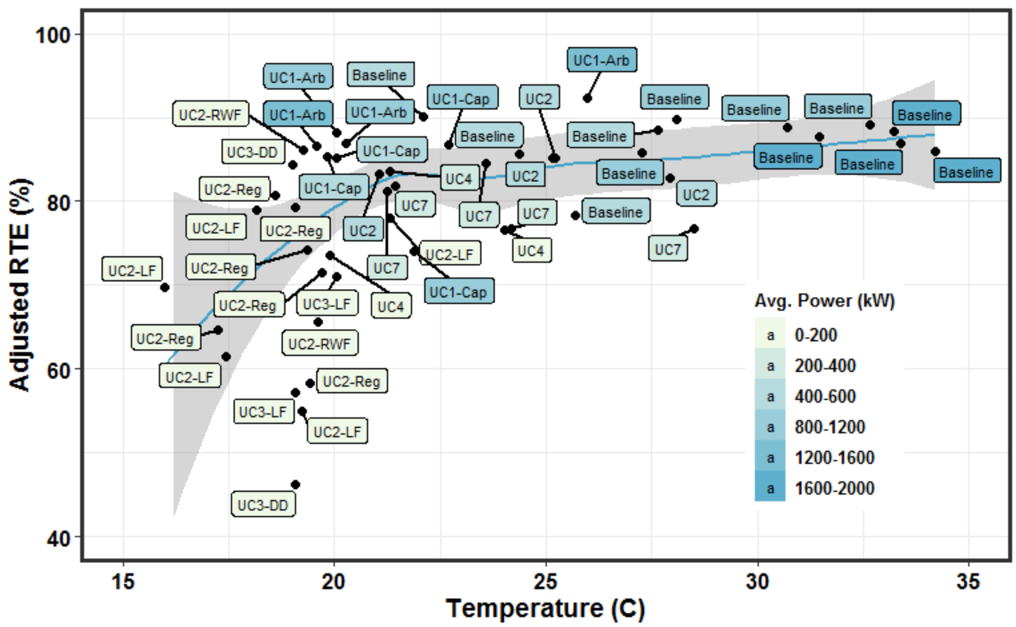

Figure 4.1. RTE without Rest or Auxiliary Analysis

Using the runs where the temperature was more than this set point of 20.3 C, the unadjusted RTE was regressed as a function of average discharge power and fraction of the time at rest, weighted by discharge energy, with the results provided in Table 4.1. The RTE drops by 0.2% for each 1% increase in rest time. The RTE increased by 10.1% for each 1,000 kW increase in average discharge power. This analysis has an adjusted R2 of 0.69. The regression results are shown in Table 4.1 and plotted in Figure 4.2.

Table 4.1. RTE Regression

Coefficient	Estimate	Std. Error	Pr(>|t|)
Intercept (%)	75.6551010	1.629268	0.0e+00
Rest Fraction (%)	-20.8675675	3.665694	4.2e-06
Avg. Dis Power (%/kW)	0.0100565	0.001491	3.0e-07

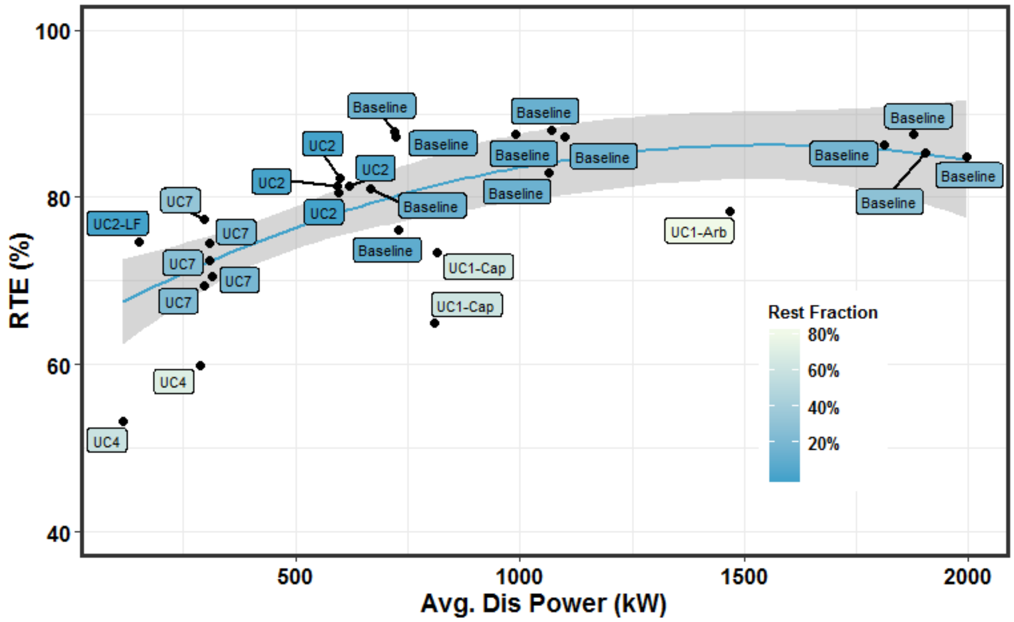

Figure 4.2. RTE as a Function of Power and Rest Fraction

4.2 Root Mean Square Error Analysis

The RMSE in the power was consolidated for Use Cases 2 and 7 and presented in Figure 4.3.

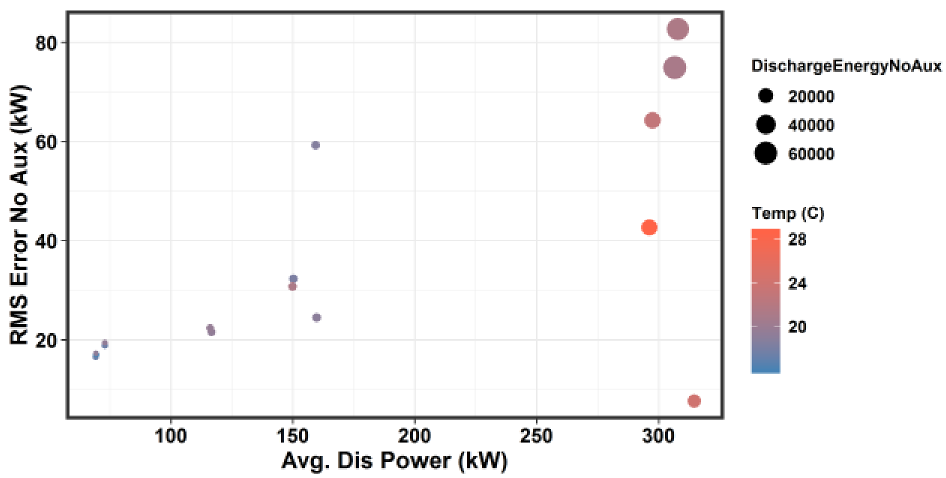

Figure 4.3. RMSE vs. Power and Temperature

A weak relationship was found, with the RMSE regressed as a function of average discharge power and average module temperature, weighted by discharge energy, with the results provided in Table 4.2. The RMSE decreases by 0.1 kW for each 1ºC increase in temperature. The RMSE increased by 305 kW for each 1000 kW increase in average discharge power. This analysis has an adjusted R^2 of 0.51.

Table 4.2. RMSE Regression

Coefficient	Estimate	Std. Error	Pr(>|t|)
Intercept (kW)	1518	517	0.01
Average Discharge Power (kW/kW)	0.305	0.0770	0.001
Average Temperature (kW/C)	-5.23	1.78	0.01

4.3 Temperature Change Analysis

The temperature rate of change was calculated for periods of charge, discharge, or rest longer than 2 hours. The average rate of change is shown in Figure 4.4, color coded by difference between battery temperature and ambient temperature from the weather report.

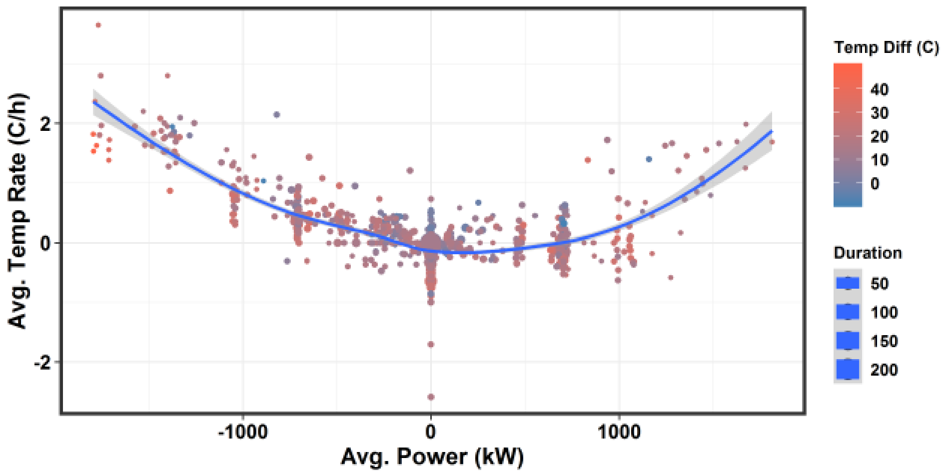

Figure 4.4. Temperature Rate vs Power and Delta Temperature

A weak relationship was found, with the battery temperature regressed as a function of power, power squared, SOC, and difference between battery temperature and weather temperature. The results are provided in Table 4.3. This analysis has an adjusted R^2 of 0.69. The negative coefficient for the power term shows an exothermic effect for charge, and the negative coefficient for the difference between weather and battery temperature shows the effect of the weather on the battery, with the temperature decreasing if the battery is warmer than the weather or increasing if the battery is colder.

Table 4.3. Temperature Rate Regression

Coefficient	Estimate	Standard Error
Power (C/h/kW)	-3.80E-04	3.09E-06
$Power^2$ ($C/h/kW^2$)	5.25E-07	3.68E-09
Del Batt Weather Temperature (1/h)	-8.68E-03	1.96E-04
SOC (C/h)	1.43E-03	8.05E-05

5.0 Conclusions

The 2-MW, 4.4-MWh Li-ion BESS near the Glacier substation is installed to provide temporary backup power to the distribution circuit to overcome outages due to frequent, vegetation-related transmission-line outages. As part of Washington CEF 1, a $3.8 million grid modernization grant was awarded to PSE to support the BESS project, plus technical support to evaluate the effectiveness and economics of the BESS project and energy storage applications in general. The energy storage benefits to be explored through this BESS project were: flexibility services (energy arbitrage, regulation up/down), primary frequency response, capacity, outage mitigation. Because BESSs are quite diverse in their characteristics, it was important to characterize their performance and stability over time using a DOE-OE standardized test procedure for energy storage.

This report documents the technical performance of the Glacier substation BESS. Baseline tests were intended to assess the general technical capability of the BESS (e.g., stored energy capacity, ramp rate performance, ability to track variable charge/discharge commands, DC battery internal resistance) while the use case tests were used to examine the performance of the BESS while engaged in a specific service (e.g., arbitrage, capacity, regulation services, load following services). The use cases for this extended analytic support work expand the initial use cases that PSE implemented in the Glacier BESS. Parameters that are important for understanding BESS performance when subjected to actual field operation for economic purposes (e.g., RTE, auxiliary consumption, command tracking performance, temperature variations, parasitic power loss during power electronics switching during rest, SOC excursions) were examined. These metrics were used to quantify performance of the BESS in several use cases, in comparison with baseline performance.

The analyses of the BESS tested performance confirm that the technical characteristics (e.g., capacity) and performance (e.g., response rate) of the Glacier BESS are generally compatible with the range of use cases investigated in this project. The detailed findings provided in this report will help PSE understand the performance of the Glacier substation BESS at its current state and will be useful when developing appropriate operational strategies. In addition, the results and lessons presented herein would also be beneficial in general for any task or effort that needs technical assessment on similar types of BESSs based on field deployment results.

Some specific conclusions are:

1. The system rated energy of 4400 kWh was not verified because the SOC range was limited to 5% at the low end and 90% at the high end. Because of the lack of SOC control, some discharges were carried out to <0.5% SOC. The cumulative discharge energy increased linearly with DOD till ~0.5% SOC. At <0.5% SOC (or >99.5% DOD), the delivered energy increased at a faster rate, possibly due to the reported SOC being less than the actual SOC.
2. Because discharge to <0.5% SOC was done only for a couple of runs, it was not possible to estimate total energy discharged down to 0% SOC.
3. Estimation of energy content for ΔSOC of 100% yielded 3,970 to 4,060 kWh.
4. There was one run conducted during the Baseline capacity test when the SOC range was 88% to 1%, with an energy content of 3,975 kWh. Extrapolating this to 100% DOD provided an estimated energy content of 4,570 kWh.
5. While the upper SOC limit for BESS was set at 90% on a few occasions only an 82% SOC was achieved during charge on a few occasions. We also determined that up to 10% SOC, the cumulative energy discharged was linear. Hence, analysis was done in the 10 to 82% SOC range.

6. The energy content in the 82 to 10% SOC range decreased from the Baseline tests to the Post Cycle 1 test at all rates. However, following a 2.5 month wait after C/6 rate test due to issues related to a remote terminal unit, the discharge capacity decreased by 10%, possibly due to BYD and/or Whitehorn crew performing string balancing and other adjustments to the BESS at the time. This makes estimation of SOH difficult because BESS performance changes after maintenance.
7. The BESS RTE during reference performance capacity tests ranged from 83 to 88% based on charge-discharge rate, auxiliary power consumption, and whether rest period and auxiliary load were included, and did not change during the test period. The RTE is maximum in the C/4 to C/2 rate.
8. The RTE varied significantly among various use cases. For the arbitrage use case with a high rest duration, the RTE decreased to as low as 62% for 89% rest time at an average power level of 1400 kW. As the average power decreased to 70 to 275 kW, the RTE decreased, as observed for frequency regulation and load following use cases with RTEs as low as 54%. For Use Case 3, distribution and load following, the RTE was in the 31 to 49% range because average power levels were <2% of the rated power, even though the rest percentages were low in the 4 to 7% range.
9. The RTE without rest increased with temperature at <20°C, while the unadjusted RTE increased with power levels and decreased with rest duration.
10. The DC battery internal resistance determined by a 10-second pulse is in the 2 to 4 mΩ range, with resistance decreasing due to a conditioning effect for Post Cycle 1 RPT and then remaining unchanged.
11. The calculated cell resistance is 0.17 to 0.34 mΩ, while the Ah-normalized resistance is 34 to 68 mΩ-Ah, which is about 2 to 4 times that of a high power cell of same chemistry (A123 Systems Incorporated, undated). This indicates that the battery cells are tailored for energy intensive applications relative to the high power cells.
12. During rest, the PCS is sometimes in switching mode and at other times it is disabled, with the PCS state changing during a rest period. During rest, because the BESS provides auxiliary load and power related to PCS switching, the difference between the average power output associated with the SOC drop during PCS switching at rest and auxiliary load is assumed to represent power consumption to support PCS switching, and is equal to ~10 kW. However, there are occasions when this difference is as high as 100 kW, indicating power consumption to support PCS switching may be as high as 100 kW.
13. The difference between DC discharge power during rest for PCS in the switching state and PCS in disabled state was also found to be ~10 kW, although there are times when this difference is as high as 100 kW, thus confirming it is the DC battery that provides power for the auxiliary load and PCS switching during rest.
14. The lack of a priori information on what happens during rest (the computer switches, does not switch, grid or battery powers auxiliary) makes it difficult to predict SOC drift during rest. This is not a big issue when PCS does not switch because auxiliary power consumes only 0.25% SOC in an hour. However, during PCS switching, the BESS power is as high as 100 kW, corresponding to a 2.5% SOC change in an hour. Hence, for tests with long rest times, the RTE is very low, and SOC drift during rest is unpredictable. To add to the confusion, there are several occasions when DC battery power is zero with PCS in a disabled state, with the SOC drop being negligible. Hence, it is important to be conservative when operating the BESS to ensure the SOC does not go below the lower limit.

15. Thermal management is based on deviation from set points of 22 to 24ºC for thermostats inside the containers. Because heating the BESS needs to overcome heat loss to surroundings, for a fixed deviation from the set point, auxiliary load is higher at low temperatures. The auxiliary load at 0°C is 20 kW, while at 40°C it is 10 kW, corresponding to an hourly drop of 0.5% SOC and 0.25% SOC, respectively.
16. Of the total test duration of 551 days, 199 days were lost for various reasons. Balance of plant (BOP) related losses contributed to 38% of the lost days, while BMS related issues contributed to 23% of the lost days, followed by site-related issues at 16%. BOP-related issues include BESS external communication hardware, internal communication within the BESS and UPS. Site-related issues include outages, communication error at recloser, and network switch failure for communication. Most of the BOP and site related issues can be resolved through learning. While outages for this report interfered with testing, the BESS is expected to provide outage mitigation when outages do occur.
17. BMS related issues included SOC drift and unbalanced strings, along with inability to control the SOC end points during operation to target SOCs. These interrelated issues can result in suboptimal operation of the BESS.
18. The BESS SOH has not degraded in the 1.5 years of testing. The resistance from in situ and ex situ methods were nearly the same, with a decrease in resistance due to conditioning of the BESS.
19. The BESS SOH in terms of energy content decreased by 6% from the Baseline tests to Post Cycle 1 tests, and by another 1% to Post Cycle 2 tests. Because the internal resistance decreased slightly over this timeframe, the associated decrease was hypothesized and confirmed to be due to an Ah capacity loss. A differential capacity analysis confirmed that capacity loss was due to formation of a solid electrolyte interphase layer that led to lithium loss at the graphite anode.
20. A communication lag of 5 to 7 seconds was observed for the BESS. Excluding the communication lag, signal tracking was excellent within 2% of BESS rated power.

6.0 References

A123 Systems Incorporated. Undated. "Nanophosphate® High Power Lithium Ion Cell ANR26650*m1-B*." Waltham, Massachusetts . Available at https://www.batteryspace.com/prod-specs/6610.pdf.

BYD. Undated. Factory Acceptance Test (FAT) of Energy Storage Systems (ESS), Glacier Energy Storage Project, Report 98223-Glacier-FAT-BYD001.

Doosan GridTech Inc. 2016a. "Products: Doosan GridTech Software™". Seattle, Washington. http://www.doosangridtech.com/products/. Accessed on December 16, 2016.

Doosan GridTech Inc. 2016b. "Applications: Doosan GridTech Distributed Energy Resource Optimizer™ (DG-DERO™). Seattle, Washington. http://www.doosangridtech.com/products/distributed-energy/applications/ Accessed on December 16, 2016.

Modular Energy Storage Architecture (MESA). 2016. *MESA Open Standards for Energy Storage – Draft*. Available at http://mesastandards.org/wp-content/uploads/2016/11/MESA-ESS-Specification-November-2016-Draft-2.pdf. Accessed on December 27, 2016.

Puget Sound Energy (PSE). 2018. *Puget Sound Energy innovation project: Glacier battery storage project – 2018 project updates*. Bellevue, Washington. Available at https://www.pse.com/pages/pse-projects/glacier-battery-storage-project. Accessed on November 29, 2018

Schweiger HO, O Obeidi, A Komesker, M Raschke, C Schiemann, M Zehner, M Gehner, M Keller, and P Birke. 2010. "Comparison of Several Methods for Determining the Internal Resistance of Lithium Ion Cells." *Sensors* 10(6):5604-5625. Available at http://www.mdpi.com/1424-8220/10/6/5604. Accessed July 3, 2017

SunSpec Alliance. 2017. *SunSpec Energy Storage Models: SunSpec Alliance Interoperability Specification*. San Jose, California. Available at http://mesastandards.org/wp-content/uploads/2017/09/SunSpec-Alliance-Specification-Energy-Storage-ModelsD4rev0.25.pdf. Accessed on February 26, 2018.

Viswanathan VV, DR Conover, AJ Crawford, S Ferreira, and D Schoenwald. 2014. *Protocol for Uniformly Measuring and Expressing the Performance of Energy Storage Systems*. PNNL-22010 Rev. 1, Pacific Northwest National Laboratory, Richland, Washington. Available at https://www.sandia.gov/ess-ssl/docs/ESS_Protocol_Rev1_with_microgrids.pdf. Accessed on January 10, 2018.

Viswanathan VV, Balducci PJ, MJE Alam, AJ Crawford, D Wu, and TD Hardy. 2017. *Washington Clean Energy Fund: Energy Storage System Performance Test Plans and Data Requirements.* PNNL-26492, Pacific Northwest National Laboratory, Richland, Washington.

Weather Underground. https://www.wunderground.com/personal-weather-station/dashboard?ID=KWADEMIN7

Appendix A

Additional Battery Design and Performance Information

A.1 Factory Acceptance Test Summary

The Factory Acceptance Test for containers 2, 3, and 4 [BYD undated) describes protective actions that should be taken when smoke or flames are detected. Actions include pressing the emergency stop button, and disconnecting the main and secondary circuit switches, followed by use of fire extinguisher, the type of which was not mentioned. Separate auxiliary supply voltage and specifications suggest the auxiliary load is powered through a separate line. The internal container temperature range was 10 to 40°C, giving some insight into the thermal management algorithm, which according to PSE staff includes a container internal set point of 22°C. When the temperature sensor in modules exceeds 57°C, the fire alarm sounds and the BESS shuts down automatically.

The following equipment were tested:

1. PCS cabinet
2. Transformer cabinet
3. Battery rack
4. Power distribution cabinet
5. Monitoring cabinet
6. Lighting system
7. Ventilation system
8. Air-conditioning system
9. Grounding system
10. Fire Protection system
11. Video monitoring system
12. Container enclosure

The test performed were:

1. Overall inspection of each container
2. Basic test
3. Communication
4. Pseudo-auto-control test (verify control functionality of DC battery, PCS, and ESS between “Supplier Master Controller and ESS”)
5. System performance test
   - Harmonic wave
   - Air conditioning output accuracy
   - Remote dispatching control

6. Alarm functionality
7. Fault recording – All battery faults recorded in battery “historical alarm interface”
8. “Produce” PCS fault – All PCS faults recorded in PCS “historical alarm interface”
9. Check PCS one-way efficiency (Some numbers listed below. Higher efficiency for charge at low power levels of ≤ 100 kW)
   – PCS power/DC Power during discharge – 73% at 10 kW, 88% at 50 kW, 90% at 100 kW, >94% at ≥ 200 kW.
   – DC power/PCS power during charge – 92% at 100 kW, 98% at 250 kW, 99% at 500 kW.
10. Test grid outage – Container charging at 500 kW for 5 minutes. Switch off the grid for 2 minutes, then switch on the grid. The BESS should resume charging at 500 kW.
11. Reactive power capability
12. 240-VAC signal shunt trip capability
13. Test operational mode change signals sent by supervisory control and data acquisition
14. Auto-control mode for current source mode.

A.2 BESS Technical Specifications

The BESS technical specification sheet follows.

Energy Storage System Technical Specification

System Technical Parameters (per Unit)			
	Item	**Parameter**	**Remarks**
1	Nominal Charge/Discharge Power	500kW	Continuous
2	Storage Energy	1.1MWh	
3	Nominal Grid Voltage	480 VAC	
4	Permissible Grid Voltage	423VAC – 528VAC	
5	Nominal Grid Frequency	60Hz	IEEE1547
6	Total Harmonic Distortion	< 3%	Nominal Power IEEE 1547
7	Power Factor	-1 to +1 adjustable continuously	
8	Permissible Ambient Temperature	-40C to +40C	
9	Permissible Ambient Humidity	10% - 95%	
10	Permissible Altitude	< 6562 feet	
11	Container Rating	NEMA 3R	
12	Response Time	< 100mSec @ BYD interface	
13	Communication Protocol	Modbus TCP/IP	

Specification of PCS (per Inverter Unit)	
DC Input Data	
Max DC Voltage	1000VDC
DC Voltage Range	780VDC – 1000VDC
Nominal Power (Charge)	500kW
Max DC Current	700A
AC Input Data	
Nominal AC Power	500kW
Normal Grid Voltage	480VAC
Permissible Grid Voltage	423VAC – 528VAC
Nominal Grid Frequency	60Hz
Permissible Grid Frequency	57Hz – 60.5Hz
Max Efficiency	97.5%
System Data	
Cooling Method	Forced Air
Noise	<80dB at 1m from container
Display	HMI
Anti-Islanding Protection	Active Passive Control&
Dimensions W*D*H	1200 * 600 * 2000mm
Reference Standards	EN61000-6-2, EN61000-6-4, IEC62109-1, UL1741, IEEE1547

- The ESS and battery cells will be lithium-iron phosphate. Each battery module will contain a communication unit to allow the battery management system (BMS) to read the cell voltage and temperature on every individual battery cell.

- The power conversion system (PCS) section of each ESS contains one (1) 500kW inverter BYD model BEG500KTL-U.

- Each container shall be equipped with the following safety features:
  a. Standard and emergency lighting
  b. Heating and cooling
  c. NFPA approved gas fire suppression system.
  d. Fire proof door separating the battery cells for the inverters.
  e. Smoke and temperature sensors.
  f. IR video cameras allowing 24 hour remote video monitoring of the entire energy storage system.
  g. Ventilation shutdown during a fire event.
  h. 24-hour remote monitoring by the battery manufacturer of battery string voltages, cell and environmental temperatures and ESS breaker settings and alarms. Monitoring is covered under the Warranty Agreement.
  i. Each 8 cell block is engineered to provide containment and shall provide containment for any leaked electrolyte.

- The specific chemistry used in the battery system is UL listed and is not subject to internal thermal runaway. The electrolyte used in the battery cells is a nontoxic fluid.

A.3 Site Drawings

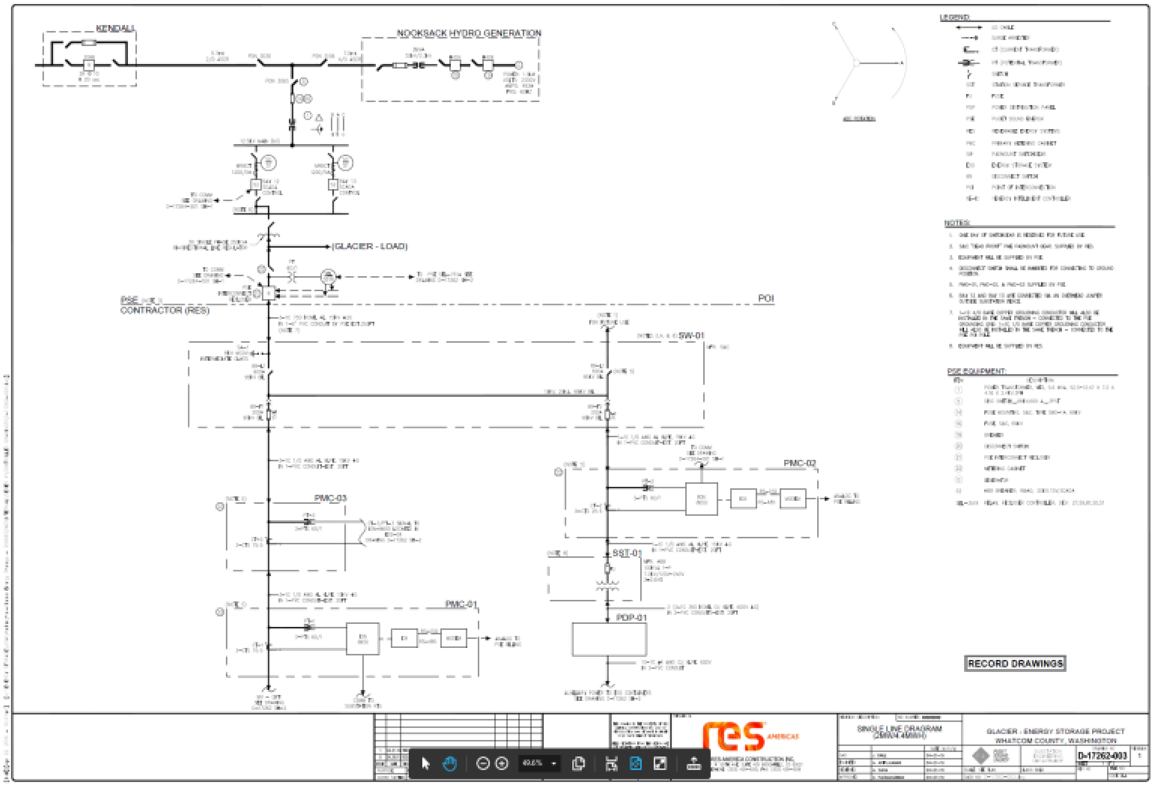

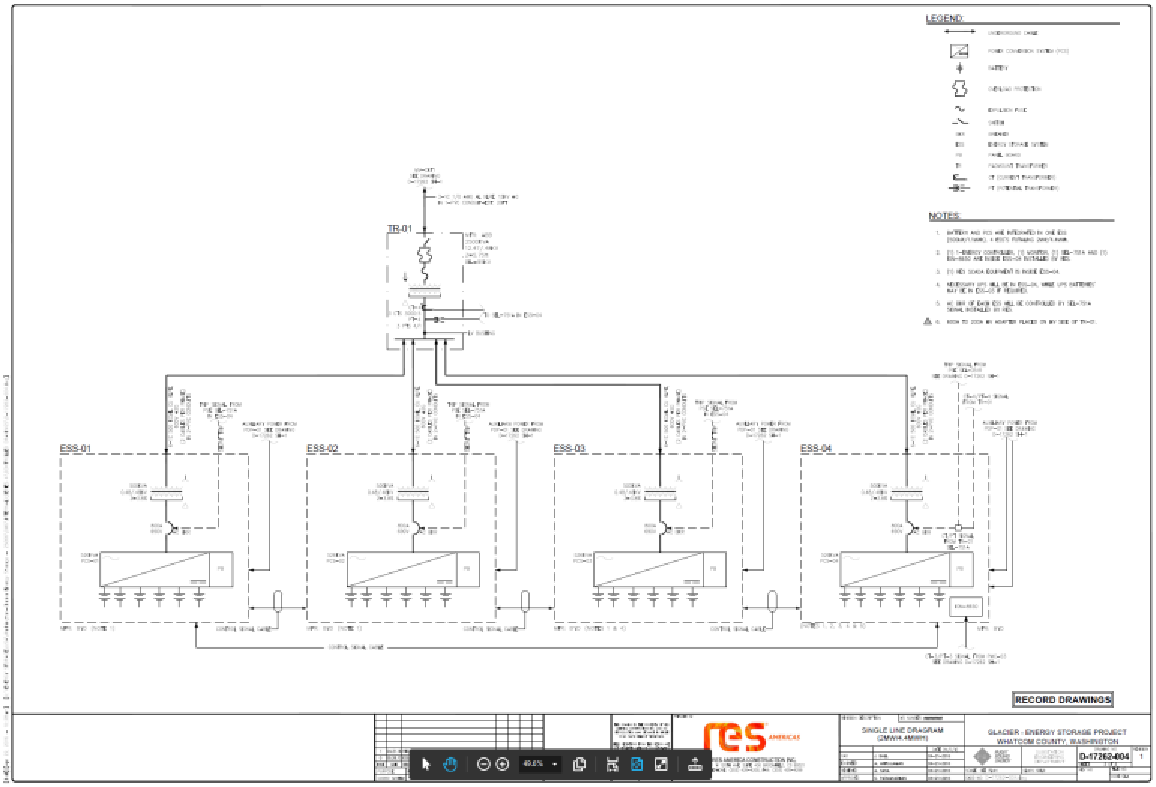

Figure A.1. Glacier Single-Line Drawings

A.4 Issues Encountered

There were multiple issues identified during testing that were not obvious or necessarily anticipated leading up to testing:

A.4.1 Data Related Issues

- The supervisory control and data acquisition system needed to be serviced by Doosan at times.
- Synchronizing data flow from various meters was labor intensive because each meter makes new comma-separated-value files when the file size reaches 10 MB.
- Sending data to PNNL required initiation from DG-IC to create and push the files out.
- A secure file transfer protocol had to be established to transfer the data from PSE to PNNL.
- To automate data transmittal, PNNL's contractor installed software on BESS computer where the data resides.
- A virtual private network connection was established in September 2016. Copying 10 MB file over the virtual private network took 3 minutes.
- Automated processing of selecting files, compressing them on the Glacier computer via a Remote Desktop Protocol session, and retrieving via a network mapped drive.
- Files from different meters were combined in the MySQL database on the PNNL computer.

A.4.2 BMS Related Issues

- Rapid swings in SOC as power magnitude and/or direction changes due to flaw in BMS algorithm to estimate SOC.
- Batteries frequently encountered unbalanced strings, resulting in end of charge SOC <75%.
- SOC range of testing reduced from 5 to 95% to 5 to 90% to avoid high voltage alarm.
- Periodic balancing needed.
- Balancing log not available, hence changes in battery performance difficult to correlate with maintenance.
- BYD balancing procedure was shared with the team. BYD balancing handwritten logs not legible.
- BESS SOC drift during rest not predictable. Changes made by BYD to the BMS software were not shared with the team.
- BYD retrofit all modules with new BMUs to improve balancing and reduce SOC drift.
- Details not shared with team.
- BYD reconfigured BMS to match actual SOC to target SOC.
- PSE unable to control end SOC to target value.
- The original 5-minute UPS caused container BMS to shut down, resulting in BYD master controller seeing no further information from the BMS.
- Situation corrected with PSE learning how to reset BYD master controller and replacing 5-minute UPS with 1-hour UPS.

- The PSE drawings shown auxiliary loads powered by a separate line. However, during discharge and rest, auxiliary loads are powered by the battery, resulting in unexpected SOC drop during rest.
- During rest, the BYD BMS puts PCS either in active mode with PCS switching or in standby mode with PCS not switching. PCS switching during rest is supported by the battery, causing a faster drop in SOC during rest. An increase in SOC drop rate of 0.25% SOC/hour was observed when PCS is in switched mode during rest.
- Thermal management using heat pumps/air conditioning units outside each container based on four thermostats located inside the container containers.
- BMS does not do thermal management based on cell or module temperature
  - A high temperature condition was found in containers after a 2000 kW capacity test performed from October 1–2, 2017, with the container temperature reaching 37ºC twice. The maximum battery temperature at the end of the test reached 45ºC, which is 5ºC lower than for capacity tests done in January and February of 2017. For the Post Cycle 2 test, the internal ambient temperature reached 42ºC, but this did not generate a high-temperature condition. This indicates that the availability of the BESS is dependent on an unknown algorithm to control container temperature and inconsistent criterion for a high-temperature condition. The high rate test was subsequently done in June 2018, when the battery reached a maximum of 48ºC, with the container temperature not displaying the high-temperature condition, even though it reached a maximum of 42ºC.
  - Based on our analysis, auxiliary power consumption increases as temperature from 24ºC. This condition is in line with PSE input that the set point for the thermostats inside the containers is 22ºC.
  - A similar relationship was also found with respect to the ambient temperature. Because the container interior temperature does depend on the ambient temperature, it is not surprising the relationships are similar.
- The difference between minimum and maximum cell temperature was as high as 20ºC at the C/2 rate, and 10ºC at the C/6 rate. Separate data were not available for each container; therefore, it is not possible to conclude if this disparity exists within a container or across containers.
- Power flow information across various containers was not available. SOC information also was not available for each container separately. Hence it was not possible to determine if the central BMS controller allocates power depending on each string status—SOC and temperature. For example, at 2000 kW, each container has to provide 500 kW, which is its maximum rating. However, at power levels less than 2000 kW, there is opportunity for the central BMS controller to direct power flow such that containers with lower SOC and/or higher temperatures during discharge are allocated less power.
- There was an instance when communication between master controller and each container stopped for an unknown reason. An outage on the Glacier line, followed by site restoration cleared the communication alarm. Such unknown causes for alarm generation and clearing adversely affect system reliability in terms of availability.
- Strings are considered balanced when their SOC is within 10 to 15% of each other. This is a wide range, and is sustainable only if the master controller allocates power to each container based on its SOC.

A.4.3 Site Related Issues

- Tests lasting more than 24 hours requires special formatting by PSE to ensure testing continues beyond 24 hours.

- Tests that have commands every few seconds require a manual start. Hence these tests cannot be scheduled sequentially in automatic mode.
- With multiple test interruptions, it was a challenge to synchronize runs with the schedule files sent by PNNL.
- Having a process that names files in an easy-to-track manner at either end would have helped.
- UPS powering Doosan Gridtech Intelligent Controller (DG-IC) faulted due to defective batteries and could not be run on bypass mode. It required a manual DG-IC restart before data could be assessed.
- There was an occasion when the GG-IC sent a signal, but the BESS did not respond. The cause is not known.
- Staff need to be onsite to verify strings are balanced using the human-machine interface.
- The power following mode of the DG-IC was not applicable to load following use case. The frequency/watt mode was more applicable. This mode has not been used by PSE; therefore, duty cycles were sent by PNNL for load following.

A.5 Detailed Pulse Testing Results

The actual SOC values during pulse testing are presented in Table A.1

Table A.1. Detailed Pulse Test Results

Scenario	Pulse	SOC	Time
Baseline	Charge	3	4
Baseline	Charge	13	4
Baseline	Charge	25	2
Baseline	Charge	35	2
Baseline	Charge	46	4
Baseline	Charge	58	2
Baseline	Charge	69	0
Baseline	Charge	79	8
Baseline	Discharge	3	2
Baseline	Discharge	13	0
Baseline	Discharge	25	2
Baseline	Discharge	35	4
Baseline	Discharge	46	2
Baseline	Discharge	58	0
Baseline	Discharge	69	4
Baseline	Discharge	79	2
Baseline	Discharge	90	4
Post Cycle 1	Charge	5	4
Post Cycle 1	Charge	10	2
Post Cycle 1	Charge	16	4
Post Cycle 1	Charge	26	2
Post Cycle 1	Charge	37	2
Post Cycle 1	Charge	47	2
Post Cycle 1	Charge	58	4
Post Cycle 1	Charge	69	2
Post Cycle 1	Discharge	5	2
Post Cycle 1	Discharge	16	4
Post Cycle 1	Discharge	26	4
Post Cycle 1	Discharge	37	2

Scenario	Pulse	SOC	Time
Post Cycle 1	Discharge	47	2
Post Cycle 1	Discharge	58	4
Post Cycle 1	Discharge	69	2
Post Cycle 1	Discharge	79	2
Post Cycle 2	Charge	23	2
Post Cycle 2	Charge	37	2
Post Cycle 2	Charge	51	2
Post Cycle 2	Charge	65	2
Post Cycle 2	Charge	78	2
Post Cycle 2	Discharge	10	4
Post Cycle 2	Discharge	23	4
Post Cycle 2	Discharge	37	4
Post Cycle 2	Discharge	51	2
Post Cycle 2	Discharge	65	2
Post Cycle 2	Discharge	78	2

Figure A.2 shows the power profile during pulse testing at various SOCs, while Figure A.3 shows the time in seconds for the BESS to reach rated power. Figure A.3 shows the voltage and current during pulse testing, while Figure A.4 plots the extreme voltage and current values during each pulse test as a function of SOC.

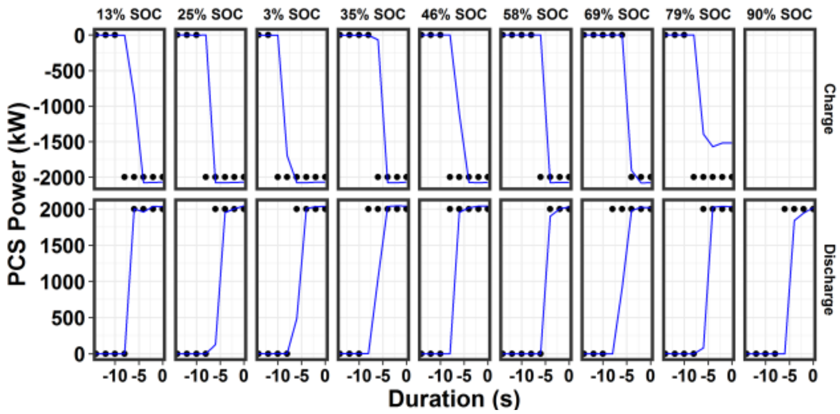

Figure A.2. Power and Requested Power during Pulse Testing

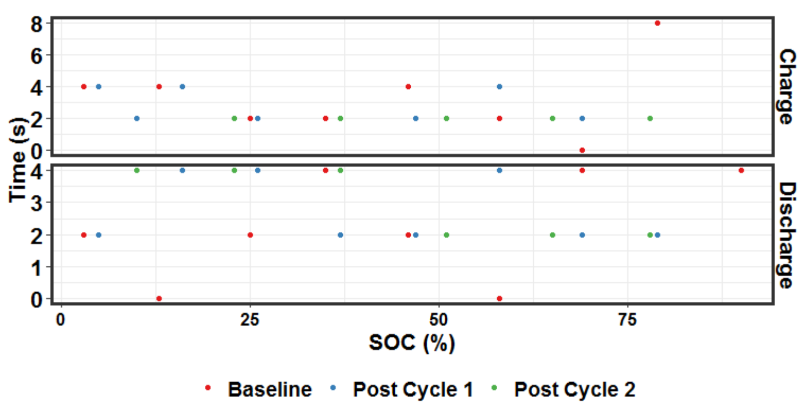

Figure A.3. Response Time vs. SOC during Pulse Testing

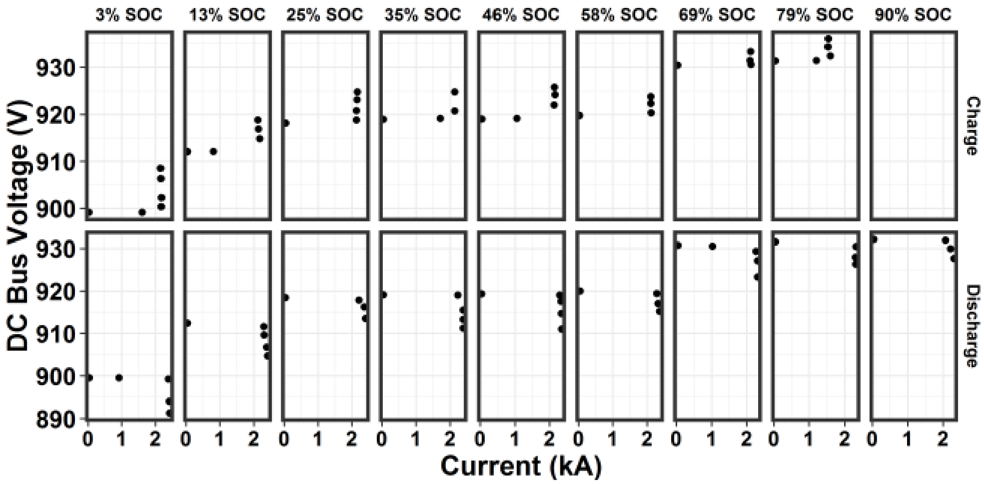

Figure A.4. Voltage vs. Current during Pulse Testing

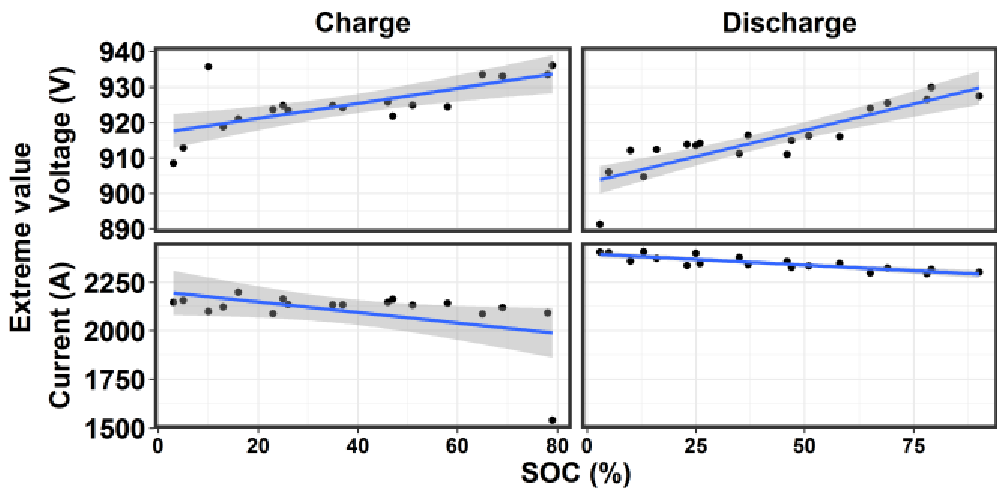

Figure A.5. Extreme Voltage vs. SOC during Pulse Testing

A.6 Individual Baseline Capacity Test Cycles

Table A.2 provides detailed information for each cycle. The RTE for each cycle is calculated by adding or subtracting the required energy to bring the BESS SOC after test to its initial state.

As discussed earlier, the BESS was subjected to various DODs during RPTs. Table A.3 shows the estimated discharge energy for 100% DOD. The Baseline tests showed energy content of ~4,600 kWh, which decreased with test duration.

Table A.2. Data for Individual Baseline Cycles

Scenario	AvgDisPower	AvgChgPower	delSOC	SOCRange	ChgEnergy	DisEnergy	RTE	ChgEnergyNoRest	RTENoRest	ChgEnergyNoAux	DisEnergyNoAux	RTENoAux	meanTemp
Baseline	1741	1998	87.0	90-3	4020	3509	87.3	4007	87.6	3979	3535	88.8	31.4
Baseline	1758	2021	87.0	90-3	4055	3552	87.6	4043	87.9	4016	3578	89.1	31.4
Baseline	1769	2030	88.0	90-2	4077	3563	87.4	4066	87.6	4040	3587	88.8	31.4
Baseline	1766	2030	87.0	89-2	4070	3557	87.4	4059	87.6	4035	3578	88.7	31.4
Baseline	1993	2009	87.0	89-2	4025	3339	83.0	4018	83.1	3997	3355	83.9	31.4
Baseline	1050	1095	87.0	94-7	4024	3408	84.7	4009	85.0	3960	3451	87.1	27.3
Baseline	724	732	93.0	97-4	4399	3663	83.3	4392	83.4	4345	3703	85.2	23.4
Baseline	724	707	93.0	95-2	4254	3663	86.1	4243	86.3	4198	3702	88.2	23.4
Baseline	694	707	93.0	93-0	4258	4219	99.1	4247	99.3	4199	4273	101.8	23.4
Post Cycle 1	729	743	84.0	87-3	3713	3299	88.8	3709	88.9	3694	3313	89.7	27.7
Post Cycle 1	715	742	85.0	87-2	3709	3238	87.3	3706	87.4	3691	3252	88.1	27.7
Post Cycle 1	716	743	85.0	87-2	3711	3239	87.3	3707	87.4	3692	3253	88.1	27.7
Post Cycle 1	714	742	84.0	86-2	3707	3234	87.2	3704	87.3	3689	3247	88.0	27.7
Post Cycle 1	1093	1117	85.0	86-1	3642	3342	91.8	3638	91.9	3628	3351	92.4	32.9
Post Cycle 1	1057	1115	84.0	85-1	3657	3234	88.4	3654	88.5	3644	3243	89.0	32.9
Post Cycle 1	1052	1112	83.4	84-0.6	3649	3219	88.2	3646	88.3	3636	3228	88.8	32.9
Post Cycle 1	1058	1114	84.0	84-0	3655	3237	88.6	3652	88.6	3642	3246	89.1	32.9
Post Cycle 1	1055	1114	84.0	84-0	3654	3227	88.3	3652	88.4	3642	3236	88.9	32.9
Post Cycle 1	1973	2023	88.0	88-0	3561	3365	94.5	3558	94.6	3552	3370	94.9	32.5
Post Cycle 1	1857	2025	83.0	83-0	3603	3168	87.9	3600	88.0	3595	3173	88.3	32.5
Post Cycle 1	1846	2017	83.0	83-0	3589	3149	87.7	3586	87.8	3581	3154	88.1	32.5
Post Cycle 1	1851	2018	83.0	83-0	3590	3152	87.8	3587	87.9	3582	3157	88.1	32.5
Post Cycle 1	1848	2017	83.0	83-0	3589	3147	87.7	3587	87.7	3581	3152	88.0	32.5
Post Cycle 2	720	719	91.0	95-4	3925	3348	85.3	3916	85.5	3867	3390	87.7	25.7
Post Cycle 2	720	711	90.0	92-2	3885	3348	86.2	3876	86.4	3827	3390	88.6	25.7
Post Cycle 2	720	712	87.0	89-2	3892	3348	86.0	3883	86.2	3834	3390	88.4	25.7
Post Cycle 2	720	710	88.0	89-1	3877	3348	86.4	3868	86.6	3819	3389	88.7	25.7
Post Cycle 2	720	711	87.0	88-1	3882	3348	86.2	3873	86.4	3824	3390	88.7	25.7
Post Cycle 2	1090	1065	97.0	98-1	3712	3234	87.1	3704	87.3	3673	3260	88.8	30.6
Post Cycle 2	1091	1063	97.0	98-1	3705	3236	87.3	3696	87.6	3665	3262	89.0	30.6
Post Cycle 2	1991	2032	88.0	89-1	3428	2778	81.0	3421	81.2	3406	2790	81.9	33.9
Post Cycle 2	1986	2023	91.0	93-2	3420	2771	81.0	3411	81.2	3396	2784	82.0	33.9
Post Cycle 2	1985	2024	91.0	97-6	3416	2775	81.2	3408	81.4	3392	2788	82.2	33.9
Post Cycle 2	1990	1989	89.0	98-9	3357	2776	82.7	3348	82.9	3332	2788	83.7	33.9
Post Cycle 2	1990	1957	88.0	98-10	3308	2777	83.9	3299	84.2	3284	2789	84.9	33.9

Table A.3. Individual Baseline Capacity Test Cycles Normalized per 100% SOC

Scenario	AvgDisPower	AvgChgPower	delSOC	SOCRange	ChgEnergy	DisEnergy	RTE	ChgEnergyNoRest	RTENoRest	ChgEnergyNoAux	DisEnergyNoAux	RTENoAux	meanTemp
Baseline	1741	1998	87.0	90-3	4621	4033	87.3	4606	87.6	4574	4063	88.8	31.4
Baseline	1758	2021	87.0	90-3	4661	4083	87.6	4647	87.9	4616	4113	89.1	31.4
Baseline	1769	2030	88.0	90-2	4633	4049	87.4	4620	87.6	4591	4076	88.8	31.4
Baseline	1766	2030	87.0	89-2	4678	4089	87.4	4666	87.6	4638	4113	88.7	31.4
Baseline	1993	2009	87.0	89-2	4626	3838	83.0	4618	83.1	4594	3856	83.9	31.4
Baseline	1050	1095	87.0	94-7	4625	3917	84.7	4608	85.0	4552	3967	87.1	27.3
Baseline	724	732	93.0	97-4	4730	3939	83.3	4723	83.4	4672	3982	85.2	23.4
Baseline	724	707	93.0	95-2	4574	3939	86.1	4562	86.3	4514	3981	88.2	23.4
Baseline	694	707	93.0	93-0	4578	4537	99.1	4567	99.3	4515	4595	101.8	23.4
Post Cycle 1	729	743	84.0	87-3	4420	3927	88.8	4415	88.9	4398	3944	89.7	27.7
Post Cycle 1	715	742	85.0	87-2	4364	3809	87.3	4360	87.4	4342	3826	88.1	27.7
Post Cycle 1	716	743	85.0	87-2	4366	3811	87.3	4361	87.4	4344	3827	88.1	27.7
Post Cycle 1	714	742	84.0	86-2	4413	3850	87.2	4410	87.3	4392	3865	88.0	27.7
Post Cycle 1	1093	1117	85.0	86-1	4285	3932	91.8	4280	91.9	4268	3942	92.4	32.9
Post Cycle 1	1057	1115	84.0	85-1	4354	3850	88.4	4350	88.5	4338	3861	89.0	32.9
Post Cycle 1	1052	1112	83.4	84-0.6	4375	3860	88.2	4372	88.3	4360	3871	88.8	32.9
Post Cycle 1	1058	1114	84.0	84-0	4351	3854	88.6	4348	88.6	4336	3864	89.1	32.9
Post Cycle 1	1055	1114	84.0	84-0	4350	3842	88.3	4348	88.4	4336	3852	88.9	32.9
Post Cycle 1	1973	2023	88.0	88-0	4047	3824	94.5	4043	94.6	4036	3830	94.9	32.5
Post Cycle 1	1857	2025	83.0	83-0	4341	3817	87.9	4337	88.0	4331	3823	88.3	32.5
Post Cycle 1	1846	2017	83.0	83-0	4324	3794	87.7	4320	87.8	4314	3800	88.1	32.5
Post Cycle 1	1851	2018	83.0	83-0	4325	3798	87.8	4322	87.9	4316	3804	88.1	32.5
Post Cycle 1	1848	2017	83.0	83-0	4324	3792	87.7	4322	87.7	4314	3798	88.0	32.5
Post Cycle 2	720	719	91.0	95-4	4313	3679	85.3	4303	85.5	4249	3725	87.7	25.7
Post Cycle 2	720	711	90.0	92-2	4317	3720	86.2	4307	86.4	4252	3767	88.6	25.7
Post Cycle 2	720	712	87.0	89-2	4474	3848	86.0	4463	86.2	4407	3897	88.4	25.7
Post Cycle 2	720	710	88.0	89-1	4406	3805	86.4	4395	86.6	4340	3851	88.7	25.7
Post Cycle 2	720	711	87.0	88-1	4462	3848	86.2	4452	86.4	4395	3897	88.7	25.7
Post Cycle 2	1090	1065	97.0	98-1	3827	3334	87.1	3819	87.3	3787	3361	88.8	30.6
Post Cycle 2	1091	1063	97.0	98-1	3820	3336	87.3	3810	87.6	3778	3363	89.0	30.6
Post Cycle 2	1991	2032	88.0	89-1	3895	3157	81.0	3888	81.2	3870	3170	81.9	33.9
Post Cycle 2	1986	2023	91.0	93-2	3758	3045	81.0	3748	81.2	3732	3059	82.0	33.9
Post Cycle 2	1985	2024	91.0	97-6	3754	3049	81.2	3745	81.4	3727	3064	82.2	33.9
Post Cycle 2	1990	1989	89.0	98-9	3772	3119	82.7	3762	82.9	3744	3133	83.7	33.9
Post Cycle 2	1990	1957	88.0	98-10	3759	3156	83.9	3749	84.2	3732	3169	84.9	33.9

A.7 Miscellaneous Battery Performance

Figure A.6 shows the cumulative discharge energy to various end SOCs for all scenarios and rates during the RPTs. As discussed earlier, at approximately <1% SOC less than the discharged energy per unit, SOC increases steeply.

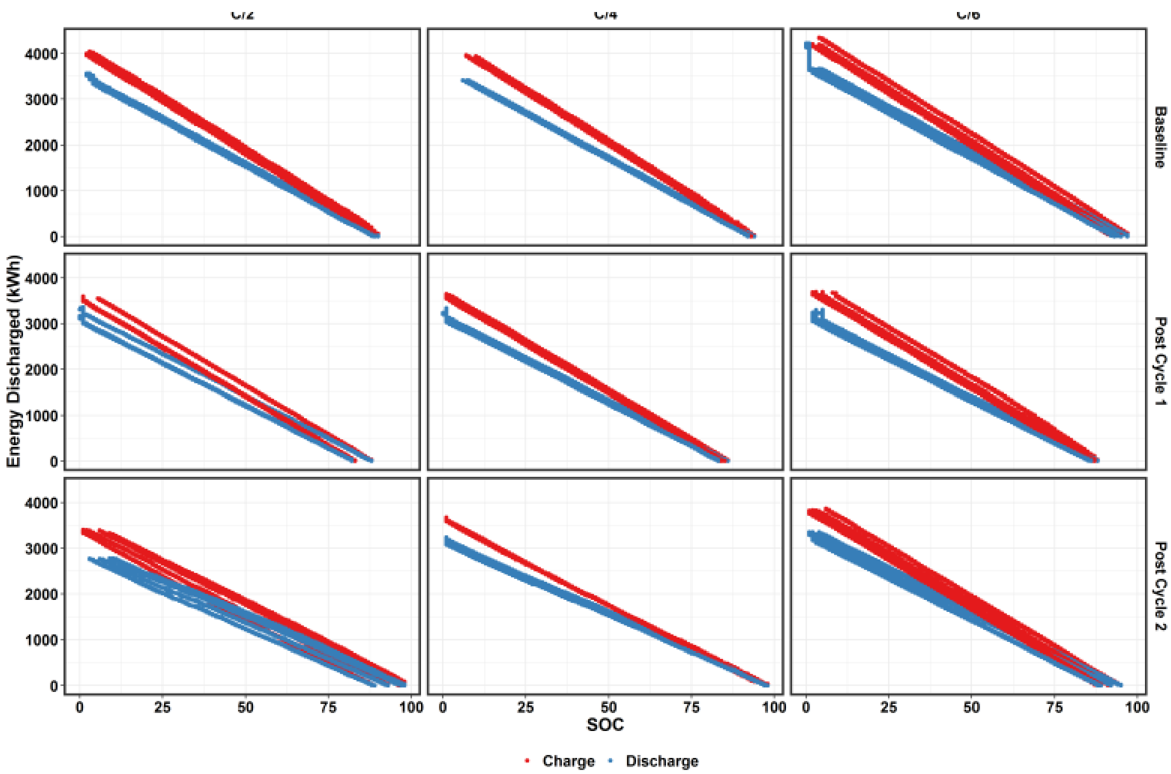

Figure A.6. Energy Discharged during Baseline Capacity Tests

As shown in Figure A.7, the cumulative energy discharged at the PCS level was 880 MWh, corresponding to 200 cycles at 100% DOD.

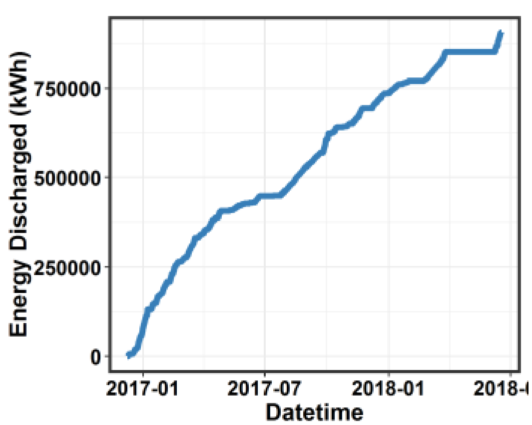

Figure A.7. Cumulative Energy Discharged vs. Time

Figure A.8 shows the SOC levels at which taper occurs at various rates of charge and discharge. Tapering was observed at SOC approximately <5% during discharge at all rates, while there does not appear to be taper during charge.

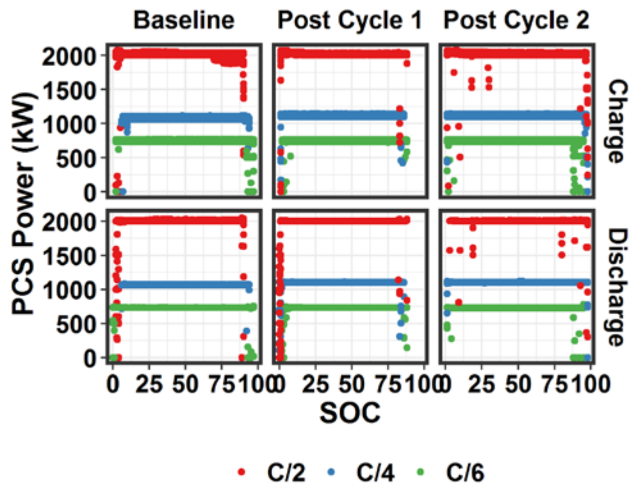

Figure A.8. PCS Power vs SOC

Figure A.9 shows the discharge DC voltage profile for the BESS during the RPTs. The discharge shape may provide insights into mechanisms for capacity loss, which will be explored at a later stage.

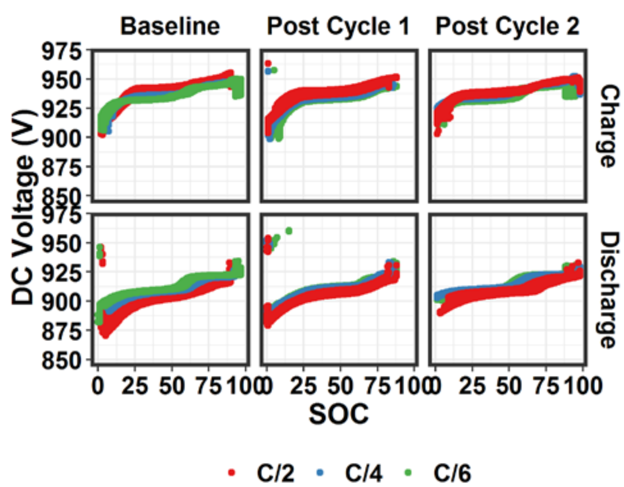

Figure A.9. Voltage vs. SOC during Baseline Capacity Tests

A.8 Islanding

In 2018, PSE successfully islanded the relevant circuit serviced by the Glacier substation. The procedure as outlined by PSE is presented below. The meter information when the Glacier circuit is placed in an islanded mode is shown in Figure A.10.

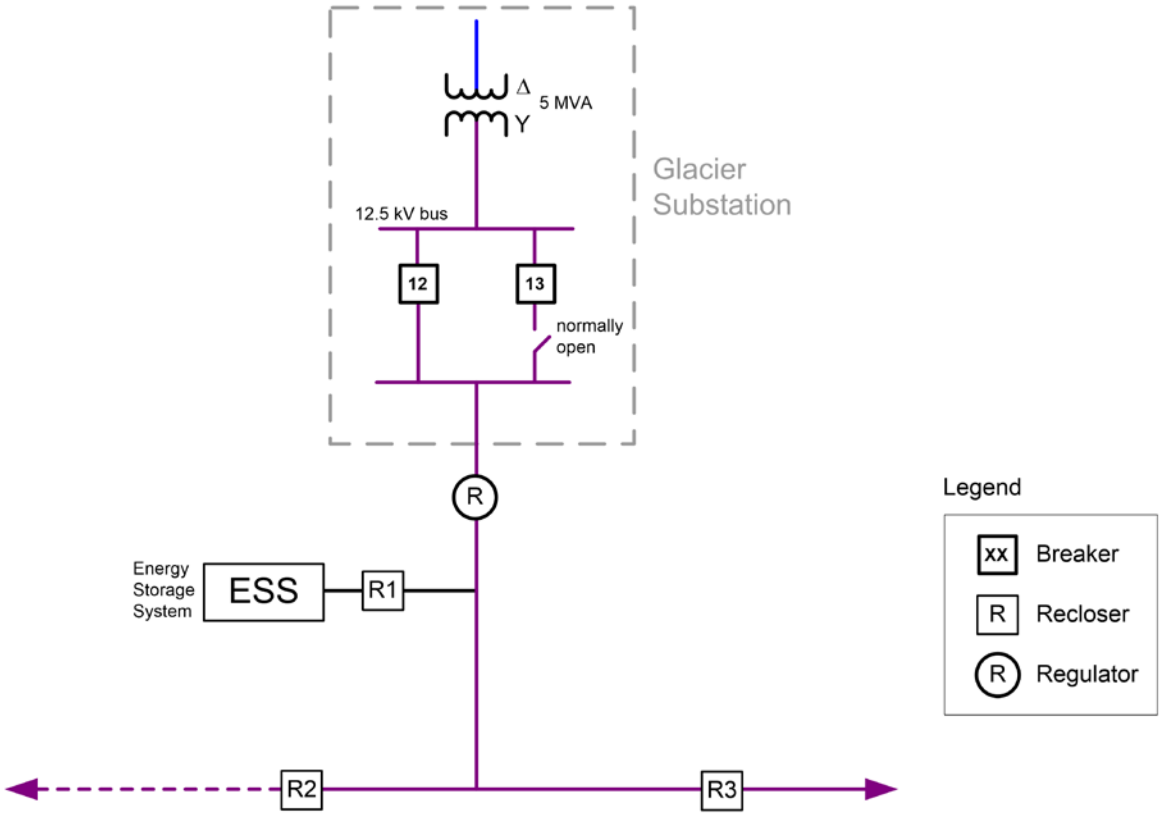

Figure A.10. Glacier System

Glacier Island Operating Procedures (updated May 29, 2016)

Purpose: The Glacier system has capabilities that allow the Glacier Substation (GLA) battery and distribution system to automatically or manually switch between islanding and grid-tied configurations. This document is intended to explain how the system works and how to use it safely.

Automation system definition: The automated islanding system consists of the following controllable devices: GLA-12 breaker, interconnect recloser R1, the GLA battery controller (1EIC), and distribution reclosers R2 and R3.

A.8.1 Procedures

To enable automation:

Automation can only be enabled when the system is in a grid-tied configuration. Before enabling automation, review energy management system (EMS) screens to verify the following:

- The GLA-12 close-block is disabled. If it is enabled, someone onsite will have to set the local/remote switch to local (wait 3 seconds) and back to remote to disable the close-block.
- The R1 close-block is disabled. If it is enabled, someone onsite will have to set the local/remote switch to local (wait 3 seconds) and back to remote to disable the close-block.
- The GLA-12 breaker is closed.

- No system components are abnormally configured; for example, GLA-13 should not be closed and circuit switcher 3065 should be closed.
- The 1EIC is in grid-tie mode.
- All alarms have been cleared.
- To restore the system after an automation fail alarm:
- Resolve all alarm conditions and re-enable automated islanding after the system has been restored to normal (see procedure to enable automation above).

To manually island remotely:

This procedure should generally only be used for testing. In all other cases, the system should only be islanded by the islanding automation scheme.

1. Disable islanding automation in EMS – SCHEME_ON/OFF.
2. Verify R1 is open.
3. Set the battery to island mode – ESS_ISLAND_GRID.
4. Open the GLA-12 breaker
NOTE: DO NOT CLOSE GLA-12 WHILE THE SYSTEM IS ISLANDED. Closing the breaker could result in injury or damage to equipment.
5. Open R2.
6. Open R3.
7. Change R1 settings to SG2 – RCL.76124_GRID_ISL.
8. Verify the 1EIC has successfully switched to island mode (this may take ~1 minute) – ESS_ISLAND_GRID.
9. Start the battery – BAT.ESS _START.
10. Close R1.

To manually restore the system from island to normal grid-tied mode remotely:

1. Disable islanding automation in EMS - SCHEME_ON/OFF.
2. Stop the battery – BAT.ESS_STOP.
3. Open R1 if not open already.
4. Set the battery to grid-tied mode - ESS_ISLAND_GRID
Note that if the generator connects to the grid in island mode, it may be out-of-phase and result in equipment damage and injury.
5. Reset GLA-12 close-block. Someone onsite will have to set the local/remote switch to local (wait 3 seconds) and back to remote to disable the close-block.
6. Close breaker GLA-12.
7. Close R2.
8. Close R3.
9. Change R1 settings to SG1 - RCL.76124_GRID_ISL.
10. Reset R1 close-block. Someone on site will have to set the local/remote switch to local (wait 3 seconds) and back to remote to disable the close-block.

11. Start the battery - BAT.ESS _START.
12. Verify the battery is in grid-tied mode (this may take ~1 minute) - ESS_ISLAND_GRID.
13. Close R1. The battery will automatically synch to the distribution system after R1 is closed.

A.8.2 Operation Details

Things that cause the automation scheme to turn off:

- If any of the remote terminal unit, GLA-12, R1, R2 or R3 are put into local mode, the scheme is disabled but will be re-enabled as soon as all components are back in "remote."
- If GLA-12 opens for a fault or through EMS, the scheme will be disabled. An operator will then need to enable automation after the system is returned to normal.
- If an isolating device (recloser, breaker…, etc.) does not open within 90 seconds after a control is issued, the auto-fail alarm is set and the scheme is turned off. The auto-fail alarm can only be reset from EMS.
- Setting the HLWS at R1 or GLA-12 will disable the GLA island automation. It will be re-enabled when the HLWS is disabled.
- Island operation:
- Reclosers R2 and R3 can be operated remotely without affecting automation, though they should not be closed remotely as this will increase the load on the battery and increase exposure to faults.
- An auto-complete alarm will be enabled for 60 seconds after the auto-scheme successfully isolates or restores the system.
- Grid-tied operation
- Disable automation if Glacier sub is reconfigured such that breaker GLA-13 is serving load.
- The open/close position of R2 and R3 will not affect grid-tied operation.
- An auto-complete alarm will be enabled for 60 seconds after the auto-scheme successfully isolates or restores the system.

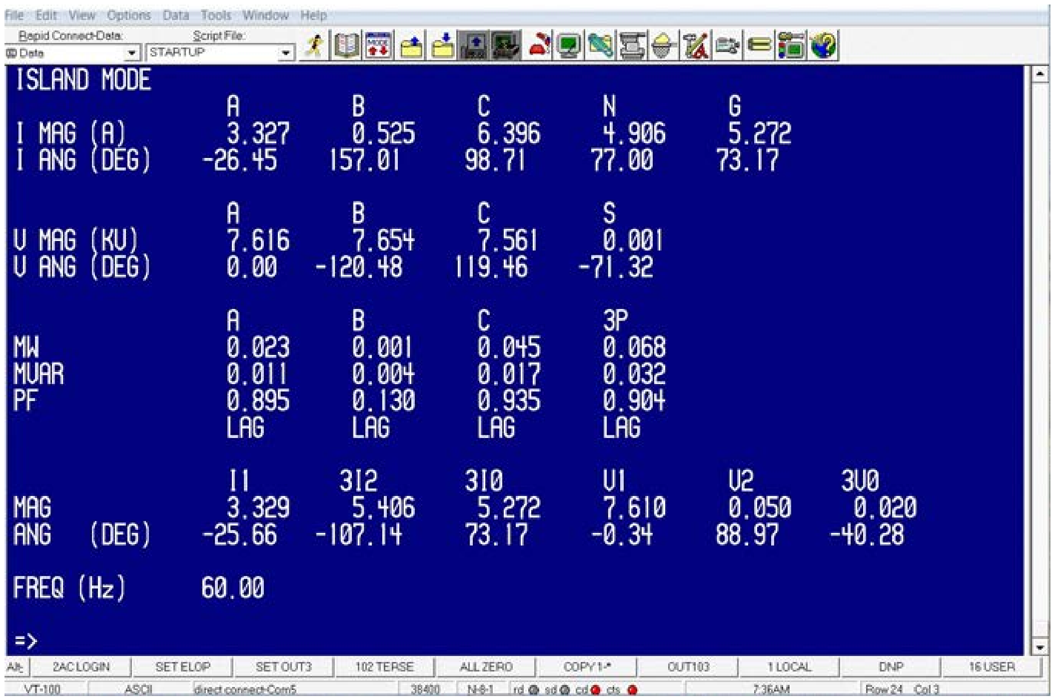

Figure A.11. Meter Information when the Glacier Circuit is in an Islanded Mode. For perspective, the normal currents when the circuit is not islanded are A-86 B-119 C-107 N-30.

Pacific Northwest
NATIONAL LABORATORY

www.pnnl.gov

902 Battelle Boulevard
P.O. Box 999
Richland, WA 99352
1-888-375-PNNL (7665)

U.S. DEPARTMENT OF
ENERGY